

# **NORTH PACIFIC RESEARCH BOARD PROJECT FINAL REPORT**

## **Walleye Pollock Recruitment and Stock Structure in the Gulf of Alaska: An investigation using a suite of biophysical and individual-based models**

### **NPRB Project 523**

**Sarah Hinckley<sup>1</sup>, Carolina Parada<sup>2</sup>, John Horne<sup>3</sup>, Albert J. Hermann<sup>2</sup>, Bernard A. Megrey<sup>1</sup>,  
Martin Dorn<sup>1</sup>**

<sup>1</sup>**National Oceanic & Atmospheric Administration, National Marine Fisheries Service,  
Alaska Fisheries Science Center, 7600 Sand Point Way NE, Seattle, WA 98115. (206-526-  
4109, sarah.hinckley@noaa.gov.**

<sup>2</sup>**Joint Institute for the Study of Atmosphere and Oceans, University of Washington, Seattle,  
WA 98195.**

<sup>3</sup>**School of Aquatic and Fisheries Science, University of Washington, Seattle, WA 98195.**

**October, 2008**

Note: Mention of trade names is for information purposes only and does not constitute endorsement by the US Department of Commerce. This report does not constitute a publication and is for information only. All data herein are to be considered provisional and shall not be cited without the author's permission.

## ABSTRACT

We developed and used a coupled model application to simulate the physical environment and the early life history of walleye pollock (*Theragra chalcogramma*) in the Gulf of Alaska (GOA). The overall goal of the modeling work has been to understand processes that influence walleye pollock recruitment, and how recruitment may fluctuate as climate changes. As part of this main goal, we have tried to illuminate aspects of the population structure of walleye pollock in the North Pacific by providing a picture of relationships between spawning locations and nursery areas. GOA and Bering Sea (BS) walleye pollock are presently managed as a separate populations – is this management scheme justified? Spawning pollock are now found in several different locations in the GOA, especially since the historical population spawning in Shelikof Strait has declined. Where do the fish from these different spawning locations go? Part of our ultimate goals with this work is to use our biophysical model to derive a model-based index of recruitment to aid managers of walleye pollock. In order to do this, we must answer these questions about stock structure and connectivity. In this project, we adapted and developed a simulation modeling application to examine some of these questions, and to aid in the development of a potential recruitment forecasting index for GOA walleye pollock. This application consists of a coupled model set: a three dimensional model of the physical environment, including currents, salinities, and temperatures, and an individual-based model (IBM) of mechanisms affecting growth and survival of young walleye pollock as they move through the environment. We present the modeling application we developed, validation exercises, and the results of simulation experiments that shed light on the complex relationship between spawning areas in the GOA, and the different nursery areas. This work has resulted in increased insight into possible connections of walleye pollock within the GOA and between the GOA and the BS.

**Keywords:** Walleye pollock, *Theragra chalcogramma*, Gulf of Alaska, Recruitment, Individual-based Modeling, Early Life History, ROMS, Connectivity

### Citation:

Hinckley, S., C. Parada, J. Horne, A.J. Hermann, B.A. Megrey, M. Dorn. 2008. Walleye pollock recruitment and stock structure in the Gulf of Alaska: An investigation using a suite of biophysical and individual-based models. North Pacific Research Board Final Report 523, ??? p.

# TABLE OF CONTENTS

## INTRODUCTION

## OVERALL OBJECTIVES

### CHAPTER 1. Java-based applications and model development for the simulation of early life history of walleye pollock in the Gulf of Alaska

- 1.1. Java application implementation and coupling the IBM to the hydrodynamic model
- 1.2. IBM model code translation and adaptation to the Java interface
- 1.3. Addition of new features to the biological compartments of the IBM
  - 1.3.1. Initial conditions
  - 1.3.2. Superindividual module
  - 1.3.3. Water density estimation
  - 1.3.4. Predation on juveniles
  - 1.3.5. Active swimming of juveniles
- 1.4. ROMS model output preparation
- 1.5. Model experiment: A year of anomalous transport
- 1.6. Initial spawning-nursery areas experiment and parameter testing
- 1.7. Addition of bioenergetic and feeding algorithms for juvenile pollock to the IBM
- 1.8. Conclusions
- 1.9. Literature Cited

### CHAPTER 2: Empirical corroboration of IBM predicted walleye pollock (*Theragra chalcogramma*) spawning-nursery area transport and survival in the Gulf of Alaska

- 2.1. Introduction
- 2.2. Methods
  - 2.2.1. Hydrodynamic model
  - 2.2.2. Walleye pollock IBM
    - 2.2.2.1. Growth and bioenergetic submodels
    - 2.2.2.2. Mortality submodel
    - 2.2.2.3. Movement submodels
  - 2.2.3. Model simulations
    - 2.2.3.1. Spatial and temporal matching of model predictions and data
    - 2.2.3.2. Prediction of potential nursery areas
- 2.3. Results
  - 2.3.1. Comparison between observed and predicted distributions
  - 2.3.2. General patterns of juvenile pollock nursery areas
- 2.4. Discussion
- 2.5. Literature Cited
- 2.6. Tables
- 2.7. Figures

CHAPTER 3. Connectivity of walleye pollock (*Theragra chalcogramma*) spawning and nursery areas in the Gulf of Alaska.

3.1. Introduction

3.2. Methods

3.2.1. Model configuration

3.2.2. Individual-based model parameters and mechanisms

3.2.3. Spatial and temporal variability of spawning areas

3.2.4. Spatial and temporal variability of nursery areas

3.2.5. Transport to and retention in nursery areas

3.3. Results

3.3.1. Retention in the spawning areas and temporal variability

3.3.2. Temporal variability of transport to nursery areas

3.3.3. Spawning in February

3.3.4. Spawning in March

3.3.5. Spawning in April

3.3.6. Spawning in May

3.4. Summary of Results

3.5. Discussion

3.6. Literature Cited

CONCLUSIONS

PUBLICATIONS

OUTREACH

ACKNOWLEDGEMENTS

LITERATURE CITED

PROJECT SYNOPSIS

## **Study Chronology**

July, 2005: Project Start

January, 2006: Progress Report

July, 2006: Progress Report

January, 2007: Progress Report

July, 2007: Progress Report

January, 2008: Progress Report

October, 2008: Final Report

This project did not build directly on previously funded NPRB projects, but benefited from the expertise of many individuals supported by NPRB over the years. This project has served as foundation for other NPRB projects. We also build on projects funded by NOAA NMFS, GLOBEC and NSF support.

## INTRODUCTION

Walleye pollock (*Theragra chalcogramma*) is an important commercial species in Alaskan waters. Pollock show high interannual variability in recruitment (Dorn et al. 2005), which is likely due to the combined effects of physical and biological processes during early life stages (Megrey et al, 1995). Knowledge of the mechanisms behind this recruitment variability will aid in the development of ways to forecast recruitment several years ahead of the entry of a pollock year-class into the fishery, providing useful information for resource managers. In addition, understanding these mechanisms should allow us to understand and predict how shifts in climate may affect recruitment.

To understand recruitment processes for walleye pollock (*Theragra chalcogramma*) in the Gulf of Alaska (GOA), and to understand how recruitment may fluctuate as climate changes, a clearer understanding of the relationships between populations spawning in different spawning locations and the juvenile nursery areas is needed. GOA and eastern Bering Sea walleye pollock are presently managed as separate populations. Is this management scheme justified? Is there transportation of eggs, larvae or juveniles between these management areas? It is necessary to answer these questions before we can use information derived from spawning stock biomasses and surveys of early life stages, along with mechanistic models of the success of early stages, to develop a biophysical model-based index of recruitment.

In this project, we developed a simulation modeling application to examine some of these questions, and to aid in the development of a potential recruitment forecasting index for GOA walleye pollock. This application consists of two previously existing models linked to form a coupled model set: a three dimensional model of the physical environment, including currents, salinities, and temperatures, and an individual-based model (IBM) of mechanisms affecting growth and survival of young walleye pollock as they move through the environment. Here we present the developments of the coupled model set (Parada et al., accepted) and the interface to these models that we developed. We also present model corroboration exercises and the results of simulation experiments that shed light on the complex relationship between spawning and nursery areas in the GOA and the BS.

Two ultimate goals of this work were: (1) to explore whether our coupled biophysical model can be used to generate an index of recruitment several years ahead of its entry into the

fishery, and (2) to understand the biophysical mechanisms behind the variability in recruitment, which will allow us to explore future effects of climate change on recruitment. The application that we have developed will not only be useful for the study of walleye pollock recruitment in the GOA, but also to study recruitment of pollock and other species in other areas, such as the Bering Sea and the West Coast of North America. It is a versatile and powerful tool.

In Chapter 1, we describe additions to the physics and to the biology of the walleye pollock IBM precursor model, the application that we have developed and the validation tests accomplished before the model was deemed ready for use. Details of the precursor models can be found in Haidvogel et al., 2000; Hermann et al. 1996a; Hermann et al. 1996b; Hermann & Stabeno 1996; Hermann et al. 2001; Hinckley et al. 1996; Hinckley et al. 2001; Megrey & Hinckley, 2001; Moore et al., 2004; and Shchepetkin and McWilliams, 2004. In Chapter 2, we describe model corroboration studies, which found the model capable of correctly simulating the movement through space of pollock eggs, larvae and juveniles, and of simulating the known nursery areas of GOA walleye pollock. In Chapter 3, we describe our final study for this project exploring the relationships or connectivity between GOA pollock spawning areas and nursery areas. This information will aid managers in making informed decisions about how to effectively manage this species, and also to understand the best way to use the coupled model set as a forecasting tool. This work will indicate what indices the model may be able to produce, and what measures may be well correlated with recruitment.

## **OVERALL OBJECTIVES**

In this project, we proposed to refine and further develop a suite of coupled models and to use these to investigate recruitment variation in, and stock structure of walleye pollock in the Gulf of Alaska. We originally proposed to develop two outputs: (1) an index of abundance of pre-recruits for managers of this stock, and (2) information on stock structure of pollock in the Gulf, as determined by the modeled success of spawning and retention of juveniles in different regions within the Gulf. We utilized a hydrodynamic model (Regional Ocean Modeling System, ROMS), adapted to this region, and we further developed our individual-based model (IBM) of the early life of walleye pollock to meet these objectives. This project directly addresses NPRB's mandate to fund research which furthers our understanding of, and ability to manage, fish populations in the Gulf of Alaska region of the North Pacific.

The objectives of this project were, of necessity, modified as we progressed through this work. The model and coupled model application took significantly more time than anticipated to develop. We decided to focus on the stock structure aspect of the work (rather than the recruitment prediction), since without better understanding of stock structure and connectivity of walleye pollock spawning and nursery areas in the GOA, we would not be in a position to derive a pre-recruitment index from this coupled model set. This goal was accomplished.

The overall objectives, as modified, were to:

1. Adapt and develop a Java application that allows us to use physical model output from the ROMS models, in conjunction with the walleye pollock IBM, to simulate the early life history of walleye pollock in the Gulf of Alaska in a user friendly, flexible manner. This application is easily adaptable for use in different simulation configurations and even different species and areas.
2. Make needed improvements to the walleye pollock IBM within the Java application, to reflect new thinking about factors governing connectivity and recruitment variability.
3. Perform model simulation experiments designed to test and corroborate the coupled model set.
4. Perform model simulation experiments designed to illuminate the relationships between different spawning areas and nursery areas of walleye pollock in the GOA. This information will be used to aid managers in assessing management strategies, and in designing potential indices to be derived from the coupled model in future studies which may be useful in forecasting year class strength.

## **CHAPTER 1: Java-based application and model development for the simulation of early life history of walleye pollock in the Gulf of Alaska**

### 1.1 Java application implementation and coupling the IBM to the hydrodynamic model

A Java programming application was adapted to simulate the early life history of walleye pollock in the Gulf of Alaska (GOA). The purpose of the study was to understand the transport and survival of walleye pollock from spawning to nursery areas. This application enabled us to track trajectories of simulated particles representing individual or groups of individual fish, and water properties (temperature, salinity) experienced by particles during transport. It uses three-dimensional fields of velocity, temperature, and salinity archived from simulations of the Regional Oceanic Modeling System (ROMS, Haidvogel et al., 2000; Moore et al., 2004; Shchepetkin and McWilliams, 2004) to track particle trajectories within the model domain. As described in Lett et al. (2008), the application offers two functioning modes. The first allows a visualization of the transport of simulated eggs and larvae in a user-friendly graphic interface showing the trajectories of all particles being transported, and the evolution of selected variables followed during simulations. Examples of variables that can be tracked include distributions of length or weight, growth curves, or number of survivors. The second mode enables batch simulations based on pre-defined sets of parameters and produces output files for each series. The program stores information on the dynamics of individuals (e.g. time, longitude, latitude, depth, length, etc.). Output files are in ASCII format for ease of post-processing. The application is distributed as a package that contains the program code and libraries (for details see <http://www.ur097.ird.fr/projects/ichthyop/>). For this project, we used one of the early releases of the Java application and adapted it to our model requirements (see below).

The Java application was coupled to the ROMS hydrodynamic model to simulate the transport of particles released in spawning areas for walleye pollock in the GOA (Figure 1.1). We used a subset of the output of the multi-decadal coupled sea-ice/ocean numerical simulations of the Northeast Pacific (NEP) region configured and run by Curchitser et al. (2005). The coupled model is based on the ROMS model implemented at 10 km resolution for a Northeast Pacific domain, which includes the Gulf of Alaska and the Bering Sea (Figure 1.2).

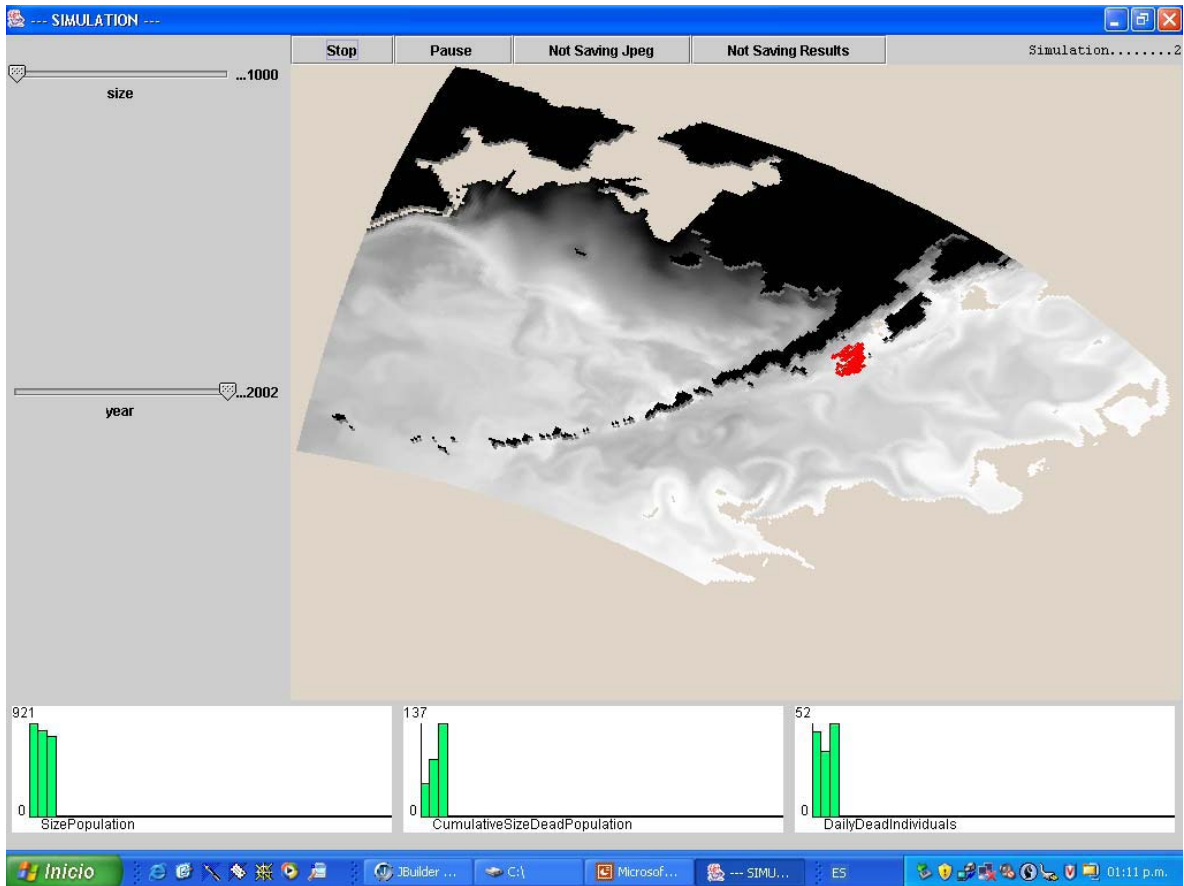


Figure 1.1. Java graphical interface showing SST and currents from ROMS model output, and in red initial positions of drifters. To the left are slider bars where parameters can be set. At the bottom are histograms or graphs showing model output.

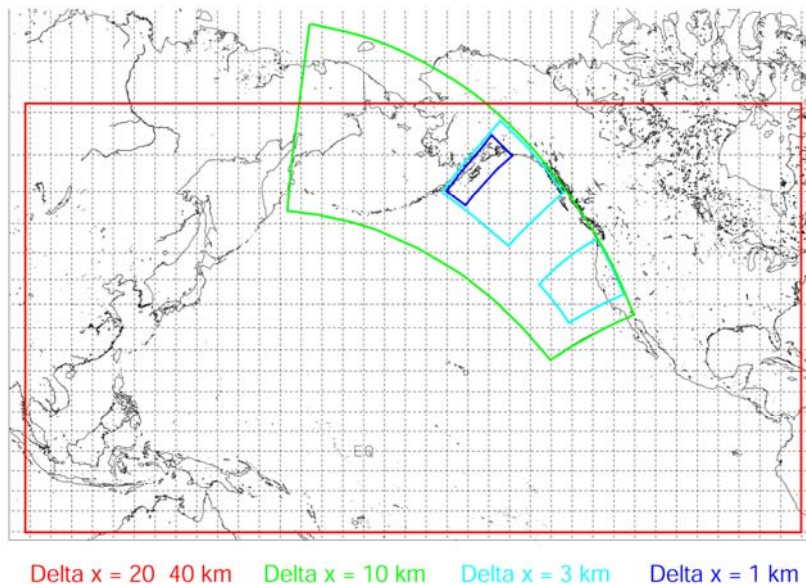


Figure 1.2. Nested grids used in the ROMS model system. The NPac grid, outlined in red, has 20-40 km horizontal resolution. The NEP grid, outlined in light green, has 10 km horizontal resolution. The CGOA grid, the northernmost of the two grids outlined in light blue, has a horizontal resolution of 3 km. The coupled model described here was run on the NEP grid.

A series of experiments was conducted to test the reliability of the particle tracking algorithm within the Java application. Two tracking algorithms were tested: one using the Euler method for solving differential equations, the other using a 4<sup>th</sup> order Runge-Kutta method. In these experiments, the number of iterations ( $i$ ) between time steps was varied from 1 to 10,000. The Runge-Kutta method was more stable than the Euler method, and converged quickly ( $i < 10$ ) to the (x, y) position (Fig. 1.3a and b). The Euler method took longer to converge ( $100 > i > 200$ ) (Fig. 1.3a and b).

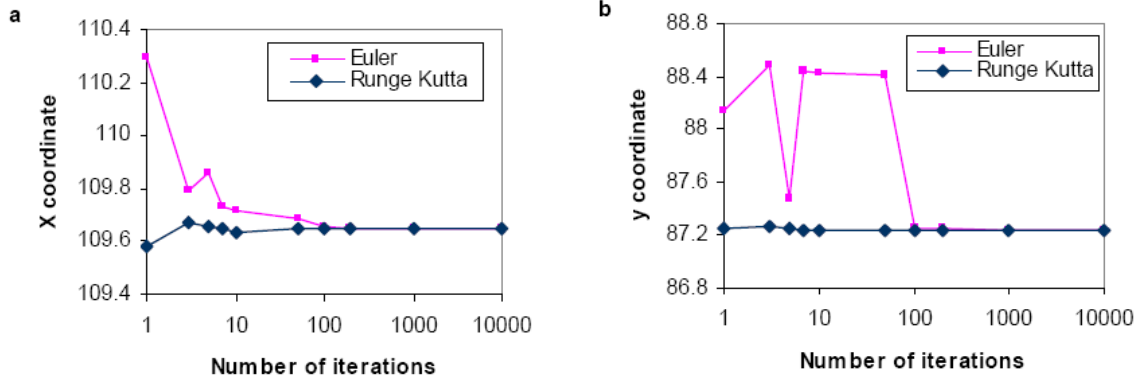
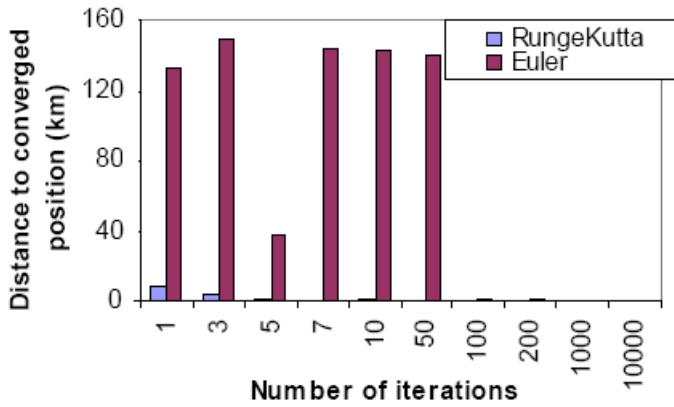


Figure 1.3. Convergence of particle positions (a) x and (b) y after a series of simulations varying the number of iterations between time steps using two algorithms for particle tracking (Euler and Runge-Kutta).

The error in displacement before convergence was very high for a low number of iterations when using the Euler method (Fig. 1.4). For  $i < 100$ , the error in displacement was higher (~130 km) than the spatial resolution of the ROMS model output. The error in



displacement when using Runge-Kutta method, was very low (Fig. 1.4).

Figure 1.4. Displacement of particles from the final position after 'i' iterations using two algorithms for tracking particles: Euler and Runge-Kutta.

## 1.2. IBM model code translation and adaptation to the Java interface

The original IBM model for walleye pollock was coded in the C programming language (Hinckley et al., 1996; Megrey and Hinckley, 2001). It has now been translated into Java, and a new model interface has been completed. All biological compartments and subroutines were translated from C to Java.

## 1.3. Addition of new features to the biological compartments of the IBM

(See Chapter 2 for details of algorithms and parameters mentioned in the next sections)

### 1.3.1. *Initial Conditions*

Algorithms were written to select spawning areas, the depth of spawning, and the timing of spawning. Eggs can be released randomly or with a stratified random distribution, at specific locations, depths, and times.

### 1.3.2. *Superindividual module*

Superindividual schemes (Scheffer et al., 1995; Megrey and Hinckley, 2001; Bartsch and Coombs, 2004) are approaches that allow the use of realistic mortality rates in IBMs by increasing the number of individuals represented by each point or float (i.e. superindividual). In this way, we can simulate larger numbers of fish in a population without significantly adding to computer processing time. The assumption behind this approach is that growth, feeding conditions, and the probability of mortality for each individual within a superindividual are the same. At the beginning of the simulation, each superindividual is assigned a “count”, indicating how many individual fish the superindividual represents. This “count” is decreased by applying a random deviate from the daily mortality rate for that particular life stage. At any point in time, the total number of individual fish is the sum of the “count” variable over all superindividuals. The value of the “count” of the superindividual at time  $t+1$  depends on that of the superindividual at time  $t$ , the mortality rate  $r$ , and the time step  $t$ .

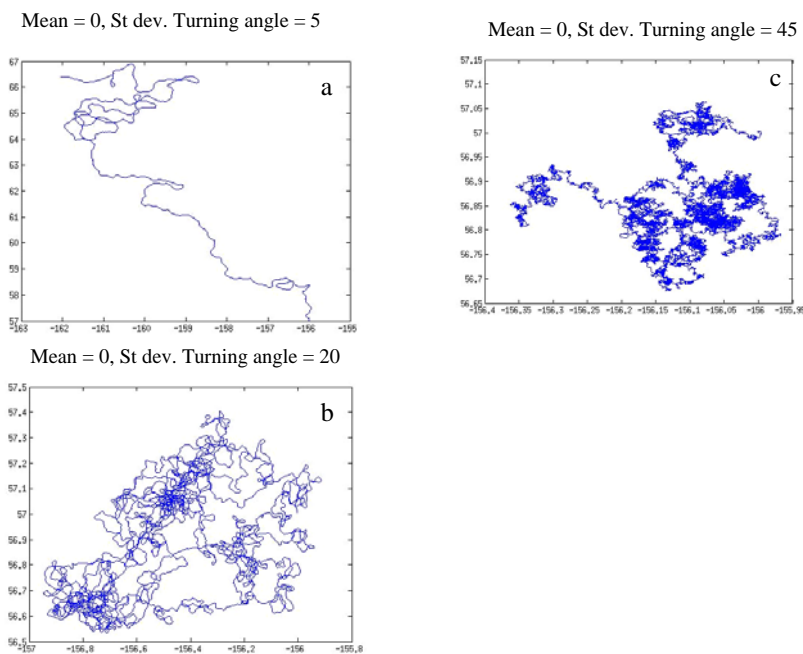
$$S_{t+1} = S_t e^{-rt} \tag{1}$$

### 1.3.3. Water density estimation

The UNESCO equation for the estimation of seawater density based on salinity and temperature was incorporated in the code to replace a linear function of salinity. The original algorithm was intended for a model which covered a more restricted domain (Parada et al., accepted) for which the linear function of density with salinity was appropriate. However the larger domain covered by the ROMS model necessitated the use of the more general UNESCO function.

### 1.3.4. Predation on Juveniles

Groundfish predation on 0-age juveniles was added to the juvenile subroutine. Predation rates were based on 8 years of groundfish predation data (K. Aydin, Alaska Fisheries Science Center, Seattle, WA, pers. comm.). For years where no data were available, an average rate over the 8 years was used. The predation rate was calculated using the total numbers of walleye pollock juveniles consumed by all groundfish predators in each year. We computed mortality rates assuming that the maximum number consumed was equivalent to a predation mortality rate of 0.3 per day (average). Predation rates for other years were standardized relative to this maximum.



### 1.3.5. Active swimming of juveniles

A correlated random walk algorithm was added to the model to simulate horizontal movement of juveniles. Examples of trajectories of a single individual (60 mm length) with mean turning angle of

0° and several different values for the standard deviation of the turning angles are shown in Figure 1.5.

Figure 1.5. Trajectories of juvenile pollock at 60 mm using different values for the standard deviation of the turning angle.

A standard turning angle deviation of 20 degrees was used in the simulations described below. When this value was used, the overall distribution of 0-age juveniles was closer to the Alaska Peninsula and patchier than simulations without active swimming of juveniles, which was what we were trying to accomplish by this addition to the model, as it is what the observations indicate.

#### 1.4. ROMS model output preparation

Outputs from ROM model runs were corrected for the time series 1978-2004 to fit the requirements of the IBM, and some faulty files were replaced. We are currently using a subset of this time series (several years in the 1980's, the 1990's, and the years 2000-2004) to perform model experiments examining walleye pollock spawning-nursery area connections.

#### 1.5. Model experiment: A year of anomalous transport

The model was run for 1985, a year for which we have data showing anomalous transport patterns of pollock eggs associated with changes in salinity (K. Bailey, Alaska Fisheries Science Center, pers. comm.). The model output matched patterns contained in the empirical data: transport of eggs in a northeasterly direction through the Shelikof Strait. Pollock eggs are usually transported to the southwest through Shelikof Strait.

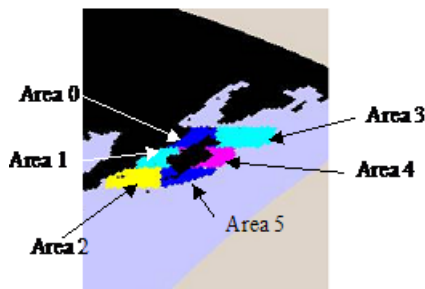


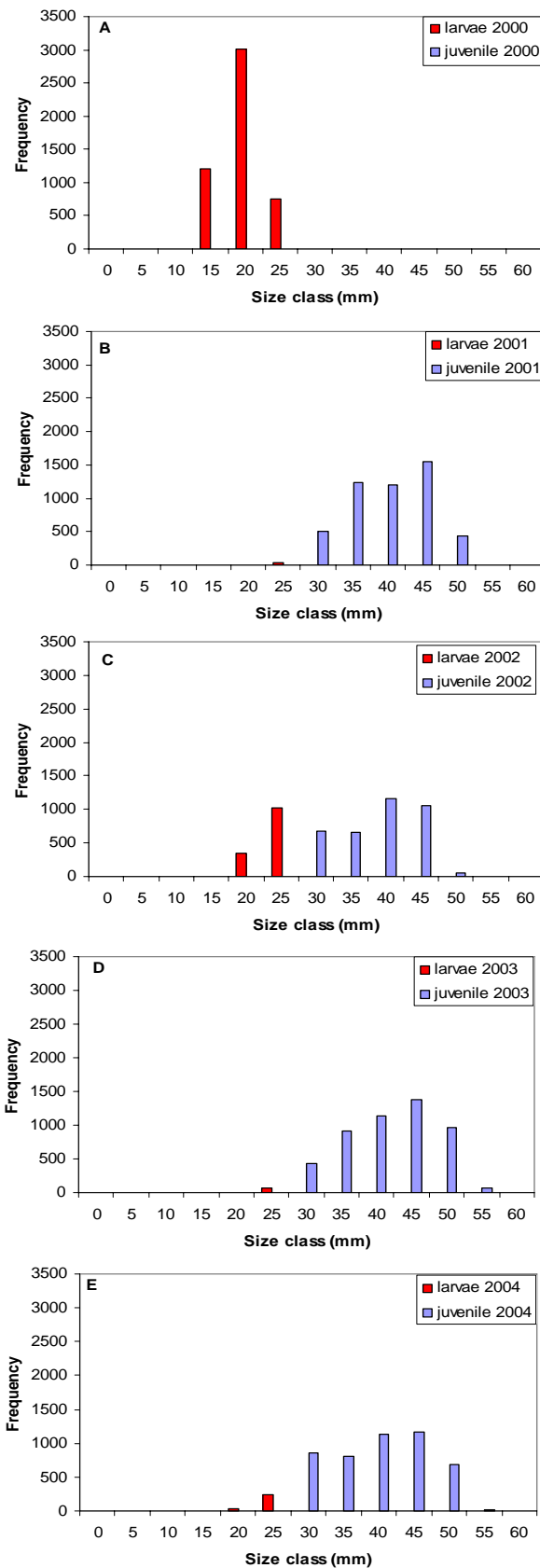
Figure 1.6. Locations of egg release in initial spawning-nursery area experiment. Areas are located around Kodiak Island.

#### 1.6. Initial spawning-nursery areas experiment and parameter testing

A second series of simulations was performed to study the relationship between spawning and nursery areas for the years 2000-2004. Eggs were randomly released in six areas in Shelikof Strait and around Kodiak Island (Fig. 1.6). The eggs were released at an average depth of 200 m, or at the bottom when depth was shallower than 200 m. The period of egg release was between 1st March and 1st April assuming a normal distribution.

Five years of ROMS output were used to provide the physical flow fields in the IBM for this experiment. A dynamic prey source was not used. A constant consumption function based on weight was used to regulate development of larvae and juvenile fish. The number of individual floats released each year was 5000. We also used the superindividual approach in the model, where each superindividual modeled represented a cohort of fish (as above) with the number proportional to the egg production for that year (given by stock assessment model values). These superindividuals were subject to a daily natural mortality caused by predation. The simulation duration was 3 months (i.e. early March until early June). At the end of the simulation, the trajectory, destination, stage (feeding larvae or juvenile), size, and count (representing the number that survived for each superindividual) were tabulated.

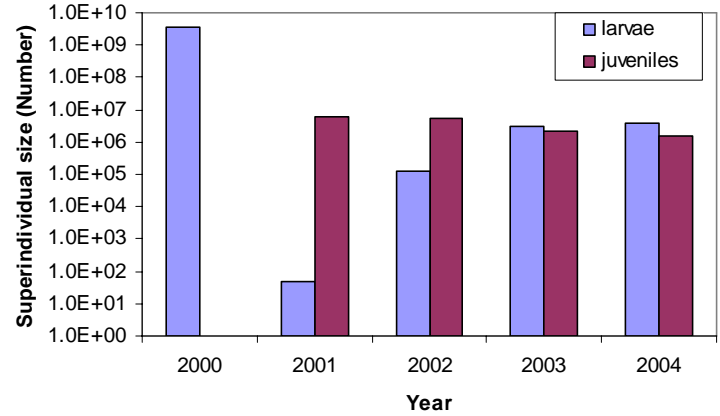
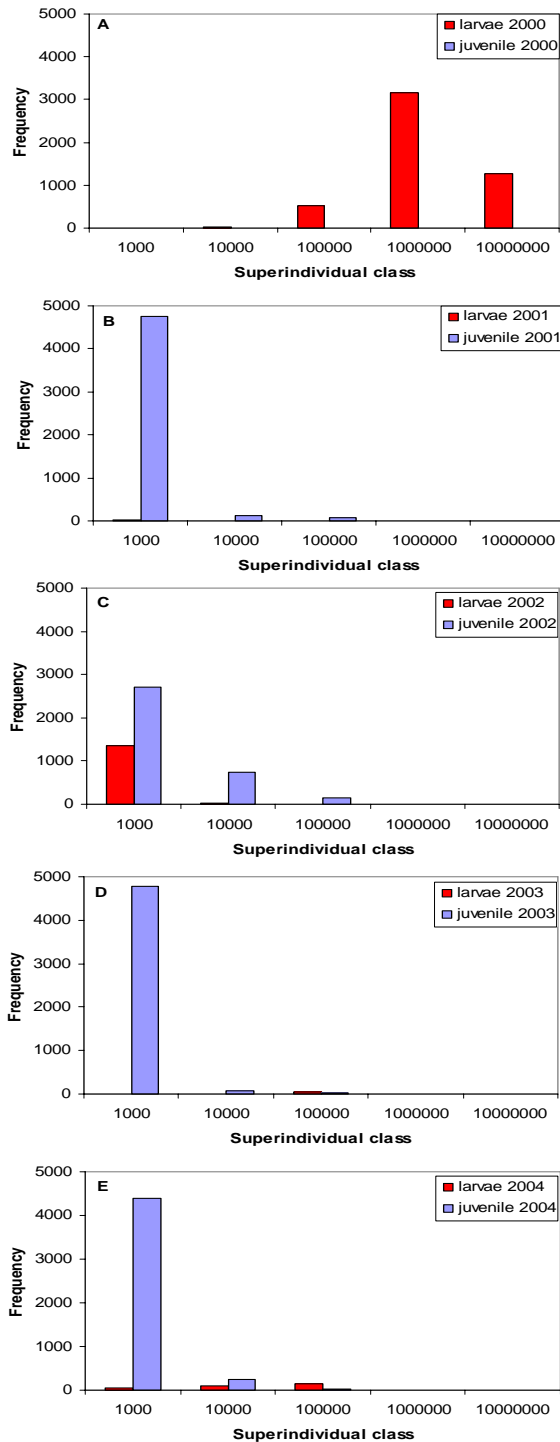
Figure 1.7 (right). Final length frequency histograms for annual simulations. The 5 years of simulations were: A) 2000, B) 2001, C) 2002, D) 2003, E) 2004.



For the year 2000 (Fig. 1.7A) slower growth and development of the individuals was observed compared to the other years, with lengths of larvae at the end of the simulation between 15-25 mm. Simulation results from 2001 and 2003 showed mainly the presence of juveniles with sizes between 30-50 mm. The years 2002 and 2004 contained a wide range of size classes (20-50 mm), with both larvae and juveniles present. The ranked order of growth was 2000<2002<2004<2003<2001.

Figure 1.8. Frequency of superindividual counts for IBM simulations for 5 years A) 2000, B) 2001, C) 2002, D) 2003, E) 2004.

Frequency distributions of the number of fish represented by each superindividual (superindividual counts, Fig. 1.8) showed that during 2000 high counts of larvae ( $10^5$ - $10^7$ ), indicated that superindividuals experienced less mortality than in the other years. In years 2001, 2003 and 2004, the fish surviving to the end of the simulation were mainly juveniles, which had experienced a higher cumulative mortality (i.e. counts of only  $\sim 10^3$  juveniles). At the end of the simulation for year 2002, both larvae and juveniles were present, with superindividual



counts of  $10^3$ - $10^5$  (Fig. 1.8).

The total number of fish that survived (sum of all superindividual counts) for each stage showed that 2000 had the highest number of larvae due to low mortality, but that no juveniles survived due to the low growth rates (Fig. 1.9). The overall number of juveniles for 2001-2004 was very similar. Results from 2001 showed a small number of surviving larvae, with an increasing trend toward

Figure 1.9. Total number of pollock surviving until the end of the simulations for 5 years (2000 to 2004), in larval and juvenile stages.

2004. This may mean that 2004 had the potential to increase the overall abundance of juveniles compared to 2001.

The overall total numbers of surviving individuals by spawning area, showed interannual variability (Table 1.1). For larvae, areas 3 and 5 were the most successful spawning grounds during 2000, with the highest numbers of survivors. In 2001, few or no larvae survived in any area. In 2003 there were no larvae from area 3, and in 2004, there were no larvae observed in area 5. For juveniles in 2001, spawning areas 0, 4, and 5 were the most successful. In 2002,

spawning areas 3 and 5 were successful, and in 2003, area 3 was the most successful in producing juveniles.

Table 1.1A. Overall total numbers by spawning areas for walleye pollock larvae. The spawning areas are shown on Figure 1.6

Area of Origin	Year				
	2000	2001	2002	2003	2004
0	224,222,876	1	43,773	280,681	1,798,595
1	245,389,679	29	54,592	405,584	879,244
2	253,171,175	18	21,595	546,590	901,951
3	1,187,468,054	0	658	0	134,016
4	553,041,453	0	8,985	1,614,660	198,883
5	1,111,716,827	0	663	352,651	0

Table 1.1B. Overall total numbers by spawning areas for walleye pollock juveniles.

Area of Origin	Year			
	2001	2002	2003	2004
0	3,654,715	10,724	126,933	766,683
1	2,142	28,026	285,408	226,894
2	7,848	69,259	183,166	320,126
3	425,255	1,895,301	1,020,924	196,457
4	935,084	749,964	320,562	98,120
5	1,226,132	2,495,944	236,649	18,433

This simulation was not designed to indicate recruitment strength, as it only runs until the beginning of June, and has no dynamic prey source. However, it does tell us that there is significant interannual variability in the number of surviving individuals from the different spawning areas. It also tells us that other regions around Kodiak besides Shelikof Strait may be important to the production of walleye pollock in the GOA. These are both important findings. The next set of simulations included realistic initial conditions for selected years and a wider range of spawning locations.

### 1.7. Addition of bioenergetic and feeding algorithms for juvenile pollock to the IBM

We added a new bioenergetics submodel to the IBM for 0-age juveniles. From the earlier experiments, it was noted that the original version of the juvenile bioenergetic equations resulted in higher than observed growth rates. Ciannelli et al.'s (1998) bioenergetics model performed better relative to the data and was therefore added to our IBM. This model also contained digestion, following Mazur et al. (2007), which was not present in the earlier version.

A feeding model was also added for juvenile pollock. This model was based on field data showing prey preference depending on juvenile walleye pollock size (M. Wilson, AFSC, Seattle, pers. comm), with an increasing shift to euphausiids from copepods as juvenile fish grew. Prey availability, in the absence of the NPZ model, was constant, but proportions of each type (small and large copepods, euphausiids) in each area were based on historical data (M. Wilson, AFSC, Seattle, pers. comm., NPRB Project 308 Final Report). Prey was set to 0 at depths >1000m (ie. off the continental shelf). In the inner shelf areas, the density of euphausiids, small copepods, and large copepods were higher (1.17838, 486.2773, 66.66362 number m<sup>-3</sup>). In the mid and outer shelf and slope areas, prey densities started low (number of euphausiids, small and large copepods were 0.294595, 121.56933, 16.665905 number m<sup>-3</sup>) up to Day of the Year (DOY) 120 and then increased up to DOY 160 (mid June) to the values for the inner shelf; based on NPZ model output for several years (Hinckley, 1999).

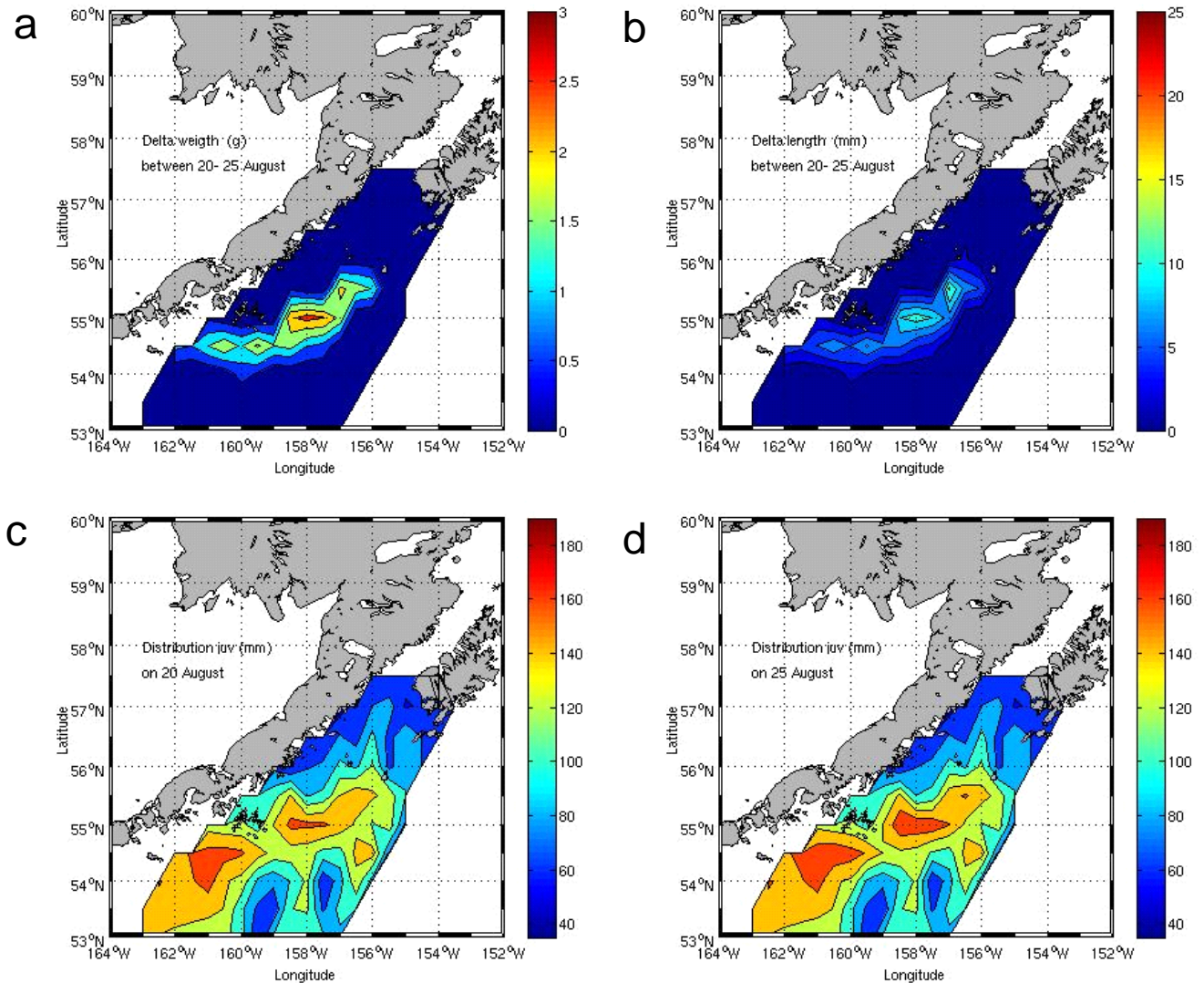


Figure 1.10. Output of the model simulation testing bioenergetics and feeding of juveniles. a. change in weight (g) between August 20-25, b. change in length (mm) between August 20-25, c. distribution of juvenile lengths on 20 August, and d. distribution of lengths on 25 August.

For the simulations to test the bioenergetics and feeding behavior rules, the model was run for 45 days (Aug-Sept), starting with a random distribution of juvenile fish lengths. One thousand individuals were released between Shelikof Strait and the Shumagin Islands. As noted above, the prey distribution had a coast-ocean gradient, with copepods and euphausiids more abundant inshore.

The results of this simulation showed individuals clustered over the outer shelf and slope, with very few transported to the nearshore regions. Figures 1.10a and b show the change in juvenile weight and length in the areas where the fish were found (where delta weight was zero)

from August 20 to August 25. The maximum change in weight in 5 days (Fig. 1.10a) was ~ 3.0 g (ie. ~0.6 g d<sup>-1</sup>), which is reasonable. The spatial distribution of length is shown in Figs. 1.10c (20 Aug.) and 1.10d (25 Aug.).

A second test of the new biology incorporated the early life history of pollock (from eggs, to early juveniles) and all of the biological mechanisms (spawning, buoyancy, vertical migration, swimming behavior, growth, mortality, starvation). The objectives of this simulation were to: 1) observe interannual variability in model variables for larvae and juvenile stages, 2) estimate the density of pollock at age-0 based on superindividual features using GIS, and 3) test the configuration to be used for the final connectivity analysis (see Chapter 3).

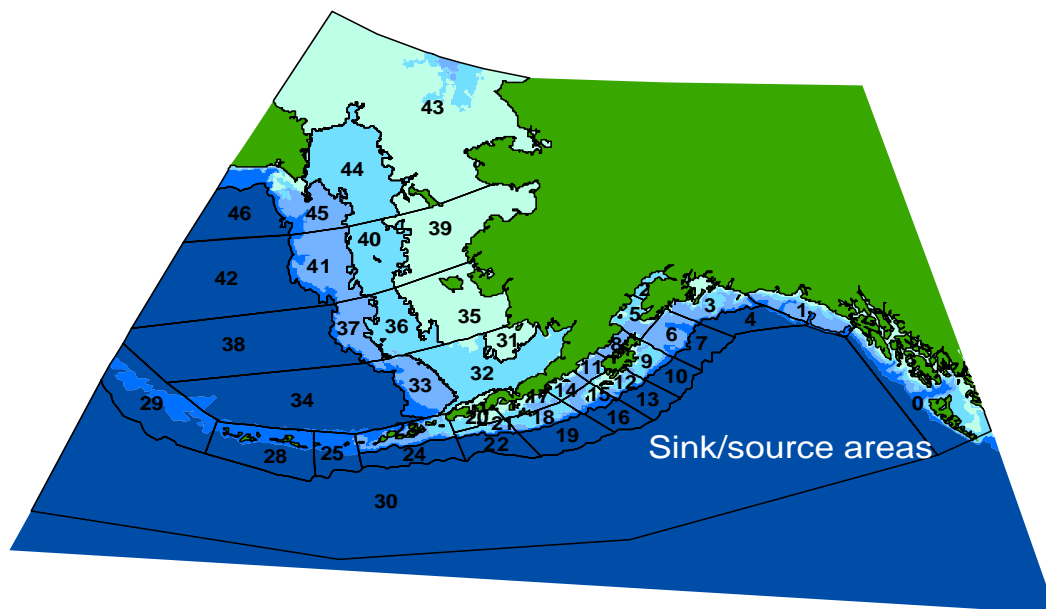


Figure 1.11. Source and sink areas used to build the connectivity matrix. Spawning (source) areas were 2, 3, 5, 6, 8, 9, 11, 12, 14, 15, 17, 18, 20, and 21. Sink areas were 0-46.

For this test, the model was run for the years 2000 to 2004. We released eggs randomly over a broad time period (February-June) over the continental shelf and slope (Prince William Sound (PWS) to the Shumagin Islands) of the GOA. Source and sink areas were defined using GIS to establish a connectivity matrix (Fig. 1.11 and Chapter 3). We released 5000 individuals in 14 spawning areas from PWS to Unimak Pass (Fig.1.12A).

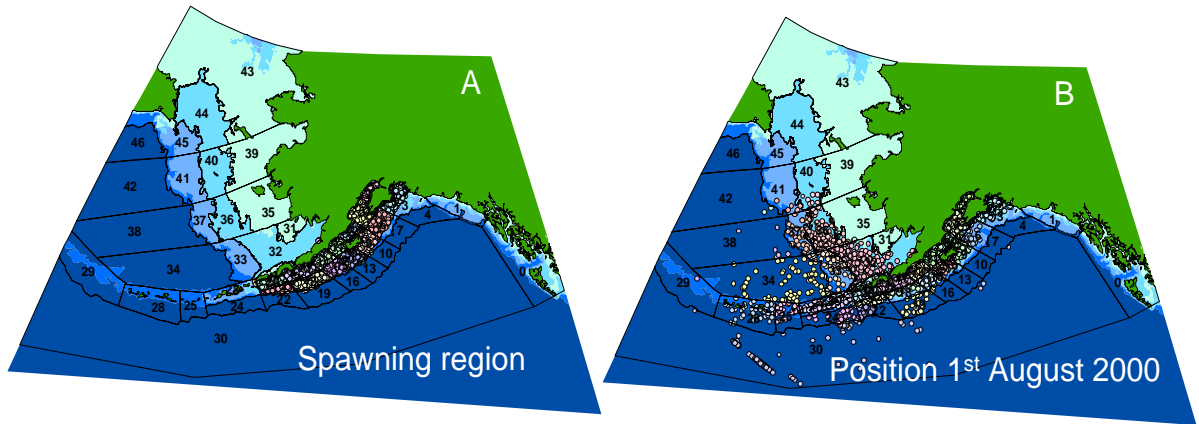


Figure 1.12. A. Regions where modeled pollock eggs were released for the years 2000-2004. B. Positions of particles (corresponding to eggs, yolksac larvae, feeding larvae, and juveniles) during the simulation on 1 August, 2000.

Overall results for this simulation for the years 2000-2004 are shown in Figure 1.13 and 1.14. Larval hatch size and larval first feeding weight modeled values agreed with literature values (Fig. 1.13A, B). Larval first feeding dates occurred in 3 distinct pulses: the first on day 20 of the simulation, between day 40 and day 90, and a third pulse at day 120 of the simulation (Fig. 1.13C). The second pulse

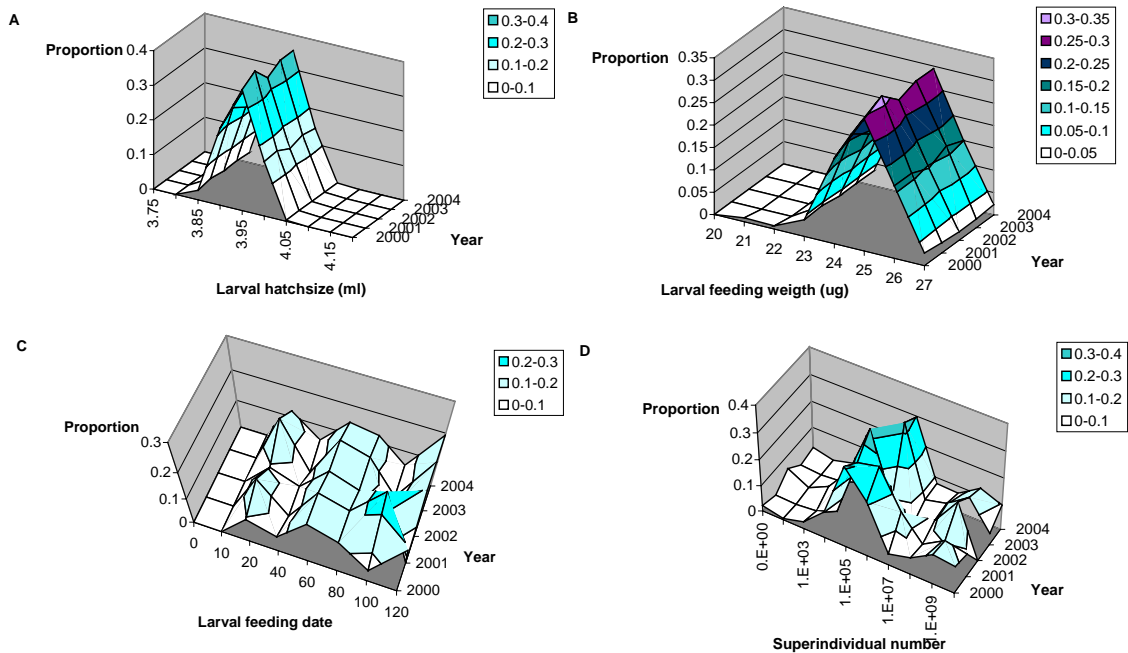


Figure 1.13. Simulation model output testing bioenergetics and feeding of juveniles and new model biology. A. Larval hatch size, B. larval first feeding weight, C. larval first feeding date, D. superindividual number.

corresponded to eggs spawned on days 30 and 60 of the simulation. During 2001 we observed a larger proportion of larvae starting to feed on day 100 (Fig. 1.13C).

The overall number of juvenile survivors was calculated by adding all juveniles that survived through September 30<sup>th</sup> of each year, times the superindividual number. We observed that survival was larger in 2001 compared to the other simulation years. A trend in increasing survival occurred from 2002 to 2004 (Fig. 1.14).

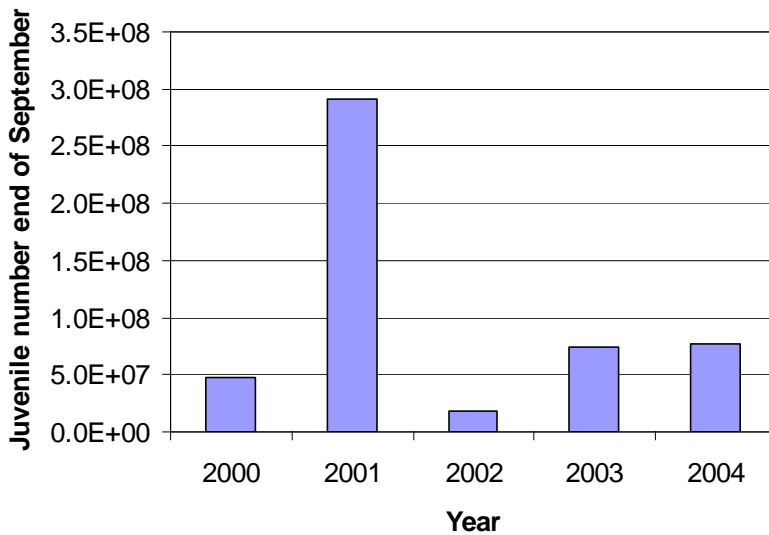


Figure 1.14. Number of juveniles at the end of the simulation (30<sup>th</sup> September) each year.

## 1.8. Conclusions

Significant methodological advances were made to the coupled model set during this project. We adapted a Java application to our previous pollock IBM which gives us a graphical user interface, makes the model faster and easier to run, and allows us to use ROMS output to provide physical flow fields. Extensive testing of the float tracking algorithm gave us confidence that the simplest method (Euler) would be adequate, if we used a higher number of iterations. The original C code was translated into Java with all the biological mechanisms that were included in the original model (Hinckley et al., 1996; Megrey and Hinckley, 2001). Important

new features were added to the simulation model: an algorithm to set initial conditions of egg release (spatial and temporal), a superindividual module, a new algorithm to estimate water density, estimates of groundfish predation on 0-age juveniles based on data, and active swimming by juveniles. We also obtained and corrected the ROMS model output for 1978-2004 to use with these model simulations.

We performed several model simulations to test model additions and to simulate particular phenomena, to see how well the model performed. We succeeded in simulating the anomalous transport seen in 1985. In an initial spawning-nursery area experiment and parameter test, we found that the model could simulate significant interannual variability in larval and juvenile length distributions and mortality, and found differences in the success of different spawning areas, including those outside of Shelikof Strait. This test also allowed us to review parameters included in the model.

We did several more tests of juvenile bioenergetics, movement, and feeding modules. The first test, focusing on the early juvenile phase, resulted in reasonable growth of juvenile walleye pollock. The second test included the whole early life history from eggs to juveniles in the fall. We found that larval variables matched values from the literature.

In conclusion, we now have an application which can reliably be used to test the main hypotheses of this project about spawning and nursery area connectivity.

#### 1.9. Literature Cited

Bartsch, J. and S. Coombs. 2004. An Individual-Based Model of the early life-history of mackerel (*Scomber scombrus*) in the eastern North Atlantic, simulating transport, growth and mortality. *Fisheries Oceanography*, 13: 365-379.

Ciannelli, L., R.D. Brodeur and T.W. Buckley. 1998. Development and application of a bioenergetics model for juvenile walleye pollock. *Journal of Fish Biology*, 52:879-898.

Curchitser, E.N., D.B. Haidvogel, A.J. Hermann, E.L Dobbins, T.M. Powell and A. Kaplan. 2005. Multi-scale modeling of the North Pacific Ocean: Assessment and analysis of simulated basin-scale variability (1996-2003). *Journal of Geophysical Research. C. Oceans* 110(C11), [np].

Dorn, M., Aydin, K., Barbeaux, S., Guttormsen, M., Megrey, B., Spalinger, K. and M. Wilkins. 2005. Assessment of walleye pollock in the Gulf of Alaska In: Appendix B. Stock assessment and fishery evaluation report for the Groundfish Resources of the Gulf of Alaska, North Pacific Fishery Management Council, P.O. Box 103136, Anchorage, AK 99510.

Haidvogel, D.B., H.G. Arango, K. Hedstrom, A. Beckmann, P. Malanotte-Rizzoli, P. and A.F. Shchepetkin. 2000. Model evaluation experiments in the North Atlantic Basin: Simulations in nonlinear terrain-following coordinates, *Dynamics Atmosphere Oceans* 32: 239-281.

Hermann, A.J., Hinckley, S., Megrey, B.A. and P.J., Stabeno. 1996a. Interannual variability of the early life history of walleye Pollock near Shelikof Strait as inferred from a spatially explicit, individual-based model. *Fish Oceanogr* 5(Suppl.1):39-57.

Hermann, A.J., Rugen, W.C., Stabeno, P.J., and N.A., Bond. 1996b. Physical transport of young pollock larvae (*Theragra chalcogramma*) near Shelikof Strait as inferred from a hydrodynamic model. *Fish Oceanogr* 5(Suppl.1):58-70.

Hermann, A.J. and P.J., Stabeno. 1996. An eddy-resolving model of circulation on the western Gulf of Alaska shelf. 1. Model development and sensitivity analyses. *J Geophys Res* 101(CI): 1129-1149.

Hermann, A.J., Hinckley, S., Megrey, B.A. and J.M., Napp. 2001. Applied and theoretical considerations for constructing spatially explicit individual-based models of marine larval fish that include multiple trophic levels. *ICES J Mar Sci* 58:1030-1041.

Hinckley, S., Hermann, A.J. and B.A. Megrey, 1996. Development of a spatially-explicit, individual-based model of marine fish early life history. *Marine Ecology Progress Series*, 139: 47-68.

Hinckley, S. 1999. Biophysical mechanisms underlying the recruitment process in walleye pollock (*Theragra chalcogramma*). PhD dissertation, University of Washington, Seattle. 258 pp.

Hinckley, S., Hermann, A.J., Mier, K.L. and B.A., Megrey. 2001. Importance of spawning location and timing to successful transport to nursery areas: a simulation study of Gulf of Alaska walleye pollock. *ICES J Mar Sci* 58:1042-1052.

Mazur, M.M., M.T. Wilson, A.B. Dougherty, A. Buchheister and D.A. Beauchamp. 2007. Temperature and prey quality effects on growth of juvenile walleye pollock *Theragra chalcogramma* (Pallas): a spatially explicit bioenergetic approach. *Journal Fish Biology*, 70: 816-836.

Megrey, B.A., Bograd, S.J., Rugen, W.C., Hollowed, A.B., Stabeno, P.J., Macklin, S.A., Shumacher, J.D. and W.J. Ingraham. 1995. An exploratory analysis of associations between biotic and abiotic factors and year-class strength of Gulf of Alaska walleye pollock (*Theragra chalcogramma*). In: Beamish RJ (ed) *Climate change and northern fish populations*. *Can Spec Pub Fish Aquat Sci* 121:227-243.

Megrey, B.A. and S. Hinckley. 2001. Effect of turbulence on feeding of larval fishes: a sensitivity analysis using an individual-based model. *ICES Journal of Marine Science* 58: 1015-1029.

Moore, J. K., D.M. Doney, C. Scott, and K. Lindsay, 2004. Upper ocean ecosystem dynamics and iron cycling in a global three-dimensional model. *Global Biogeochemical Cycles* 18, [np].

Scheffer, M., J.M. Baveco, D.L. DeAngelis, K.A. Rose and E.H. Van Nes. 1995. Super-individuals: a simple solution for modelling large populations on an individual basis. *Ecological Modeling*, 80: 161–170.

Shchepetkin, A.F. and J.C. McWilliams. 2005. The Regional Ocean Modeling System: A split-explicit, free-surface, topography-following coordinate ocean model, *Ocean Modeling*, 9: 347-404.

## **CHAPTER 2: Empirical corroboration of IBM-predicted walleye pollock (*Theragra chalcogramma*) spawning-nursery area transport and survival in the Gulf of Alaska**

**(Draft Manuscript – Citation is not allowed without author permission)**

C. Parada<sup>a,c</sup>, S. Hinckley<sup>b</sup>, J. Horne<sup>c</sup>, M. Mazur<sup>a</sup>

<sup>a</sup>*Joint Institute for the study of Atmosphere and Ocean (JISAO) University of Washington, Box 355672, Seattle, WA 98195*

<sup>b</sup>*Alaska Fisheries Science Center, National Oceanographic and Atmospheric Administration (NOAA), 7600 Sand Point way NE, Seattle, WA, 98115*

<sup>c</sup>*School of Aquatic and Fishery Sciences, University of Washington, Box 355020, Seattle, WA, 98195*

### **2.1. Introduction**

Understanding the role of nursery areas in the recruitment of marine fish populations enables fisheries managers to target conservation efforts and improve management decisions that preserve diversity and protect natural resources. Even though the term “nursery area” is broadly used in the ecological literature, there is not a consistent definition. The term nursery area was first applied by Harden Jones (1968) to describe the movement by fish species with complex life cycles and larval stages that are transported to estuarine systems where they grow and then move to adult habitats (Deegan, 1993). Beck et al. (2001) reviewed the role of nursery areas for marine fish and invertebrates and defined the term as an area where the contribution per unit area to the production of recruits to the adult populations is greater, on average, than production from other regions in which juveniles occur. In their definition, nursery habitats must support an important contribution to adult recruitment which result from any combination of factors such as density, growth, survival of juveniles, and movement to adult habitat (Beck et al., 2001). We assume herein that nursery areas are habitats characterized by high growth, density, and survival of juveniles.

Walleye pollock is an important fishery in the Gulf of Alaska (GOA), and has a life history where spawning and nursery habitat are separated. Currents in the region where pollock spawn are advective, but information on the location and relative importance of spawning and nursery areas in the GOA is limited, as surveys do not cover all spawning and nursery areas every year. Historically, a majority of walleye pollock spawning was located between Kodiak Island and the Alaska Peninsula in an area known as Shelikof Strait (Fig. 2.1; Kendall et al., 1987; Schumacher and Kendall, 1991). Positively buoyant eggs are released between mid-March and early May in this area, with peak spawning at the beginning of April. By May, early larvae are advected southwest in the Alaska Coastal Current (ACC) along Alaska Peninsula. By summer and through

early fall, juveniles arrive at the Shumagin Islands nursery area (Hinckley et al., 1991; Spring and Bailey 1991; Wilson et al., 1996; Hinckley et al., 2001). The Shumagin Islands region was proposed to be the nursery area that ensures success of the GOA walleye pollock population (Hinckley et al., 1991; Wilson et al., 1996). More recently, other potential spawning and nursery areas have been reported (Bailey et al., 1999; Wilson, 2000; Mazur et al., 2007), but their relative contribution to the GOA population is not known. Ciannelli et al (2007) discuss the relative importance and stability of spawning areas over time. Spatial and temporal variability in spawning and variability in current flows may determine arrival at and use of nursery habitat in GOA and explain some of the variability in walleye pollock recruitment.

A suite of biophysical models consisting of an individual-based model (IBM) coupled to a hydrodynamic model, can be used to assess which GOA areas have the potential to be nursery areas for juvenile walleye pollock. The spatially-explicit and Lagrangian features of biophysical models allow tracking of individuals from release locations to destinations and recording of trajectories during this period. Previous efforts using this technique in the GOA were used to explore the life history of walleye pollock (e.g. Hinckley et al., 1996, Hinckley et al., 2001, Megrey & Hinckley, 2001; Hermann et al., 2001) and to examine how biological and physical factors influence recruitment (Parada et al., accepted).

The utility of IBM models to assess the potential connectivity between spawning and nursery areas has not been determined. Can this set of coupled models reproduce distributions of different life stages of walleye pollock, including the juvenile nursery areas, observed during a year with surveys of spawning adults, larvae, and September 0-age juveniles? If so, then we should be able to use the model to examine connections between spawning and nursery areas. If we randomly scatter pollock eggs over the known range of pollock spawning in the GOA, and tabulate locations and abundances of juveniles at the end of the simulation, do distribution and abundance patterns resemble what we have observed? This study examines spatial and temporal coincidence between model outputs and observed distributions of walleye pollock successive life stages in the GOA during a single year (1987), and analyzes modeled nursery areas as compared to observed ones in the GOA.

## 2.2. Methods

### 2.2.1 *Hydrodynamic model*

The biophysical model couples the Regional Ocean Modeling System (ROMS) circulation model with an individual based model (IBM) of walleye pollock life history. ROMS is a free-surface, hydrostatic primitive equation, ocean circulation model that employs a nonlinear stretched vertical coordinate to follow the bathymetry. Horizontal space is discretized using orthogonal curvilinear coordinates on an Arakawa C grid. Numerical details can be found in Haidvogel et al. (2000), Moore et al. (2004), and Shchepetkin and McWilliams (2005). Within the ROMS model, water current and temperature resolution in the Gulf of Alaska (GOA) was set at 10 km using the Northeast Pacific (NEP) grid (Fig. 1.2, see Curchitser et al. (2005) for physical model details). First, 1987 was simulated, for the purposes of model comparison to data. Then six more years were simulated to examine whether the model was capable of replicating observed juvenile nursery areas in an average sense (ie. over more than year) using 3 years prior to (1978, 1982, 1988) and 3 years after (1992, 1999, 2001) the shift in the control of recruitment in the GOA from Bailey's hypothesis (Bailey, 2000). The ROMS simulations were run with forcing (winds, freshwater runoff, and boundary conditions) appropriate for each year. The hydrodynamic model produces daily averaged output consisting of salinity and temperature fields, and 3D water velocities, which were used to drive the IBM.

### 2.2.2. *Walleye pollock IBM*

The walleye pollock IBM simulated four development stages (eggs, yolk-sac larvae, feeding larvae, and juveniles) from spawning to the fall of the 0-age year. The IBM of Hinckley et al. (1996) and Megrey and Hinckley (2001) was expanded to include bioenergetic and swimming submodels for juveniles plus coupling to the ROMS model instead of the Spectral Primitive Equation Model (SPEM).

#### 2.2.2.1. Growth and bioenergetic submodels

Mortality and growth were stage-dependent in the IBM and were modeled following Hinckley et al. (1996) and Megrey and Hinckley (2001). Egg development was calculated as a function of age and temperature using 21 development stages (Blood et al., 1994). Eggs hatched when they reached stage 21 and passed into the yolk-sac larval stage. Yolk-sac larval dry weight was a function of standard length (Yamashita & Bailey 1989), which was determined by the egg diameter at hatch (Hinckley 1990). Growth of yolk-sac larvae depended on the number of degree

days experienced, which were accumulated every day post-hatch using temperatures from the physical model for each location and time step. Once the yolk-sac was depleted, if feeding was successful, surviving larvae entered the feeding larvae stage and a feeding probability was calculated at each time step. Predation mortality mechanisms are described in section 2.2.2.2. Dry weight of feeding larvae depended on assimilation efficiency (Houde, 1989), consumption (modified from MacKenzie et al., 1990), and daily respiration rate (Yamashita and Bailey, 1989). Feeding rules and the transition from first feeding to feeding larvae were modeled according to Hinckley, 1999.

Prey consumption by juveniles was estimated utilizing the foraging model for planktivorous fish implemented by Ciannelli et al. (1998) (Tables 2.1 and 2.2), which was developed by Bevelhimer and Adams (1993), evaluated by Stockwell and Johnson (1997), and subsequently field tested by Stockwell and Johnson (1999). For a full description of this modeling approach, see Eggers (1977) and Stockwell and Johnson (1997, 1999).

A Gerritsen and Strickler (1977) encounter rate model, as simplified by Evans (1989), was used to estimate the number of each prey type encountered by juvenile pollock per time step (Eggers, 1977). We assumed that the visual field of foraging pollock was uniform within the search volume and did not attempt to account for differences in prey position within the visual field (Mazur and Beauchamp 2006). Reaction distance (cm) was set constant for daytime feeding and juvenile pollock were only allowed to feed during lighted periods of the diel cycle. *In situ* observations of juvenile pollock feeding confirmed that little feeding occurs outside of lighted periods (Mazur et al. 2007). Prey consumption estimates per time step were generated using a functional response based on prey encounters rather than weight (cf. Bevelhimer & Adams 1993, Stockwell & Johnson 1997). The prey field constructed for the model was based on associations of small copepods, large copepods, and euphausiids with bathymetry from field data collected during 2000 and 2001 cruises (see Table 2.3).

Consumption of each prey type was partitioned based on walleye pollock body length relative to prey length, and summed to estimate the total number of each prey type potentially available for consumption per hour (Table 2.3). Prey consumption was not allowed to exceed the theoretical maximum daily consumption (C-max) for pollock of each length as estimated by the bioenergetics model (Hanson et al.; 1997; Ciannelli et al., 1998). Consumption of prey during each time step only occurred when the stomach was not full following digestion.

The bioenergetics of juvenile walleye pollock was based on Ciannelli et al.'s, (1998) model modified for spatially-explicit requirements. Energy consumed (C) was allocated between metabolism (R), egestion (F), excretion (U), and growth (G) (Hewett and Johnson, 1992):

$$C=R+F+U+G \quad (1)$$

Digestion was modeled hourly (Elliott and Pearson 1978) using walleye pollock evacuation rates from Merati & Brodeur (1996) and Mazur et al. (2007). Numbers of each potential prey type were converted to weights and added to the ration based on available stomach capacity and prey preference. Net growth was estimated using the bioenergetics model and the amount of available prey energy digested on an hourly time step (Stockwell and Johnson 1997). Net growth estimates (mass, g) were updated each time step and converted to growth in length (mm) for use in subsequent time steps.

#### 2.2.2.2. Mortality submodel

The daily probability of survival for eggs, yolk-sac larvae, feeding larvae, and juveniles is characterized as an exponential function dependent on the instantaneous daily mortality rate at the respective stage. This submodel assumed that each particle represented a batch of eggs released in a spawning area. Computational constraints restricted the maximum number of particles to 5000 per simulation. Simulations run with a larger number of particles showed the same retention patterns. To maintain realistic mortality rates within the population, each particle was considered a superindividual made up of many individuals (Scheffer et al., 1995; Megrey & Hinckley, 2001) that grew from eggs to juveniles and subject to stage-specific mortality (Table 2.4). Each superindividual contained an initial number of eggs proportional to the egg production estimated by the walleye pollock stock assessment for that year (Dorn et al., 2005). The number of surviving superindividuals was assessed at each time step. Starvation mortality was also included, by removing those individuals whose weight fell below a stage- and size-specific critical level.

#### 2.2.2.3. Movement submodels

Each batch of individuals that was assigned to a particle which moved according to the  $u$ ,  $v$ , and  $w$  velocity components in a Lagrangian pathway. Particle tracking was based on the Euler method. Particle trajectories were monitored using a Java tool aligned with the ROMS native

grid (Lett et al., 2008) resulting in a unique combination of growth, distribution, and survival for each superindividual.

Horizontal and vertical movements of individuals were stage specific. The vertical position of each egg depended on the terminal velocity and the vertical component of water velocity,  $w$ , from the ROMS model at each time step. The terminal velocity was calculated using Sundby (1983) when Reynolds numbers (Re) were less than 0.5. Yolksac larvae were assumed to remain at the depth of hatch until first-feeding. Feeding larvae began diel migrations at 6 mm, with swimming speeds a function of length (Kendall et al., 1987; 1994). Larvae reached their maximum depth at midday and minimum depth at dusk. Larvae were deeper in the water column at night compared to crepuscular periods (i.e. dusk or dawn). Horizontal position of eggs and larvae were mainly influenced by the  $u$  and  $v$  components of the fluid field.

New algorithms were developed for vertical and horizontal movements of juveniles and added to the original IBM of Hinckley et al. (1996). Vertical positions of juveniles at each time step,  $Z_{j,t+1}$  (m), were calculated based on the depth at the previous time step ( $Z_{j,t}$ ), the vertical mean velocity ( $w_j$ ), and the time step ( $\Delta t$ ).

$$Z_{j,t+1} = Z_{j,t} + w_j \Delta t \quad (1)$$

The mean magnitude of  $w_j$  depended on the length of walleye pollock juveniles (Table 2.2) and was sampled randomly from a triangular distribution<sup>1</sup> to select a value at each time step. The direction of  $w_j$  (upward or downward) was a random variable. The final depth (m) of each particle at each time step was bounded according to the hour (h) of the day in a 24 hour cycle (Equations 2 to 6).

$$h < 2 \quad 40 < Z_{j,t+1} < 60 \quad (2)$$

---

<sup>1</sup> The triangular distribution is a continuous probability distribution with lower limit a, mode c and upper limit b.

$$f(x|a, b, c) = \begin{cases} \frac{2(x-a)}{(b-a)(c-a)} & \text{for } a \leq x \leq c \\ \frac{2(b-x)}{(b-a)(b-c)} & \text{for } c \leq x \leq b \\ 0 & \text{for any other case} \end{cases}$$

$$2 < h < 5 \quad 40 < Z_{j_{t+1}} < 110 \quad (3)$$

$$5 < h < 14 \quad 90 < Z_{j_{t+1}} < 110 \quad (4)$$

$$14 < h < 18 \quad 40 < Z_{j_{t+1}} < 110 \quad (5)$$

$$h > 18 \quad 40 < Z_{j_{t+1}} < 60 \quad (6)$$

Horizontal positions of juveniles were determined using a correlated random walk based on Kareiva and Shigesada (1983). We modeled trajectories as a sequence of straight line moves in which juvenile displacement depended on juvenile length. The position of the juvenile superindividual at each time step,  $X_{j_{t+1}}$  and  $Y_{j_{t+1}}$ , depended on the position in the previous time step,  $X_{j_t}$  and  $Y_{j_t}$ , the length of the juvenile  $L_j$ , and the turning angle,  $\alpha_{t+1}$ . Turning angles were measured relative to the previous direction of movement using:

$$\alpha_{t+1} = \alpha_t + \theta_j \quad (7)$$

where  $\alpha_{t+1}$  is the turning angle at time  $t + 1$ ,  $\alpha_t$  was the turning angle at the previous time step, and the angle  $\theta_j$  was chosen from a normal random probability distribution

$$X_{j_{t+1}} = X_{j_t} + L_j \cos(\alpha_{t+1}) \quad (8)$$

$$Y_{j_{t+1}} = Y_{j_t} + L_j \sin(\alpha_{t+1}) \quad (9)$$

### 2.2.3. Model simulations

Two simulation experiments were run to: (1) examine spatial and temporal matching between model predictions and observed distributions of successive life stages of walleye pollock in the GOA during 1987, and to (2) predict potential nursery areas in the GOA using model runs from multiple years.

#### 2.2.3.1. Spatial and temporal matching of model predictions and data

The objective of this experiment was to use the coupled model to hindcast distributions of larvae in May, late larvae and early juveniles in June/July, and later juveniles in August-September for the year 1987. This was during a time period when spawning in Shelikof Strait was the dominant source of eggs and larvae for the GOA. Model output was compared with results from young larval survey distributions from 18 to 29 May of that year, late larvae and young juvenile survey distributions sampled between 18 June and 16 July, and late juvenile

survey distributions from 12 August to 20 September (Hinckley et al., 1991). Initial conditions for the simulation (egg locations) were based on the distribution of walleye pollock eggs found during an April survey (EcoFOCI, Hinckley et al., 1991) in Shelikof Strait. Initial numbers of eggs corresponded to egg production estimates from the 1987 stock assessment (Table 2.5). Eggs were released in Shelikof Strait (area 11 in Fig.1.11). The model was run and the distribution of surviving larvae in May, late larvae and early juveniles in June/July, and later juveniles in August/September was tabulated. The location and timing of each walleye pollock stage was compared to those observed during the surveys.

#### 2.2.3.2. Prediction of potential nursery areas

To identify potential nursery areas (*PNA*) for walleye pollock spawned in the Gulf of Alaska, the IBM was run for a suite of 6 years: 1978, 1982, 1988, 1992, 1999, 2001 (see Section 2.1). Eggs were released in 14 initial spawning areas (Fig. 1.11), identified as potential spawning areas, over 4 months in spring: Feb, Mar, Apr, May, which spans the bulk of known walleye pollock spawning in the GOA (M. Dorn, Alaska Fisheries Science Center, Seattle, WA, pers. comm.). The model was run for all parameter conditions described above, initializing the number of eggs according to the egg production estimates from the stock assessment for each year (Table 2.4). At the end of the simulation year, locations of juveniles at day of the year (DOY) 215 were recorded and *PNA*s were observed based on areas of surviving juvenile concentration.

### 2.3. Results

#### 2.3.1. *Comparison between observed and predicted distributions*

The observed distribution of early walleye pollock larvae in May 1987 showed high densities in a patch east of the Sutwik and Semidi Islands, 130 km downstream of the spawning region in Shelikof Strait (Fig. 2.2a). Although the survey area was restricted (Fig. 2.2b), the model output essentially matches the timing and location of maximum density of early larvae observed. One notable difference was that the predicted distribution showed a larger area of moderately high densities of early larvae to the east of the Semidi Islands. Modeled distributions of late larval and early juvenile walleye pollock in June and July, 1987 were concentrated between the Semidi and the Shumagin Islands (Fig. 2.2c). The survey data contained high density peaks in the same area (Fig. 2.2d) during this period, and also showed walleye pollock to the east of this region. The modeled distribution of later 0-age juvenile walleye pollock in August and

September in the GOA was located around the Shumagin Islands (Fig. 2.2e) with highest densities to the east of the Shumagin Islands. Maximum densities in the survey data were found to the west of the Shumagins (Fig. 2.2f), not far west of the peak of the modeled densities. The model predicted no significant numbers of walleye pollock juveniles to the east of this general area, however small areas of concentration near Sutwik Island and on the northeast side of Kodiak Island were seen in the data. The survey data (Fig. 2.2f) indicated that juvenile walleye pollock were found in Unimak Pass, possibly transiting to the Bering Sea. The modeled distribution at this time (Fig. 2.2e) indicated movement of juveniles to the Bering Sea. In summary, the model predicted the timing and locations of different life stages of walleye pollock released from Shelikof Strait that matched those observed in the 1987 survey data, with minor location differences.

To examine whether modeled walleye pollock juveniles that ended up in the area to the east of the Shumagin Islands (area 17, Fig. 1.11) could have been spawned in regions other than Shelikof Strait, we examined the spawning location of all surviving juveniles in area 17 during 1987 (see Figure 1.11 for source-sink regions). The number of fish that arrived in area 17 from each potential spawning area for all fish spawned in March is shown in Figure 2.3a. The majority of surviving juveniles were released in area 6, offshore from the Kenai Peninsula between Prince William Sound and Kodiak Island. Smaller numbers originated in Areas 9 (east of Kodiak Island), 11 (Shelikof Strait), 12 (southeast of Kodiak Island) and Area 15 (Trinity Island region). Of those fish released in April (Fig. 2.3b), the major contributors to surviving juveniles were Areas 6, 9, 11 and 12. The Shelikof Strait spawning contribution to area 17 was predicted to be more important in March, when spawning actually occurs, than in April. In this model experiment, fish were released in a stratified random manner over a broad geographic range within the GOA; we interpret these results as illustrating where fish “could” have been spawned.

### *2.3.2. General patterns of juvenile pollock nursery areas*

The distribution of surviving juveniles modeled for 1987, from simulations using particles released from 14 spawning areas in the GOA during March, April and May is summarized in Figure 2.4a. The model domain was subdivided into three main distributional areas: Gulf of Alaska (GOA), Aleutian Islands (AL), and Bering Sea (BS). A surprising result (Fig. 2.4b) was the concentration of juvenile walleye pollock in the central and southern Bering Sea (Areas 33, 34, 36, 37, 38, 41, see Fig. 1.11) that were spawned in the GOA. The overall

percentage of GOA spawned fish found on DOY 215 in the BS was 67.7%. The main area for surviving juveniles in the GOA was the east Shumagin Island region (area 17, Fig. 1.11). Other areas of concentration in the GOA during 1987 included the area northeast of Kodiak Island, and near the Semidi Islands (Fig. 2.4b). Overall, 20% of GOA spawned fish remained in the GOA. The AL region (area 28) contained moderately high densities of surviving juveniles comprising 12.3% of the original number spawned in the GOA.

*PNA*s varied in location among the six simulation years. The Semidi and Shumagin Islands areas had consistent high concentrations of juvenile walleye pollock in all years, especially in 1978, 1982, 1988 and 2001 (Fig. 2.5). Northeast and southeast of Kodiak appear to be important *PNA*s in 1978, 1992, and 2001. The BS is a recurring *PNA* with high densities of surviving juveniles during all years, although it was less important in 1988 and 1999, when juvenile densities were lower there compared to the GOA and the AL. Concentrations of juvenile walleye pollock were predicted to occur in the AL region during 1999 and 2001. Averaging over all years, the *PNA* pattern was characterized by a large region in the central and southern BS, areas east of Kodiak Island and around the Semidi to Shumagin Islands in the GOA, and one area in the AL (Fig. 2.6).

#### 2.4. Discussion

The location and timing of the maximum densities of early and late larvae, and early juveniles matched the corresponding distributions seen in the 1987 survey data. The location of the maximum density of late juveniles predicted by the model did not exactly match the location of the distribution of late juvenile from the survey data. The surviving late juveniles in the model and the survey data were both found near the Shumagin Islands, but at a finer spatial resolution, the location of the maximum density was west of the Shumagin Islands in the survey data, compared to east of the Shumagins as predicted by the model. However, the eastern limit of late juvenile distribution, ie. to the east of the Shumagin Islands and in a near-coastal band from Wide Bay to Unimak Pass were almost identical in both the survey data and model predictions. The agreement between survey data and model predictions based on corresponding data patterns (*sensu* Grimm et al., 2005) demonstrate the ability of this biophysical model suite to predict the location and timing of early life stages of walleye pollock in the GOA. The movement submodel used for juvenile pollock, based on a correlated random walk, produced a distribution of early juveniles that agreed with the survey data. Some improvement of the match between survey data and model predictions could be made by refinements to the swimming algorithm of late juveniles

by including factors such as swimming directionality, however this level of refinement may not be necessary to obtain a good picture of juvenile distribution.

Two other results from the model predictions were striking: 1) the model correctly predicted the Shumagin Islands area as the most consistent potential nursery area in the GOA, and 2) surviving modeled juveniles in the Shumagin Islands could have been spawned in Shelikof Strait during April (the model experiment included spawning areas which were not necessarily observed via surveys for each year). This prediction is consistent with literature studies and confirms the idea of the Shelikof spawning area-Shumagin Island nursery area pair (Hinckley et al. 1991). Model predictions of nursery areas northeast of Kodiak Island and around the Semidi Islands are also supported in the literature. A portion of the fish retained around Kodiak Island (Wilson, 2000), may be advected into the Alaskan Stream and lost from the population (Bailey et al., 1999), or transported to other nursery areas such as the Semidi Islands (Mazur et al., 2007). There is no field evidence to support this speculation other than results from parasite studies that found juvenile walleye pollock found in bays east of Kodiak Island (Fig. 2.1) did not originate in Shelikof Strait, unless there were anomalous currents (Bailey et al., 1999); implying that areas other than Shelikof Strait may serve as spawning areas.

The Bering Sea was predicted to be an important potential nursery (or loss) area. This result has implications for management of walleye pollock in the GOA and the BS as the two are currently managed as separate stocks. This issue, plus an assessment of whether the GOA pollock populations should be managed as a single stock, will be further assessed and discussed in Chapter 3, which describes the full spawning-nursery area connectivity study.

There were potential constraints implied in our combination of the IBM with this physical flow model. One constraint was the limitations of the hydrodynamic model. The ROMS output used in these simulations had a 10 km resolution near the coast and did not accurately characterize physical processes that operated at finer scales. A second potential constraint was the accuracy of the bathymetry and its influence on water movement. Bottom topography in the ROMS model grid used (NEP) was smoothed in some regions (e.g. depths in Shelikof Strait averaged 100 m in the model while actual bottom depths are more like 200 m with some areas of 300 m). This may influence flow patterns in coastal areas. Recent model-data comparisons between the ROMS output and GOA oceanographic data indicate that the ROMS model output includes many circulation features in the northeast Pacific, including variable flow

of the Alaska Coastal Current and sea surface height (Hermann et al., In review). Given the independent validation, we found that the IBM coupled model retained sufficient oceanographic features to allow corroboration of our model predictions with early life history survey data.

## 2.5. Literature Cited

Bailey, K.M., Bond, N.A., Stabeno, P.J., 1999. Anomalous transport of walleye pollock larvae linked to ocean and atmospheric patterns in May 1996. *Fisheries Oceanography* 8: 264-273.

Bailey, K.M. 2000. Shifting control of recruitment of walleye pollock *Theragra chalcogramma* after a major climatic and ecosystem change. *Mar Ecol Prog Ser* 198:215-224.

Beck, M.W., Heck, K.L., Able, K.W. Jr., Childers, D.L., Eggleston, D.B., Gillanders, B.M., Halpern, B., Hays, C.G., Hoshino, H., Minello, T.J., Orth, R.J., Sheridan, P.F., and Weinstein, M.P. 2001. The identification, conservation, and management of estuarine and marine nurseries for fish and invertebrates. *BioScience* 51: 633-641.

Bevelhimer, M.S., S.M. Adams. 1993. A bioenergetic analysis of diel vertical migration by kokanee salmon, *Oncorhynchus nerka*. *Can. J. Fish. Aquat. Sci.* 50: 2336-2349.

Blood D.M., Matarese, A.C., Yoklavich, M.M., 1994. Embryonic development of walleye pollock *Theragra chalcogramma*, from Shelikof Strait, Gulf of Alaska. *Fish. Bull. US* 92, 207-222.

Ciannelli, L., Brodeur, R.D., Buckley, T.W., 1998. Development and application of a bioenergetics model for juvenile walleye pollock. *J. Fish Biol.* 52, 879–898.

Curchitser, E.N., Haidvogel, D.B., Hermann, A.J., Dobbins, E.L., Powell, T., Kaplan, A., 2005. Multi-scale modeling of the North Pacific Ocean: Assessment of simulated basin-scale variability (1996-2003). *J. Geophys. Res.* 110, C11021, doi:10.1029/2005JC002902.

Deegan, L.A., 1993. Nutrient and energy transport between estuaries and coastal marine ecosystems by fish migration. *Can. J. Fish. Aquat. Sci.* 50, 74-79.

De Robertis, A., Ryer, C. H., Veloza, A. and Brodeur, R. D. (2003). Differential effects of turbidity on prey consumption of piscivorous and planktivorous fish. *Canadian Journal of Fisheries and Aquatic Sciences* 60, 1517–1526.

Dorn, M., Aydin, K., Barbeaux, S., Guttormsen, M., Megrey, B., Spalinger, K., Wilkins, M., 2005. Assessment of walleye pollock in the Gulf of Alaska In: Appendix B. Stock assessment and fishery evaluation report for the Groundfish Resources of the Gulf of Alaska, North Pacific Fishery Management Council, P.O. Box 103136, Anchorage, AK 99510.

Dumont, H. J., I. Vande Velde, S. Dumont. 1975. The dry weight estimate of biomass in a selection of cladocera, copepoda and rotifera from the plankton, periphyton and benthos of continental waters. *Oecologia* 19: 75-97.

Eggers, D. M. 1977. Nature of Prey Selection by Planktivorous Fish. *Ecology* 58(1): 46-59.

Elliott, J. M., W. Davison. 1975. Energy equivalents of oxygen consumption in animal energetics. *Oecologia* 19(3): 195-201.

Elliott, J. M., L. Persson. 1978. The estimation of daily rates of food consumption for fish. *J. Anim. Ecol.* **47**: 977-991.

Evans, G.T. 1989. The encounter speed of moving predator and prey. *Journal of Plankton Research.* 11(2): 415-417.

Gerritsen, J., J. R. Strickler. 1977. Encounter probabilities and community structure in zooplankton: a mathematical model. *J. Fish. Res. Bd. Can.* 34: 73-82.

Grimm, V., Revilla, E., Berger, U., Jeltsch, F., Mooij, W.M., Railsback, S.F., Thulke, H., Weiner, J., Wiegand, T. and D.L. DeAngelis. 2005. Pattern-Oriented Modeling of Agent-Based Complex Systems: Lessons from Ecology. *Science*, 310(5750): 987 – 991. DOI: 10.1126/science.1116681

Haidvogel D.B., Wilkin J.L., Young R.E., 1991. A semi-spectral primitive equation ocean circulation model using vertical sigma and orthogonal curvilinear horizontal coordinates. *J. Comput. Phys.* 94,151-185.

Harden Jones, F.R. 1968. Biological aspects of fish migration. Chapter 2 *In: Fish Migration*, Edward Arnold Ltd. London.

Hermann A.J., Stabeno P.J. 1996. An eddy-resolving model of circulation on the western Gulf of Alaska shelf. 1. Model development and sensitivity analyses. *J. Geophys. Res.* 101(CI), 1129-1149.

Hermann, A.J., Curchitser, E.N., Dobbins, E.L., Haidvogel, D.B. 2008. A comparison of remote versus local influence of El Nino on the coastal circulation of the Northeast Pacific. *Deep Sea Research II*, in review.

Hewett, S.W., Johnson, B.L., 1992. Fish Bioenergetics Model 2, an upgrade of ' A generalized bioenergetics model of fish growth for microcomputers. ' University of Wisconsin Sea Grant Technical Report Number WIS-SG-92-250, 79 pp.

Hinckley, S., Bailey, K.H., Picquelle, S.J., Shumacher, J.D., Stabeno, P.J., 1991. Transport, distribution, and abundance of larval and juvenile walleye pollock (*Theragra chalcogramma*) in the western Gulf of Alaska. *Can. J. Fish. Aquat. Sci.* 48, 91-98.

Hinckley S., Hermann A.J., Megrey B.A. 1996. Development of a spatially explicit, individual-based model of marine fish early life history. *Mar. Ecol. Prog. Ser.* 139, 47-68.

Hinckley, S., Hermann, A.J., Mier, K.L., Megrey, B.A., 2001. Importance of spawning location and timing to successful transport to nursery areas: a simulation study of Gulf of Alaska walleye pollock. *ICES J. Mar. Sci.* 58, 1042-1052.

Houde, E.D., 1989. Comparative growth, mortality, and energetic of marine fish larvae: temperature and implied latitudinal effects. *Fish. Bull.* US 87,471-495.

- Kareiva, P.M., Shigesada, N., 1983. Analyzing insect movement as a correlated random walk. *Oecologia*. 56,234-238.
- Kendall, A.W., Clarke, M.E., Yoklavich, M.M., Boehlert, G.W., 1987. Distribution, feeding, and growth of larval walleye pollock, *Theragra chalcogramma*, from Shelikof Strait, Gulf of Alaska. *Fish. Bull.*, US 85,499-521.
- Kendall, A.W., Incze, L.S., Ortner, P.B., Cummings, S.R., Brown, P.K., 1994. The vertical distribution of eggs and larvae of walleye pollock (*Theragra chalcogramma*) in Shelikof Strait, Gulf of Alaska. *Fish. Bull.* US 92,540-554.
- Lett, C., Verley, P., Mullon, C., Parada, C., Brochier, T., Penven, P., Blake, B., (2008). A Lagrangian tool for modelling ichthyoplankton dynamics. *Environmental Modelling & Software*, 23(9):1210-1214.
- Link J., T. A. Edsall. 1996. The effect of light on lake herring (*Coregonus artedii*) reactive volume. *Hydrobiologia* **332**: 131-140.
- MacKenzie, B.R., Leggett, W.C., Peters, R.H., 1990. Estimating larval fish ingestion rates: can laboratory derived values be reliably extrapolated to the wild? *Mar. Ecol. Prog. Ser.* 67, 209-225.
- Mazur, M. M., D. A. Beauchamp. 2006. Linking piscivory to spatial-temporal distributions of pelagic prey fishes with a visual foraging model. *Journal of Fish Biology* **69**: 151-175.
- Mazur, M.M., Wilson, M.T., Dougherty, A.B., Buchheister, A, Beauchamp, D.A., 2007. Temperature and prey quality effects on growth of juvenile walleye pollock *Theragra chalcogramma*: a spatially explicit bioenergetics approach. *J. Fish. Biol.* 70, 816-136.
- Megrey, B.A., Hinckley, S. 2001. Effect of turbulence of larval fishes: a sensitivity analysis using an individual-based model. *ICES J. Mar. Sci.* 58,1015-1029.
- Merati, N. & Brodeur, R. D. (1996). Feeding habits and daily ration of juvenile walleye pollock, *Theragra chalcogramma*, in the western Gulf of Alaska. In *Ecology of juvenile walleye pollock, Theragra chalcogramma* (Brodeur, R. D., Livingston, P. A., Loughlin, T. R. & Hollowed, A. B. eds), pp.65-79. U.S. Department of Commerce, NOAA Technical Report NMFS 126.
- Parada, C., Hinckley, S., Horne, J., Dorn, M., Hermann, A., Megrey, B. Comparing simulated walleye pollock recruitment indices to data and stock assessment models from the Gulf of Alaska. Accepted. *Mar. Ecol. Prog. Ser*
- Scheffer, M., Baveco, J. M., DeAngelis, D. L., Rose, K. A., Van Nes, E. H. 1995. Super-individuals: a simple solution for modelling large populations on an individual basis. *Ecol. Mod.* 80, 161-170.
- Schumacher, J.D., Kendall, A.W. Jr., 1991. Some interactions between young pollock and their environment in the western Gulf of Alaska. *Calif. Coop. Oceanic. Fish. Invest. Rep.* 32, 22-40.
- Spring, S., Bailey, K.M., 1991. Distribution and abundance of juvenile pollock from historical shrimp trawl surveys in the western Gulf of Alaska. AFSC Processed Report 91-18, 66p. Alaska Fish. Sci. Cent., Natl. Mar. Fish. Serv., NOAA, 7600 Sand Point Way NE, Seattle WA 98115.

- Sogard, S. M., Olla, B. L. 2000. Endurance of simulated winter conditions by age-0 walleye pollock: effects of body size, water temperature and energy stores. *Journal of Fish Biology* **56**, 1-21.
- Stabeno P.J., Hermann A.J. 1996. An eddy resolving model of circulation on the western Gulf of Alaska shelf. II. Comparison of results to oceanic observations. *J. Geophys. Res.* 101: 1151-1161.
- Stockwell, J.D., Johnson, B.M. 1997. Refinement and calibration of a bioenergetics-based foraging model for kokanee. *Can. J. Fish. Aquat. Sci.* 54: 2659-2676.
- Stockwell, J.D., and B.M. Johnson. 1999. Field evaluation of a bioenergetics-based foraging model for kokanee (*Oncorhynchus nerka*). *Can. J. Fish. Aquat. Sci.* 56(Suppl. 1): 140-151.
- Sundby, S., 1983. A one-dimensional model for the vertical distribution of pelagic fish eggs in the mixed layer. *Deep Sea Res.* 30, 645-661.
- Svetlichny, L.S. and E.S. Hubareva. 2005. The energetics of *Calanus euxinus*: locomotion, filtration of food and specific dynamic action. *Journal of Plankton Research* 27: 671-682.
- Wilson, M.T., Brodeur, R.D., Hinckley, S., 1996. Distribution and abundance of age-0 walleye pollock, *Theragra chalcogramma*, in the western Gulf of Alaska during September 1990. In: Brodeur RD, Livingston PA, Loughlin TR, Hollowed AB (eds) *Ecology of Juvenile Walleye pollock, Theragra chalcogramma*, U.S. Dep. Commer., NOAA Tech. Rep. NMFS 126 p 11-24.
- Wilson, M.T., 2000. Effects of year and region on the abundance and size of age-0 walleye pollock, *Theragra chalcogramma*, in the western Gulf of Alaska, 1985-1988. *Fish. Bull.*, U.S. 98, 823-834.
- Wilson, M.T., Jump, C. and J.T., Duffy-Anderson. 2006. Comparative analysis of the feeding ecology of two pelagic forage fishes: capelin *Mallotus villosus* and walleye pollock *Theragra chalcogramma*. *Marine Ecology Progress Series*, 317: 245-258.
- Winter, A., Swartzman, G., Ciannelli, L., 2005. Early- to late- summer population growth and prey consumption by age-0 pollock, in two years of contrasting pollock abundance near the Pribilof Islands, Bering Sea. *Fisheries Oceanography*. 14(4): 307-320.
- Yamashita, Y., Bailey, K.M., 1989. A laboratory study of the bioenergetics of larval walleye pollock, *Theragra chalcogramma*. *Fish. Bull.* US 87,525-536.

## 2.6. Tables

Table 2.1. Variables of the bioenergetic model used for juvenile walleye pollock. (Ciannelli et al. 1998)

Variables of bioenergetic model	Functions
<i>Consumption</i>	$C = A_c \cdot W^{B_c} f(T)P$ $f(T) = V^X e^{(X(1-V))}$ $V = (T_{cm} - T)/(T_{cm} - T_{co})$ $X = (Z^2(1 + (1 + 40/Y)^{0.5})^2 / 400$ $Z = \ln(Q_c)(T_{cm} - T_{co})$ $Y = \ln(Q_c)(T_{cm} - T_{co} + 2)$
<i>Respiration</i>	$R = (A_r W^{B_r} f(T)Am) + D_s(C - F)$ $f(T) = V^X e^{(X(1-V))}$ $V = (T_{rm} - T)/(T_{rm} - T_{ro})$ $X = (Z^2(1 + (1 + 40/Y)^{0.5})^2 / 400$ $Z = \ln(Q_r)(T_{rm} - T_{ro})$ $Y = \ln(Q_r)(T_{rm} - T_{ro} + 2)$ $R_j = R \cdot convj$
<i>Egestion</i>	$F = F_a C$
<i>Excretion</i>	$U = U_a(C - F)$

Table 2.2. Parameters for bioenergetic and feeding model of juvenile walleye pollock.

Parameter description and unit	Symbol	Value	Reference
<b>Consumption (gg-1 day-1)</b>	<i>C</i>		
Proportion of maximum consumption	<i>P</i>	0-2	1
Intercept of the allometric function	<i>Ac</i>	0.38	1
Slope of the allometric function	<i>Bc</i>	0.68	1
Temperature dependence coefficient	<i>Qc</i>	2.6	1
Optimum temperature for consumption (°C)	<i>Tco</i>	10	1
Maximum temperature for consumption (°C)	<i>Tcm</i>	15	1
<b>Respiration (gg-1 O<sub>2</sub> day-1)</b>	<i>R</i>		
Intercept of the allometric function	<i>Ar</i>	0.0075	1
Slope of the allometric function	<i>Br</i>	0.251	1
Temperature dependence coefficient	<i>Qr</i>	2.6	1
Optimum temperature for respiration (°C)	<i>Tro</i>	13	1
Maximum temperature for respiration (°C)	<i>Trm</i>	18	1
Proportion of assimilated energy lost for Specific Dynamic Action	<i>Ds</i>	0.125	1
Multiplier for active metabolism	<i>Am</i>	1	1
Respiration in Joules	<i>Rj</i>		
Conversion from g of oxygen to joules	<i>convj</i>	13560	2
<b>Egestion</b>	<i>F</i>		
Proportion consumed energy	<i>Fa</i>	0.15	1
<b>Excretion</b>	<i>U</i>		
Proportion of assimilated energy	<i>Ua</i>	0.11	1
<b>Digestion (gg<sup>-1</sup> day<sup>-1</sup>)</b>	<i>D</i>		
Stomach capacity			3
Digestion coefficient	<i>dc</i>	0.25	1
Parameters of feeding model			
Pollock swimming speed (m s <sup>-1</sup> )	<i>Pss</i>	0.15	4
Euphausiid swimming speed (m s <sup>-1</sup> )	<i>Ess</i>	0.0285	16
Large copepod swimming speed (m s <sup>-1</sup> )	<i>Lcss</i>	0.01	17
Small copepod swimming speed (m s <sup>-1</sup> )	<i>Scss</i>	0.002	17
Reactive distance (m)	<i>rd</i>	0.1	5
Handling time (seconds prey <sup>-1</sup> )	<i>t<sub>h</sub></i>	0.33	6
Minutes to hours	<i>conv</i>	60	-
Probability of prey preference			
Euphausiids	<i>PpE</i>	0 (size class 1)** 0.1429 (size class 2)**	14 14

		0.8571 (size class 3)**	14
Large copepods	<i>PpLc</i>	0.127 (size class 1)**	14
		0.2381 (size class 2)**	14
		0.6349 (size class 3)**	14
Small copepods	<i>PpSc</i>	0.6481 (size class 1)**	14
		0.32419 (size class 2)**	14
		0.02781 (size class 3)**	14
Mean weight Euphausids (g)	<i>MwE</i>	0.0402	7
Mean weight Large Copepods(g)	<i>MwLc</i>	0.00056743	8
Mean weight Small Copepods(g)	<i>MwSc</i>	0.0001122	8
Energy euphausid	<i>EnE</i>	5949	3
Energy large copepod	<i>EnLc</i>	5319	3
Energy small copepod	<i>EnSc</i>	3040	3
Transferemce energy grams pollock		4050	3

\*\* Size class correspond to 1: 25 <= length < 40, 2: 120 > length >= 40 and 3: length >= 120 juvenile walleye pollock.

<b>Variables of Feeding model</b>	<b>Functions</b>	<b>Reference</b>
<i>Total prey available per juvenile pollock</i>	$Tp = numE \cdot PpE + numLc \cdot PpLc + numSc \cdot PpSc$	9
<i>Number euphausids consumed per hour</i>	$nEch = (SvE \cdot numE \cdot PpE) / (1 + SvE \cdot t_h) \cdot conv$	10, 6
<i>Number large copepods consumed per hour</i>	$nLcch = (SvLc \cdot numLc \cdot PpLc) / (1 + SvLc \cdot t_h) \cdot conv$	10, 6
<i>Number small copepods consumed per hour</i>	$nScch = (SvSc \cdot numSc \cdot PpSc) / (1 + SvSc \cdot t_h) \cdot conv$	10, 6
<i>Weight euphausids consumed per hour</i>	$wEch = nEch \cdot MwE$	
<i>Weight large copepods consumed per hour</i>	$wLcch = nLcch \cdot MwLc$	
<i>Weight small copepods consumed per hour</i>	$wScch = nScch \cdot MwSc$	
<i>Search volume for euphausids</i>	$SvE = PI \cdot rd^2 \cdot sqrt \cdot (Pss^2 + Ess^2)$	11
<i>Search volume for large copepods</i>	$SvLc = PI \cdot rd^2 \cdot sqrt \cdot (Pss^2 + Lcss^2)$	11
<i>Search volume for small copepods</i>	$SvSc = PI \cdot rd^2 \cdot sqrt \cdot (Pss^2 + Scss^2)$	11
<i>Stomach capacity per hour</i>	$Sc = (Sc + Tp) - Dh$	1
<i>Digestion per hour</i>	$Dh = (Sc + Tcons) - ((Sc \cdot e^{-dc}) + \frac{(Tcons)}{dc \cdot (1 - e^{-dc})})$	12, 13

W=weight (g), T=temperature (°C)

(1) Ciannelli et al. (1998), (2) Elliott and Davidson (1975), (3) Mazur et al. (2007), (4) Sogard & Olla (2002), (5) Link & Edsall (1996), (6) Stockwell & Johnson (1997), Winter et al. (2005), (8) Dumont et al. (1979), (9) Eggers (1977), (10) Gerritsen and Strickler (1977), (11) Evans (1989), (12) Elliott & Persson (1978), (13) Bevelhimer & Adams (1993), (14) Wilson et al. (2006), (15) Hinckley, 1999, (16) De Robertis et al. (2003), (17) Svetlichny and Hubareva (2005).

Table 2.3. Values and functions of prey field (num m<sup>-3</sup>) assigned for the feeding model associated to different environmental conditions for juvenile walleye pollock.

Prey category	Variable	Environmental condition	Value (number m <sup>-3</sup> )	Reference
<i>Euphausids</i>	<i>numE</i>	$h < 1000\text{ m}$	1.178	Wilson et al., (2006)
		$h \geq 1000\text{ m}$	None	
		$jd < 120$ **	0.2946	Hinckley, 1999
		$160 \geq jd \geq 120$ **	$numE = 0.0221(jd + \frac{it}{24}) - 2.3566$	Hinckley, 1999
		$jd > 160$ **	0.2946	Hinckley, 1999
<i>Large copepods</i>	<i>numLc</i>	$h < 1000\text{ m}$	66.663	Wilson et al., (2006)
		$h \geq 1000\text{ m}$	None	
		$jd < 120$ **	16.666	Hinckley, 1999
		$160 \geq jd \geq 120$ **	$numLc = 9.1177(jd + \frac{it}{24}) - 972.55$	Hinckley, 1999
		$jd > 160$ **	16.666	Hinckley, 1999
<i>small copepods</i>	<i>numSc</i>	$h < 1000\text{ m}$	486.277	Wilson et al., (2006)
		$h \geq 1000\text{ m}$	None	
		$jd < 120$ **	121.569	Hinckley, 1999
		$160 \geq jd \geq 120$ **	$numSc = 1.2499(jd + \frac{it}{24}) - 133.33$	Hinckley, 1999
		$jd > 160$ **	121.569	Hinckley, 1999

h = bathymetry, jd = julian day, \*\*In the Semidi region see Fig. 2.1.

Table 2.4. Mortality rates for egg, larvae and juveniles of walleye pollock used for IBM experiments.

Year	Daily mortality rates		
	Eggs*	Feeding larvae*	Juveniles**
1987	0.226	0.064	0.00005
1988	0.300	0.036	-
1989	0.170	0.157	-
1990	0.150	0.073	0.01400
1991	0.220	0.126	-
1992	0.184	0.049	-
1993	-	0.038	0.00607
1994	-	0.057	-
1996	-	0.037	0.01076
1999	-	-	0.00157
2001	-	-	0.00353
Other	0.205***	0.0200***	0.00509

\*For egg and larvae daily mortality rates for pollock and methods of calculations, see Bailey et al. 2000, \*\* Juveniles daily mortality was inferred from stomach contents from groundfish consumption and normalized to a maximum mortality, for missing values we used an average of the available data, \*\*\* average values for missing years (Bailey pers. comm.),

Table 2.5. Egg production for stock assessment estimates Dorn et al., (2005) for years of the IBM simulation.

Year	Egg production
1978	$1.593 \cdot 10^{14}$
1988	$1.194 \cdot 10^{14}$
1999	$5.513 \cdot 10^{13}$
1982	$1.677 \cdot 10^{14}$
1992	$8.62 \cdot 10^{13}$
2001	$5.01 \cdot 10^{13}$

2.7. Figures

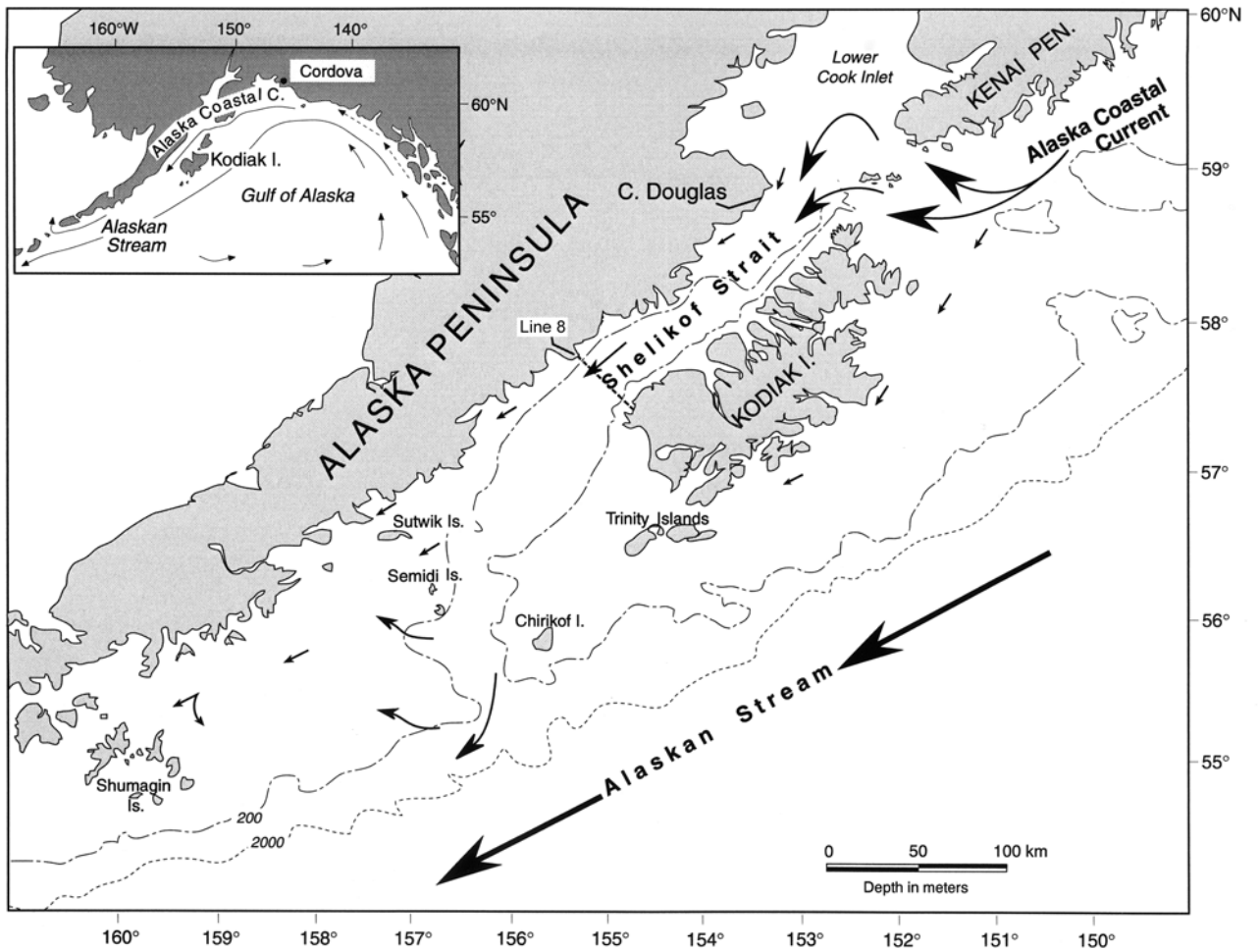


Figure 2.1. The western Gulf of Alaska.

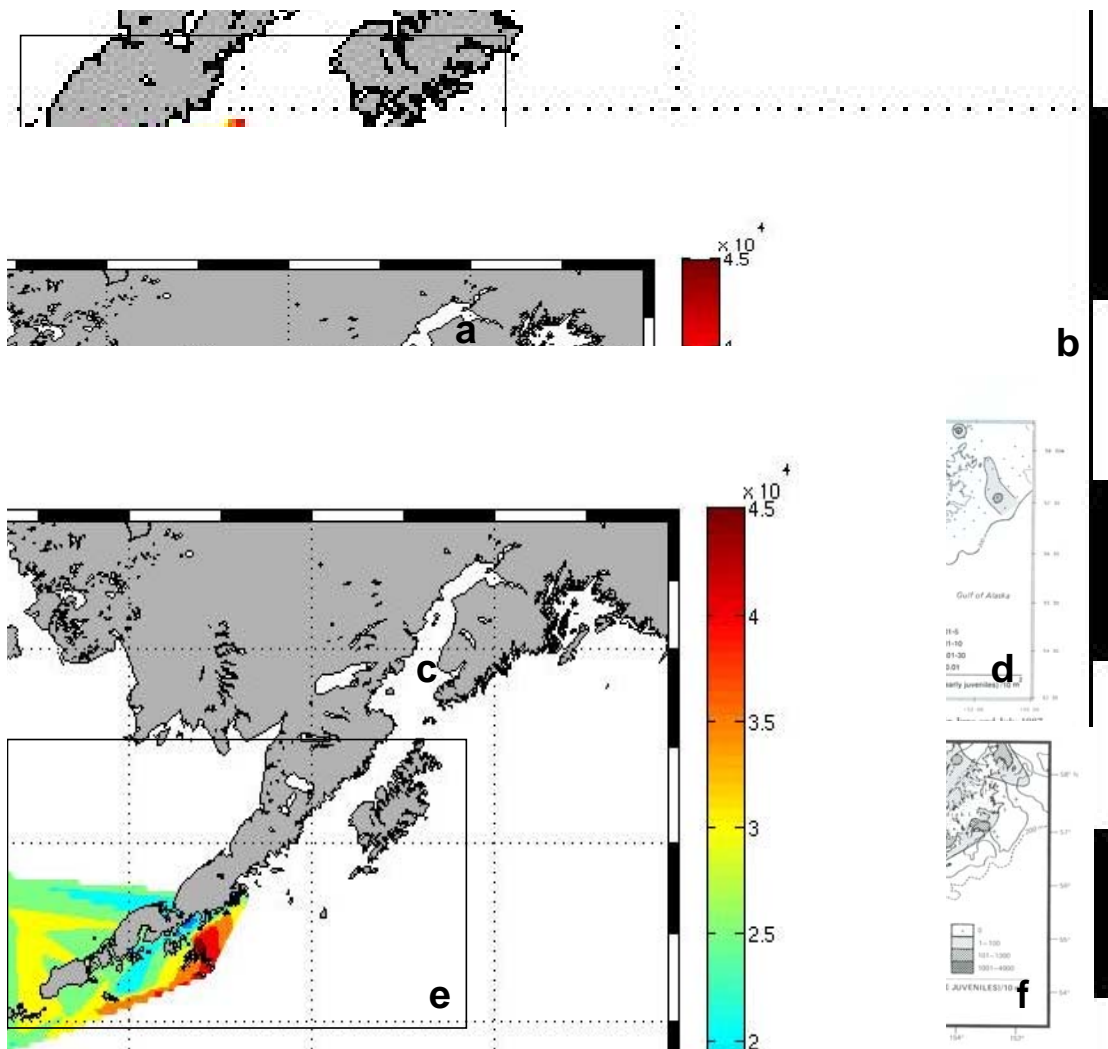


Figure 2.2. Distribution of early walleye pollock larvae in May 1987 a) model and b) data. Distribution of late larval and early juvenile walleye pollock in June and July 1987 c) model and d) data. Distribution of late juvenile walleye pollock in August and September 1987 e) model and f) data. Areas with no larvae are white.

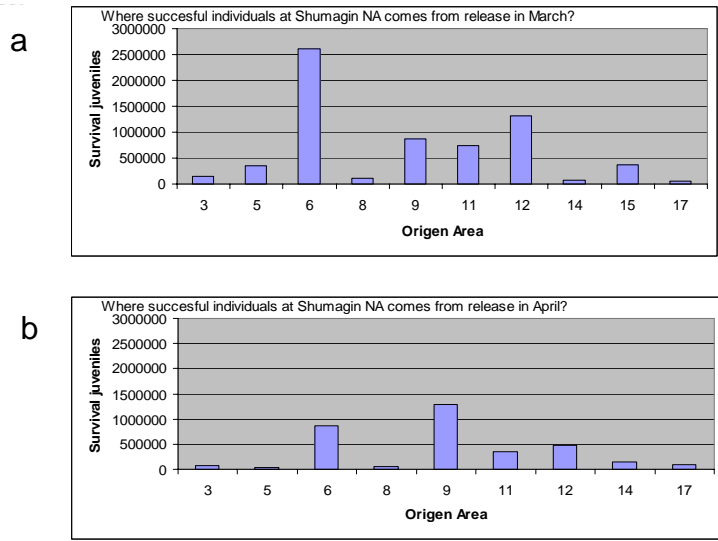


Figure 2.3. Density of juvenile walleye pollock that were found on DOY 215 in area 17 (the east Shumagins) 1987 by spawning region and date of release a) March and b) April.

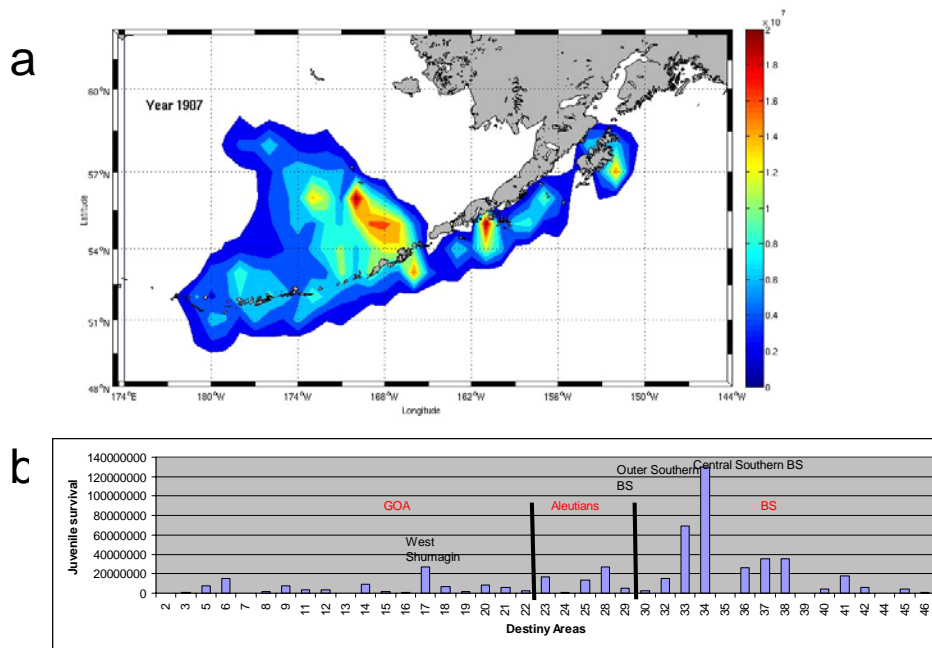


Figure 2.4. a) Contour map of modeled juvenile density at DOY 215 in 1987 showing potential nursery areas through the whole domain. b) Modeled juvenile density at DOY 215 in 1987 discretized by region: Gulf of Alaska (GOA), Aleutians and Bering Sea (BS).

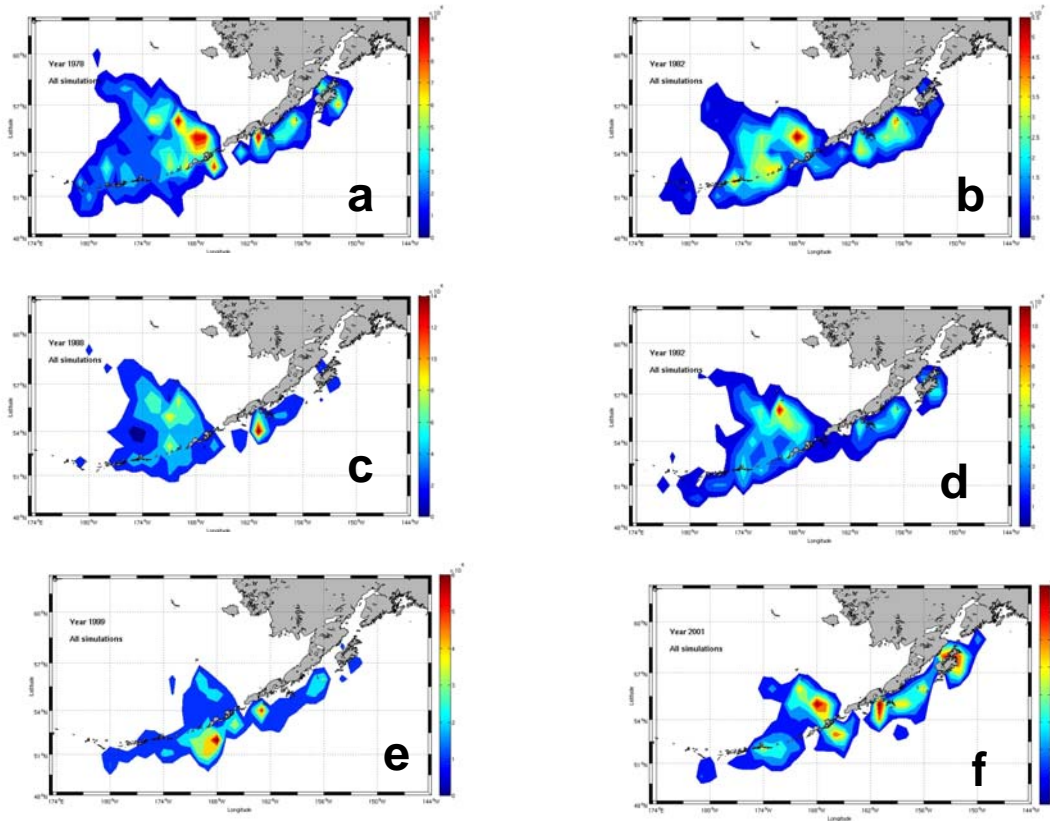


Figure 2.5. a) Contour map of modeled juvenile density on DOY 215 showing potential nursery areas through the whole domain in years a) 1978, b) 1982, c) 1988, d) 1992, e) 1999, and f) 2001.

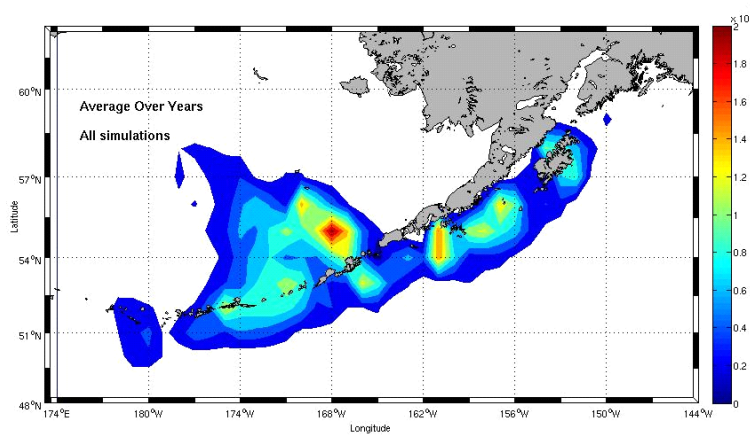


Figure 2.6. Contour map of modeled juvenile density on DOY 215 showing potential nursery areas throughout the whole domain averaged over all years of the simulation.

## **CHAPTER 3: Connectivity of Walleye Pollock (*Theragra chalcogramma*) Spawning and Nursery Areas in the Gulf of Alaska**

**(Draft Manuscript – Citation is not allowed without author permission)**

C. Parada<sup>a,c</sup>, S. Hinckley<sup>b</sup>, J. Horne<sup>c</sup>

<sup>a</sup>*Joint Institute for the Study of Atmosphere and Ocean (JISAO) University of Washington, Box 355672, Seattle, WA 98105*

<sup>b</sup>*Alaska Fisheries Science Center, National Oceanographic and Atmospheric Administration (NOAA), 7600 Sand Point Way NE, Seattle, WA, 98115*

<sup>c</sup>*School of Aquatic and Fishery Sciences, University of Washington, Box 355020, Seattle, WA, 98195*

### **3.1. Introduction**

The continuing debate over the efficacy of spatial fishery management necessitates the development of techniques to explain spatial dynamics of marine populations. The logistical constraints of tracking small organisms over hundreds of kilometers emphasize the need when investigating larval dispersal (Willis *et al.* 2003; Sale *et al.* 2005). Computer simulation models have contributed to understanding the kinematics of older life stages, but the dispersal, survival, and connectivity between spawning and nursery areas remains unresolved for many marine populations (Beck *et al.* 2001; Cowen *et al.* 2007). Since connectivity plays an important role in local and metapopulation dynamics, community structure, and genetic diversity (Hastings and Harrison, 1994), understanding the connectivity among life stages within and across populations provides information to evaluate and design management strategies. The term connectivity is derived from metapopulation analyses: dynamic interactions between geographically separated populations via the movement of individuals (North *et al.*, In press). In this study we refer to connectivity as the dynamic interaction between geographically separated spawning and nursery areas via the combined effect of individual movement and currents on transport. Connectivity is defined in practice here as the proportion of age-0 juveniles that are found on September 1st in a specific nursery area. Nursery areas are defined as the areas of accumulation of age-0 juvenile that contain more than 5% of survivals from the initial release.

Linkages between populations occur through movements of individuals, either by adult locomotion or by dispersal of pelagic eggs, larvae, and, to some extent, juveniles (Levins 1969; Botsford *et al.* 2001). Almost all fish produce larvae that can spend days, weeks, or months drifting, eating, and growing in the plankton (Gaines *et al.* 2007). Corresponding scales of dispersal from release sites can vary by more than six orders of magnitude, ranging from meters

to hundreds of kilometers (Cowen et al. 2000; Gaines et al. 2007; Pineda et al. 2007). In regions with complex horizontal circulation patterns, trajectories of individual fish may differ widely, resulting in differing histories of exposure to environmental variables such as temperature, salinity, and predators and prey, leading to variability in growth and survival among individuals. Single species populations are often divided into subpopulations, with important connections among groups, and intermixing of these subpopulations can be related to spatial dynamics of spawning and nursery areas based on individual movements and currents. Understanding transfers between spawning and nursery areas provides insight into stock and population structure.

Walleye pollock (*Theragra chalcogramma*) is a dominant component of the Gulf of Alaska (GOA) ecosystem, but knowledge of the mechanisms underlying variability in recruitment is incomplete. Adult walleye pollock are known to spawn from late March to early April at the southwestern end of Shelikof Strait, between Kodiak Island and mainland Alaska (Kendall et al., 1987; Schumacher & Kendall 1991). Eggs are fertilized at depths between 150 and 200 m, and hatch into larvae after a period of about 2 weeks. These larvae rise to the upper 50 m of the water column and drift in prevailing currents for the next several weeks (late April through mid-May). Larger larvae undergo diel migrations between 15 and 50 m. Currents may carry the larvae southwestward along the Alaska Peninsula, or offshore along the shoreward edge of the Shelikof sea valley southwest of Shelikof Strait. Only a small portion of the larvae hatched from the spawned eggs survive. By mid-summer, many of the survivors have been advected to the Shumagin Islands about 300 km southwest of the spawning site (Hinckley et al., 1991). The prevailing hypothesis is that Shelikof Strait is the main spawning area and the Shumagin Islands provides the main nursery area in the GOA. Other spawning areas have been observed from spawner biomass acoustic surveys, but potential contributions to walleye pollock populations in the GOA by these spawning areas are not known.

Gulf of Alaska walleye pollock are currently managed as a single stock, independent of Bering Sea and Aleutian Islands walleye pollock. The separation of stocks into eastern Bering Sea and Gulf of Alaska is based on studies of larval drift from spawning locations (Hinckley et al., 2001), [s1]and genetic studies of allozyme frequencies (Grant and Utter 1980; Olsen et al. 2002, mtDNA variability (Mulligan et al. 1992; Shields and Gust 1995; Kim et al. 2000), and microsatellite (O'Reilly et al. 2004) allele variability. It is important to note that data used for the larval transport study did not include encompass the entire GOA and that genetic analyses have not provided definitive results on the separation or mixing of genetic population components.

The alternate approach of examining connectivity between adult spawning and juvenile retention areas may contribute to the understanding of walleye pollock population structure. Understanding linkages between specific spawning locations and the destinations of surviving juveniles may be used to justify management units of northeast Pacific walleye pollock and aid in the conservation of population genetic components.

In this study we use a spatially-explicit IBM coupled to a hydrodynamic model to reveal patterns of potential connectivity of walleye pollock between spawning sites within the GOA, and retention of surviving juveniles in the GOA, Bering Sea (BS), or the Aleutians (AL). Spatially explicit IBMs are efficient Lagrangian tracking tools in connectivity studies (Werner et al., 2001, North et al., In press) and can be paired with geographic information systems (GIS). GIS is used to delineate source populations and potential nursery habitat along an individual's trajectory. Our goal is to understand the structure of the walleye pollock populations in Alaskan continental shelf and slope waters, through modeling the life history from eggs to age-0 juveniles.

### 3.2. Methods

The modeling approach coupled a biophysical model, the Regional Ocean Modeling System (ROMS), with a modified individual based model (IBM) of walleye pollock life history (Hinckley et al, 1996; Megrey and Hinckley, 2001).

#### 3.2.1. *Model configuration*

A multidecadal (1978-2003) simulation of water currents and temperatures was conducted for the Gulf of Alaska using the ROMS hydrodynamic model with the 10 km Northeast Pacific (NEP) grid (Fig. 1.2). Details of this simulation can be found in Curchitser et al. (2005). The model is a free-surface, hydrostatic primitive equation ocean circulation model that uses a nonlinear stretched terrain following vertical coordinates. The grid is curvilinear and pie-shaped from 20.6° to 71.6°N and from 145.8° to 247.6°E. Horizontal space is discretized using orthogonal curvilinear coordinates on an Arakawa C grid (numerical details can be found in Haidvogel et al. 2000; Moore et al. 2004; Shchepetkin and McWilliams, 2005). The use of 30 vertical levels ensures high resolution near the surface. At the horizontal boundaries facing the open ocean, an implicit, active, radiative boundary scheme (Marchesiello et al. 2001), is forced by seasonal time-averaged outputs from a basin scale ocean model. The model was forced with

monthly averaged fluxes of wind, heat, and salinity from the Comprehensive Ocean-Atmosphere Data Set (COADS) ocean surface climatology, with a horizontal spatial resolution of 0.5° (Da Silva et al. 1994). The circulation model simulation was started from rest, and summer values were used for initial conditions. As the model domain is relatively small, the model reached equilibrium after a spin-up period of about 2 years. The circulation model was run for 50 years using interannual variability in the forcing fields.

The 6 coupled model run years included 3 years before (1978, 1982, 1988) and 3 years after (1992, 1999, 2001) the shift in control of recruitment dynamics of walleye pollock in the GOA characterized by an increase of juvenile pollock mortality due to a gradual build-up of groundfish predators during the mid- and late-1980s (Bailey et al. 2000). The particular forcing scenario imposed on the physical model each year consisted of winds, freshwater input, and boundary conditions for each different year (see Curchitser et al., 2005 for details of configuration). The hydrodynamic model produced daily averaged output consisting of salinity and temperature fields, and 3D velocities. These physical variables were used to drive the IBM model over the same years. The IBM was run independently of the ROMS model runs. Details of the physical model simulations and the assessment of the model's ability to reproduce observed variability and their impact in the northeast Pacific can be found in Curchitser et al. (2005).

### *3.2.2. Individual-based model, parameters, and mechanisms*

Individual eggs, larvae, and juveniles were treated as particles with vertical (and in the case of juveniles, horizontal) locomotory capability. Each particle was tracked through space over time using a Java-based float tracking application that used modeled velocities from ROMS output at particle locations to compute movements (see Chapter 1 for details). The IBM was run from February 1<sup>st</sup> to September 1<sup>st</sup> in each model year. The biological mechanisms and parameter values used for this experiment matched those used in Chapter 2, and included early life stage processes for eggs, yolk-sac and feeding larvae, and age-0 juvenile pollock.

### *3.2.3 Spatial and temporal variability of spawning areas*

To examine potential spatiotemporal variability in the number of surviving juveniles from spawning locations, we varied the spatial and temporal spawning parameters in the IBM.

Table 3.1 shows areas and months of release for each year of the simulation. The timing of egg release was set to 1<sup>st</sup> February, 1<sup>st</sup> March, 1<sup>st</sup> April, and 1<sup>st</sup> May. Also shown in Table 3.1 are the fourteen initial release areas with codes corresponding to the spawning and nursery areas in Figure 3.1. Names and numbers of all of the areas in the model domain, and the sector associated with each area are shown in Table 3.2 and Figure 3.2.

The 14 spawning areas selected for the simulations were either areas where spawning has been observed during surveys of walleye pollock egg distribution, or during acoustic surveys of GOA walleye pollock biomass (Table 3.3). Table 3.3 lists known or suspected walleye pollock spawning areas in the Gulf of Alaska, the corresponding name and number of the area in the model domain, and the most likely spawning time for each area. In Morzhovoi Bay trawl catches were predominately males, so it is unclear whether this location is actually used as a spawning area.

#### 3.2.4. *Spatial and temporal variability of nursery areas*

The term *nursery area* was defined in this study as regions where age-0 juvenile pollock ( $\geq 25$  mm SL) were concentrated on September 1st and represented more than 5% of all survivors. The hydrodynamic model domain was divided into 46 smaller areas according to bathymetry and topography (islands, sounds, passes, bays, straits). Potential nursery areas included regions where juveniles have been sampled in FOCI surveys or during NMFS acoustic surveys of the walleye pollock biomass (Table 3.4). The simulated number of surviving 0-age juveniles in each area was tabulated.

#### 3.2.5. *Transport to and retention in nursery areas*

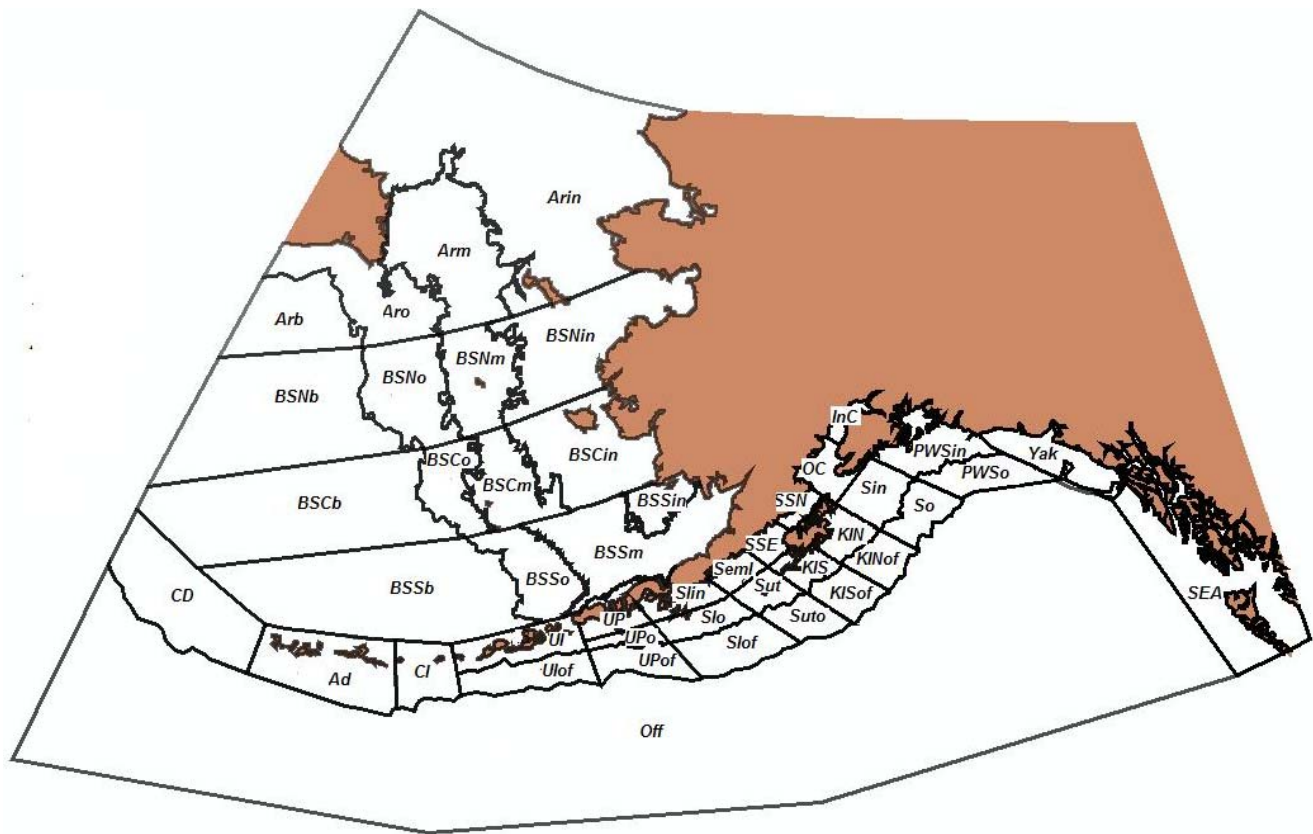
To examine contributions of surviving juveniles by spawning areas within the model domain, the proportion of juveniles from each spawning area was tabulated by month and year. To examine the relative contributions we calculated two variables: (1) retention and (2) transport of modeled age-0 juveniles to nursery areas. *Retention* was defined as the proportion of eggs released in a spawning area that on the 1<sup>st</sup> of September was still in the same spawning area. *Transport* was defined as the proportion of eggs released in a spawning area that went to area *X*. Variable values were initially averaged over all release years and months, and then separated by month and by year. The objective of this analysis was to identify regions where surviving juveniles were concentrated and report retention and transport proportions that exceeded 5% of

the surviving population. To examine the connectivity between spawning and nursery areas we created a connectivity matrix by month. We discuss model results relative to what is known or suspected about walleye pollock spawning and nursery areas.

Table 3.1. Spatial (*spawning areas*) and temporal (*month*) release parameters used in the simulation.

Parameter	Number	Description
<i>Spawning Area</i>	2	Inner Cook (InC)
	3	Prince Williams Sound Inner (PWSin)
	5	Outer Cook Inlet(OC)
	6	Seward Inner (Sin)
	8	Shelikof Strait North (SSN)
	9	Kodiak Island North (KIN)
	11	Shelikof Strait Exit (SSE)
	12	Kodiak Island South (KIS)
	14	Semidi Islands (SemI)
	15	Sutwik Island (Sut)
	17	Shumagin Islands Inner (SIin)
	18	Shumagin Islands Outer (SIo)
	20	Unimak Pass (UP)
21	Unimak Pass Outer (UPo)	
<i>Date of release</i>	1st February	
	1st March	
	1st April	
	1st May	
<i>Year of simulation</i>	1978, 1982, 1992, 1999, 2001	

Figure 3.1. Map of the numbers of the regions used to set initial conditions of release of particles (spawning areas) in South East Alaska (SEA), the Gulf of Alaska (GOA), the Aleutians (AL) and the Bering Sea (BS) sectors. The area numbers and corresponding names are listed in Table 3.2. The spawning regions are Inner Cook (InC), Prince Williams Sound Inner (PWSin), Outer Cook (OC), Seward Inner (Sin), Shelikof Strait North (SSN), Kodiak Island North (KIN), Shelikof Strait Exit (SSE), Kodiak Island South (KIS), Semidi Islands (SemI), Sutwik (Sut), Shumagin Islands Inner (Slin), Shumagin Islands Outer (Slo), Unimak Pass (UP), Unimak Pass Outer (UPo). The name and the corresponding number of the areas where the destiny of particles is counted are listed in Table 2. The areas that were assessed as nursery areas where the same spawning areas plus the areas: South East Alaska (SEA), 1: Yakutat (Yak), Prince Williams Sound Outer (PWSo), Seaward Offshore (So), Kodiak Island North Offshore (KINof), Kodiak Island South Offshore (KISof), Sutwik Offshore (Suto), Shumagin Islands Offshore (Slof), Unimak Pass Offshore (UPof), Unalaska Island (UI), Unalaska Island (Ulof), Chagulak Island (CI), Adak (Ad), Cobra Dane (CD), Offshore (Off), Bering Sea South Inner domain (BSSin), Bering Sea South Middle



domain (BSSm), Bering Sea South Outer domain (BSSo), Bering Sea South Basin (BSSb), Bering Sea Central Inner domain (BSCin), Bering Sea Central Middle domain (BSCm), Bering Sea Central Outer domain (BSCo), Bering Sea Central Basin (BSCb), Bering Sea North Inner domain (BSNin), Bering Sea North Middle domain (BSNm), Bering Sea North Outer domain (BSNo), Bering Sea North Basin (BSNb), Arctic Inner domain (Arin), Arctic Middle domain (Arm), Arctic Outer domain (Aro), Arctic Basin (Arb).

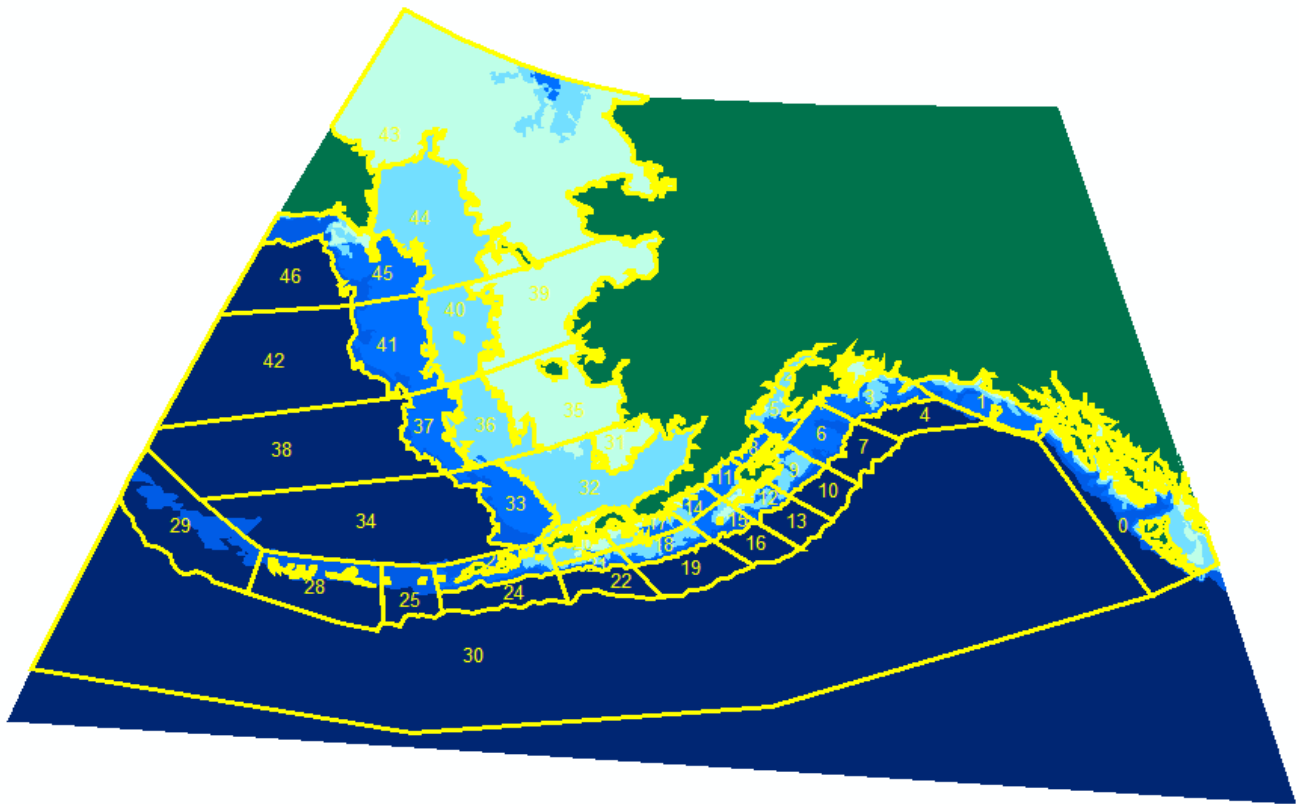


Figure 3.1b. Map of the numbers of the regions used to set initial conditions of release of particles (spawning areas) in South East Alaska (*SEA*), the Gulf of Alaska (*GOA*), the Aleutians (*AL*), the Bering Sea (*BS*), and the Arctic region (*Ar*) sectors. The area numbers and corresponding names are listed in Table 3.2.

Table 3.2. Names and numbers of all areas used in the simulation. The fourteen initial areas of release (spawning areas) are indicated by asterisks.

Region number	Region name	Sector
0	South East Alaska ( <i>SEA</i> )	SEA
1	Yakutat ( <i>Yak</i> )	GOA
2*	Inner Cook Inlet ( <i>InC</i> )	GOA
3*	Prince Williams Sound, Inner ( <i>PWSin</i> )	GOA
4	Prince Williams Sound, Outer ( <i>PWSo</i> )	GOA
5*	Outer Cook Inlet ( <i>OC</i> )	GOA

6*	Seward, Inner ( <i>Sin</i> )	GOA
7	Seward, Offshore ( <i>So</i> )	GOA
8*	Shelikof Strait North ( <i>SSN</i> )	GOA
9*	Kodiak Island North ( <i>KIN</i> )	GOA
10	Kodiak Island North Offshore ( <i>KINof</i> )	GOA
11*	Shelikof Strait Exit ( <i>SSE</i> )	GOA
12*	Kodiak Island South ( <i>KIS</i> )	GOA
13	Kodiak Island South Offshore ( <i>KISof</i> )	GOA
14*	Semidi Islands ( <i>SemI</i> )	GOA
15*	Sutwik Island ( <i>Sut</i> )	GOA
16	Sutwik Island, Offshore ( <i>Suto</i> )	GOA
17*	Shumagin Islands, Inner ( <i>SIin</i> )	GOA
18*	Shumagin Islands, Outer ( <i>SIo</i> )	GOA
19	Shumagin Islands, Offshore ( <i>SIof</i> )	GOA
20*	Unimak Pass ( <i>UP</i> )	GOA
21*	Unimak Pass, Outer ( <i>UPo</i> )	GOA
22	Unimak Pass, Offshore ( <i>UPof</i> )	GOA
23	Unalaska Island ( <i>UI</i> )	AL
24	Unalaska Island ( <i>UIof</i> )	AL
25	Chagulak Island ( <i>CI</i> )	AL
28	Adak ( <i>Ad</i> )	AL
29	Cobra Dane ( <i>CD</i> )	AL
30	Offshore ( <i>Off</i> )	GOA, AL
31	Bering Sea South, Inner domain ( <i>BSSin</i> )	BS
32	Bering Sea South, Middle domain ( <i>BSSm</i> )	BS
33	Bering Sea South, Outer domain ( <i>BSSo</i> )	BS
34	Bering Sea South, Basin ( <i>BSSb</i> )	BS
35	Bering Sea Central, Inner domain ( <i>BSCin</i> )	BS
36	Bering Sea Central, Middle domain ( <i>BSCm</i> )	BS
37	Bering Sea Central, Outer domain ( <i>BSCo</i> )	BS
38	Bering Sea Central, Basin ( <i>BSCb</i> )	BS
39	Bering Sea North, Inner domain ( <i>BSNin</i> )	BS
40	Bering Sea North, Middle domain ( <i>BSNm</i> )	BS
41	Bering Sea North, Outer domain ( <i>BSNo</i> )	BS

42	Bering Sea North, Basin ( <i>BSNb</i> )	BS
43	Arctic, Inner domain ( <i>Arin</i> )	Ar
44	Arctic, Middle domain ( <i>Arm</i> )	Ar
45	Arctic, Outer domain ( <i>Aro</i> )	Ar
46	Arctic Basin ( <i>Arb</i> )	Ar

---

Gulf of Alaska (GOA), Aleutians (AL), Bering Sea (BS), Arctic (Ar)

Table 3.3. Known or suspected walleye pollock spawning areas in the Gulf of Alaska. The spawning areas and spawn timing in each area, and the corresponding name and number of the spawning areas used in the model experiment are indicated.

Observed Spawning areas in Gulf of Alaska	Spawning Timing (likely occurrence)	Modeled areas corresponding to the observed spawning areas	
		Region number	Region name
Morzhovoi Bay*	Mid to late February	20	Unimak Pass ( <i>UP</i> )
Sanak Trough	Early to mid February	21	Unimak Pass Outer ( <i>UPo</i> )
Shumagin Gully	Mid to late February	17	Shumagin Islands Inner ( <i>SIin</i> )
Chirikov shelf break	Late March to early April	15	Sutwik Island ( <i>Sut</i> )
Shelikof Strait	Late March to early April	8	Shelikof Strait North ( <i>SSN</i> )
		11	Shelikof Strait Exit ( <i>SSE</i> )
Marmot Bay	Late March to early April	9	Kodiak Island North ( <i>KIN</i> )
Middleton Island	Late March to early April	6	Seward Inner ( <i>Sin</i> )
Entrance to Prince William Sound	Late March to early April		Prince Williams Sound Inner
		3	( <i>PWSin</i> )

---

\* Trawl catches nearly all males, so it is unclear whether this is actually a spawning area.

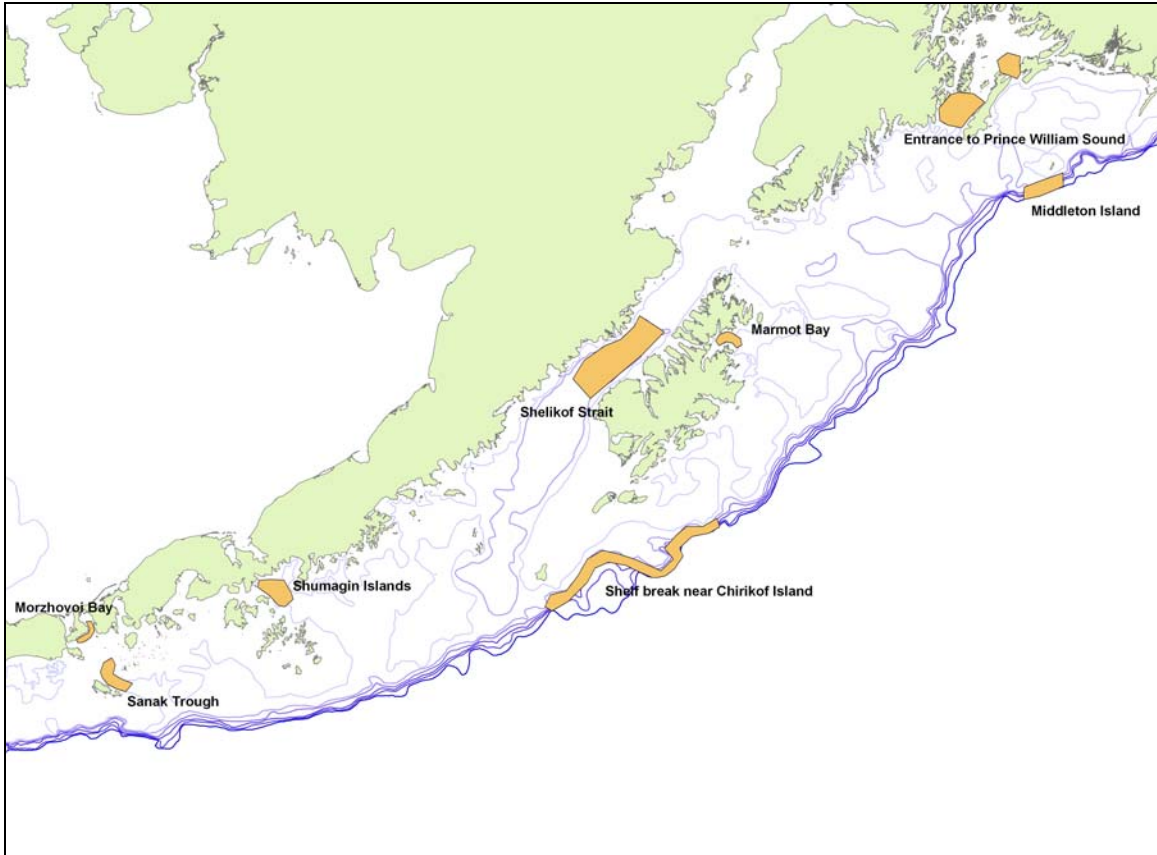


Figure 3.2. Walleye pollock observed spawning areas in the Gulf of Alaska

Table 3.4. Known or suspected walleye pollock nursery areas in the Gulf of Alaska. Observed nursery areas and the corresponding region name and number in the model are indicated.

Observed Nursery areas in Gulf of Alaska *	Modeled areas corresponding to the nursery areas	
	Region number	Region name
Shumagin area from Semidis islands to Unimak Pass	14	Semidi Islands ( <i>SemI</i> )
	15	Sutwik Island ( <i>Sut</i> )
	17	Shumagin Islands Inner ( <i>SIin</i> )
	18	Shumagin Islands Outer ( <i>SIo</i> )
	20	Unimak Pass ( <i>UP</i> )
	21	Unimak Pass Outer ( <i>UPo</i> )
North of Kodiak Island	5	Outer Cook Inlet ( <i>OC</i> )
	6	Seward Inner ( <i>Sin</i> )
North East of Kodiak Island	9	Kodiak Island North ( <i>KIN</i> )
Southwest of Unimak Pass	20	Unimak Pass ( <i>UP</i> )

\* Matt Wilson pers. comm.

### 3.3. Results

#### 3.3.1. *Retention in the spawning areas and temporal variability*

The maximum mean retention of age-0 juvenile walleye pollock over all years, months, and all spawning areas by September 1<sup>st</sup> was 0.28 in the *Shumagin Islands Inner area (SIin)*. This was followed by *Prince William Sound Inner area (PWSin)* and *Outer Cook Inlet (OC)* area with retention proportions of 0.22 (Fig. 3.3a). The *Seward Inner area (Sin)* retained 7% of the spawned eggs. Retention values did not exceed 5% in other spawning areas (Fig. 3a). For retention levels > 5%, monthly variability in the release time of spawning showed that the later the spawning occurred, the higher the proportion of retention. Eggs spawned in February resulted in the lowest proportion of retention, and those spawned in May showed the highest retention (Fig. 3b). These results indicate that the highest cumulative mortality was experienced by individuals spawned in the early months, as indicated by the monotonic increase of numbers over time, as expected. A contrasting example occurred within the *SIin* spawning area, however. The retention of May-spawned age-0 juveniles in September decreased relative to those spawned in April (Fig. 3b). In the *InC* spawning area, retention was only observed among eggs released in April and May, with May showing the highest level of retention (8%) from that site. Across sites, interannual variability in retention was low, with the highest variability observed within spawning sites (Fig.3c). Spawning areas *SIin*, *PWSin*, *OC*, and *Sin* consistently contained the overall highest retention rates, but locations differed among years (Fig.3c).

#### 3.3.2. *Temporal variability of transport to nursery areas*

The highest proportion of age-0 juveniles that were alive on September 1<sup>st</sup> across years occurred in the *Shumagin Islands Inner area (SIin)*, followed by *Semidi Islands (SemI)*, and *Outer Cook Inlet (OC)* (Fig. 3.4). In the Bering Sea, the highest proportion of age-0 juveniles were found in the *Bering Sea South Basin (BSSb)* area, followed by the *Bering Sea South Outer domain (BSSo)*, the *Bering Sea Central Outer domain (BSCo)*, and the *Bering Sea Central Middle domain (BSCm)* areas. Timing of egg release affected survival, with transport to *SemI*, *OC*, and *BSSo* areas increasing from release dates February to May, with simultaneous decreases in *BSCm* and *BSCo* areas. Transport into *SIin* and *BSSb* nursery areas increased among eggs released up to April and then decreased during May (Fig. 3.4). Transport and retention values have not been corrected for cumulative mortality.

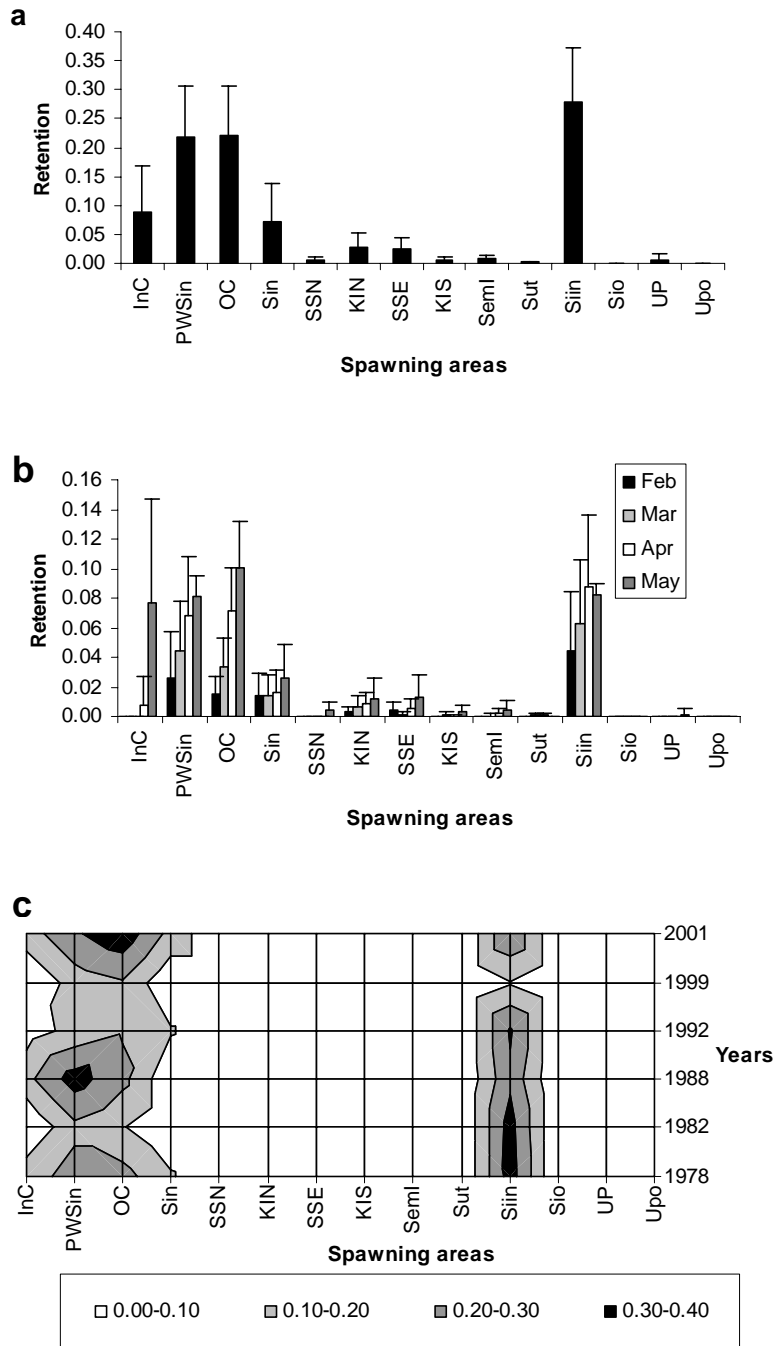


Figure 3.3. Retention of juvenile age-0 walleye pollock in each spawning area. a. Proportion of juvenile age-0 retained in spawning areas where released, over all simulations. b. Proportion of juvenile age-0 retained in spawning areas where released, by month of release (1<sup>st</sup> February, 1<sup>st</sup> March, 1<sup>st</sup> April, 1<sup>st</sup> May). c. Proportion of juvenile age-0 retained in spawning areas where released, by year of release (1978, 1982, 1988, 1992, 1999, 2001) over all spawning monthsXXXX.

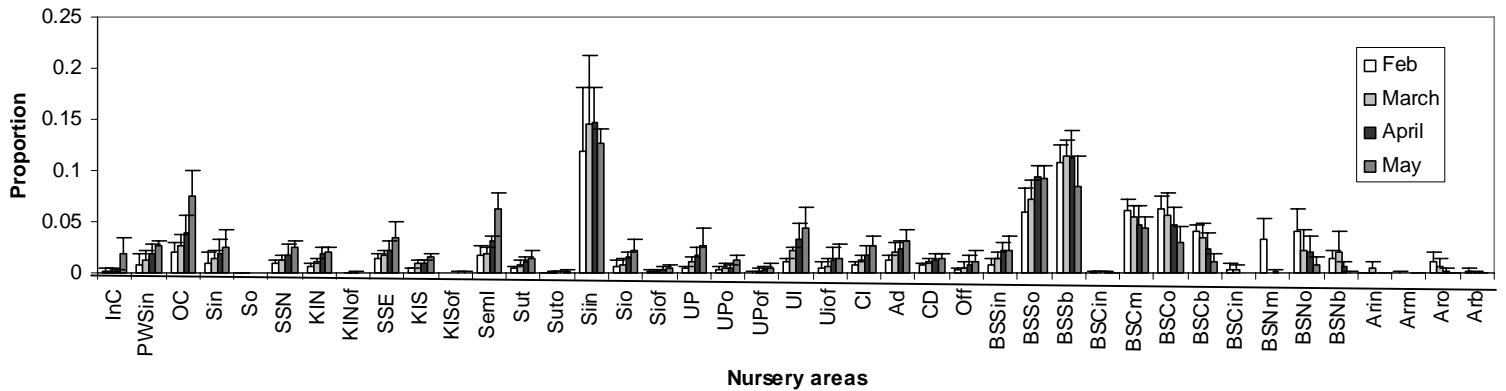


Figure 3.4. Proportion of age-0 juveniles that were alive at the end of the simulation (September 1<sup>st</sup>) in a given nursery area. The bars represent the month of release of the eggs, to observe the temporal variability of nursery areas due to differential timing of the spawning process.

### 3.3.3. Spawning in February

For eggs released on February 1<sup>st</sup>, the largest transport to nursery areas was to the *Slin* in the GOA and to *BSSb* in the BS with proportions of 0.12 and 0.11. A group consisting of *BSSo*, *BSCm*, and *BSCo* in the Bering Sea all had transport proportion values of 0.06 (Fig. 3.5).

To identify where individuals that were transported to nursery areas originated, and whether there was any monthly variability due to the timing of spawning, we built spawning and nursery area connectivity matrices over all years and then by month. The most likely nursery area was the Shumagin Islands inner area (*Slin*) with particles originating from spawning areas on the inner side of the continental shelf, upstream of *Slin*, but with considerable retention also occurring within *Slin*. Weaker transport to this area was seen from spawning areas located on the outer edge of the continental shelf of GOA, including from Seward inner (*Sin*), Kodiak Island North (*KIN*), Kodiak Islands South (*KIS*), and Sutwik Island (*Sut*) areas. Retention values of ~ 1% were seen in *Slin* (Fig. 3.6).

The second important February nursery area was located in the Bering Sea South basin (*BSSb*) with 11% of transport to that nursery region. Spawning areas where those age-0 juveniles originated were in the GOA at the outer edge of the continental shelf (*Sin*, *KIN*, *KIS*, *Sut*, *Slo*, and *UPo*), with transports values ranging between 10 and 25% (Fig.3.6). Age-0 juveniles located in

*BBSb* nursery area were also spawned along the inner edge of the GOA continental shelf, from the Shelikof Strait Exit (SSE), the Semidi Islands (*SemI*), the Shumagin Islands inner (*SIin*), and Unimak Pass (*UP*) areas, with transport proportions ranging between 5 and 10% (Fig. 3.6).

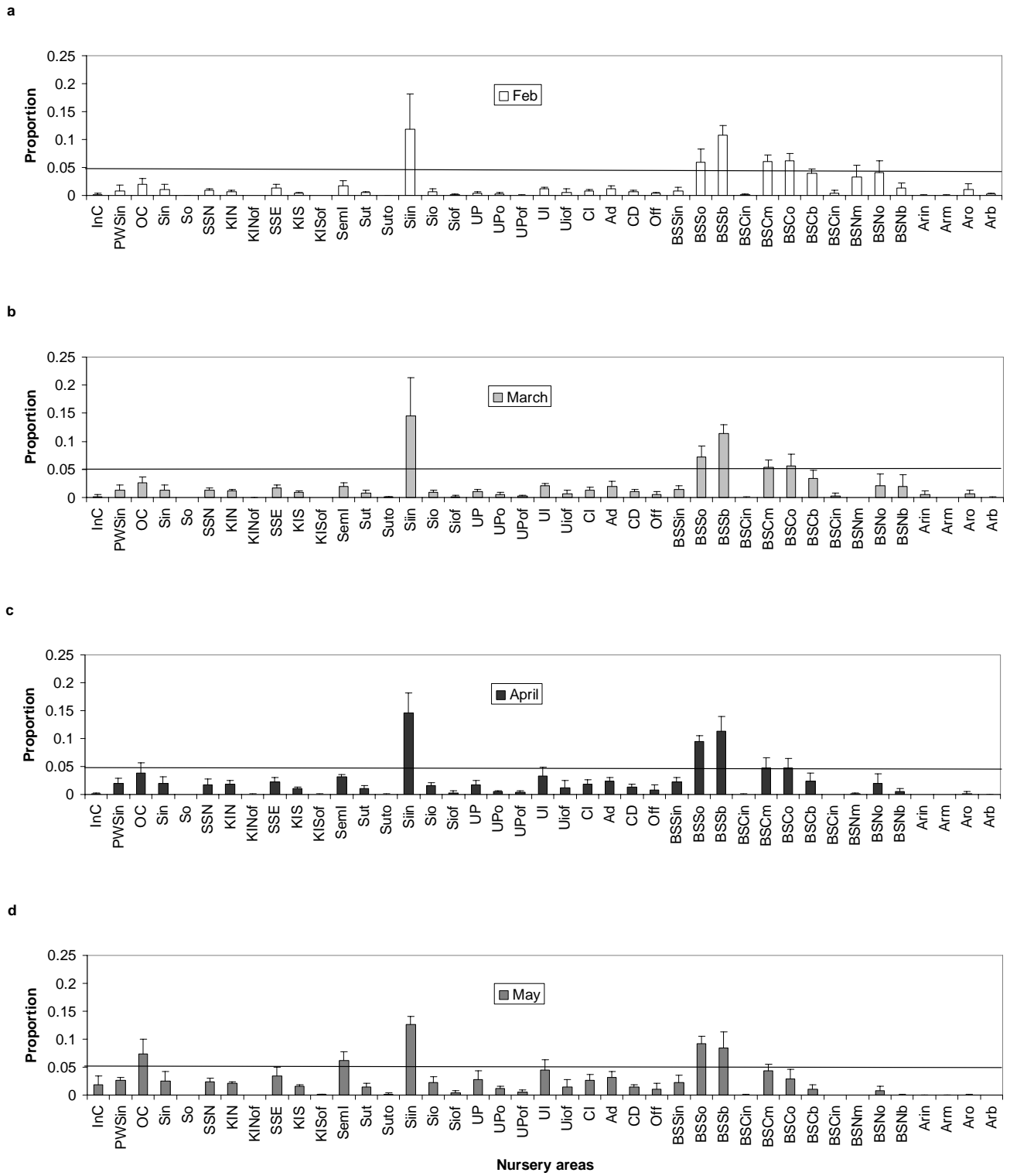


Figure 3.5. Proportion of age-0 juveniles that were alive at the end of the simulation (September 1<sup>st</sup>) in a given nursery area for eggs released in (a) February, (b) March, (c) April and (d) May.

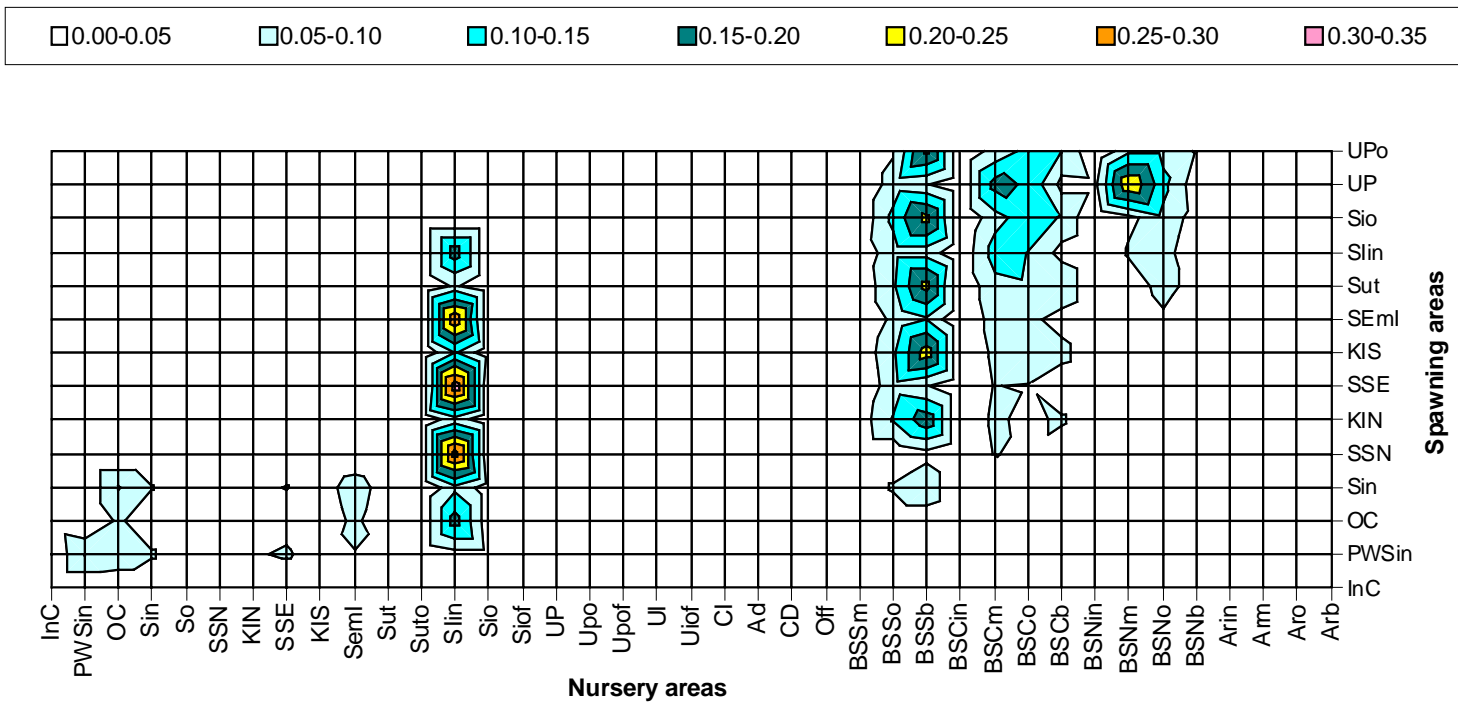


Figure 3.6. Connectivity matrix showing transport between spawning and nursery areas for eggs released in February.

The third most important nursery areas in February were located in the Bering Sea South Outer domain (*BSSo*), the Bering Sea Central Middle domain (*BSCm*), and the Bering Sea Central Outer domain (*BSCo*) with 5% of age-0 juveniles (Fig. 3.6). Age-0 juveniles in *BSSo* originated from *Sin*, *KIN*, *Sut*, *Slo*, and *UPo* (all along the outer edge of the continental shelf in the GOA). Surviving juveniles were also spawned in *SSE*, *SemI*, *SIin*, and *UP*, which are located along the inner edge of the continental shelf in the GOA. *BSSb* and *BSSo* showed the same connectivity routes and transport pattern of particles, ie. these areas were characterized by having the same spawning areas as the source of individuals (Fig. 3.6). The *BSNo* nursery area in the Bering Sea was mainly connected to the *UP* (20%) spawning area.

Nursery areas *BSCm* and *BSCo* contained a primary regions of spawning contributions which was located on the inner edge of the continental shelf of GOA. Transport proportions to these areas were highest from the southwest spawning areas and decreased among spawning regions to the north (i.e. Outer Cook Inlet (*OC*) toward Shelikof Strait North (*SSN*), *SSE*, *SemI*, *SIin*, and *UP*). In the Bering Sea Central nursery areas, a secondary spawning origin was associated with the outer edge of the GOA continental shelf, with transport proportions increasing from Seward inner (*Sin*) through *KIN*, *KIS*, *Slo*, to *UPo* (Fig.3.6). Other nursery and spawning areas had retention values around 5% (e.g. Fig. 3.3a and b), and nursery areas (e.g. *SSE* and *SemI*) with transport values around 5% (Fig.6). .

#### 3.3.4. Spawning in March

The transport of March spawned eggs resembled patterns observed among February spawned eggs. The highest transport of particles was into *SIin* in the GOA and *BSSb* in the BS, with a transport proportions of 0.15 and 0.11. A group of Bering Sea areas (*BSSo*, *BSCo*, *BSCm*) all had transport proportions ranging from 5 to 7% (Fig. 3.5b). Transport probabilities increased by at least 10% in March, relative to February, with values ranging between 45 and 50% (Fig. 3.7). In March, there were two main routes to the *SIin* area from spawning areas, a primary route associated with the inner edge of the GOA continental shelf and a secondary route along the outer edge. *SIin* also retained particles that were spawned in the region in March. There were two main nursery areas in the Bering Sea: (1) *BSSb* and *BSSo*, which showed the same connectivity pattern between spawning and nursery areas along the outer edge of the continental shelf (from *Sin* to *UPo*), and secondarily along the inner edge of the continental shelf of the GOA (from *SSE* to *UP*); (2) *BSCm* and *BSCo* also contained two routes with origins primarily along the inner edge

of the continental shelf. As predicted, contributions to these nursery areas increased with proximity to the spawning areas. This pattern also occurred along the secondary route to these Bering Sea nursery areas (i.e., along the outer edge of the shelf) with the exception of *UPo* where the transport probability to nursery areas was lower. The small probabilities of retention that were observed during February in *PWSin* and *OC* were intensified during March (Fig. 3.7) to 15-20% and 10-15%, respectively. The *BSNo* nursery area was connected to the *UP* (10-15%) spawning area, with a level of connectivity that decreased in March compared to that observed during February.

The nursery area *OC* was connected to spawning areas *PWSin*, *OC*, and *Sin* (10-15%); the nursery area *Sin* was connected with *Sin* and *PWSin*; the nursery area *SSN* was connected to *OC* and *Sin*; and the nursery area *KIN* was connected to *PWSin*, all of them showing a transport probabilities of about 5%. Also, the *SSE* nursery area was connected to *OC* (5%) and *SemI* with *OC* (10%) and *Sin* (5%).

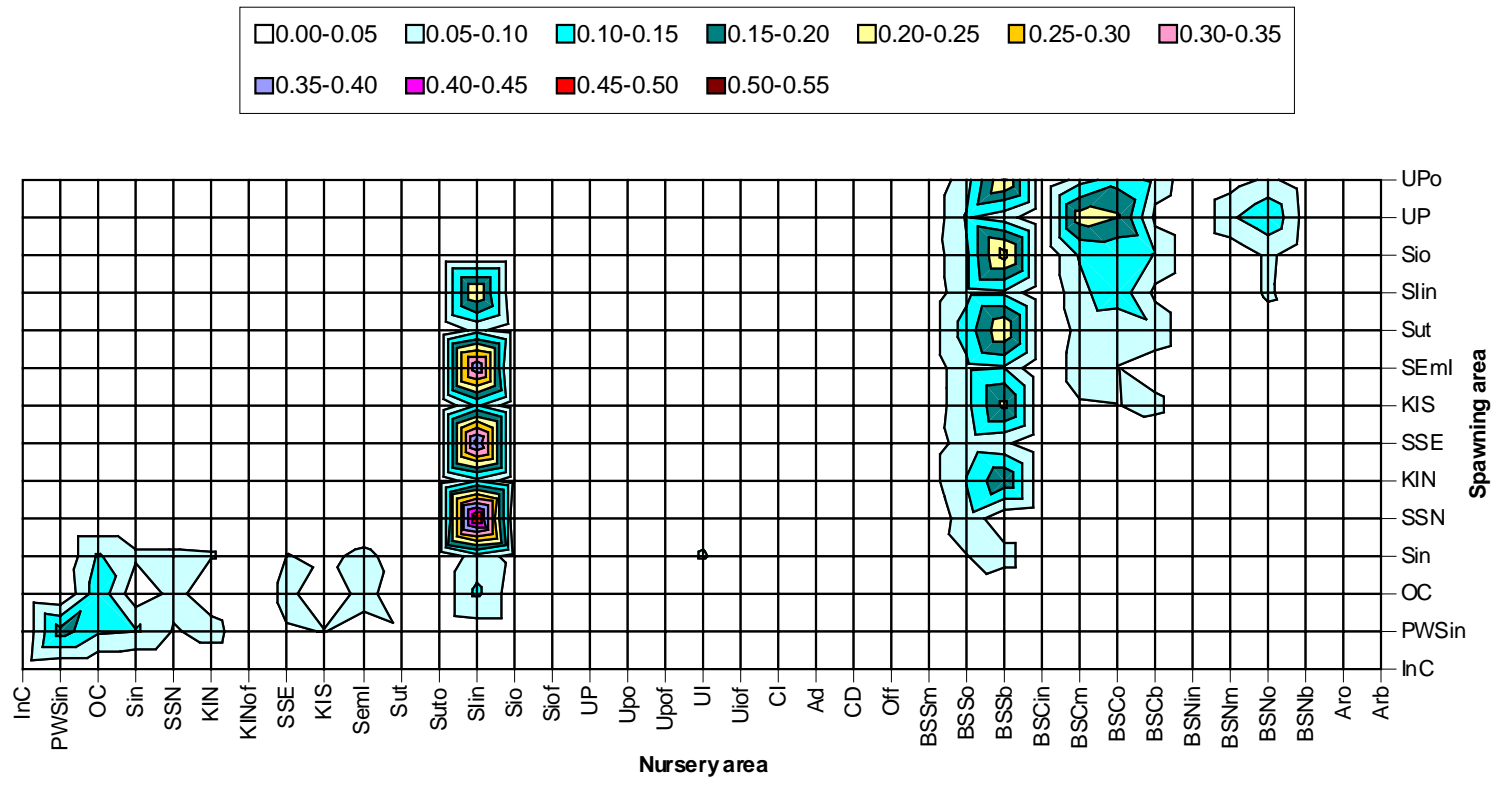


Figure 3.7. Connectivity matrix between spawning and nursery areas for the simulation where eggs were released in March.

### 3.3.5. Spawning in April

For eggs released in April, some transport patterns to nursery areas differed from previous spawning months. High transport proportions to *SIin* in the GOA and *BSSb* in the BS continued as a common feature of all months with a transport probabilities of 0.15 and 0.11. In contrast with previous spawning months, areas associated with Prince William Sound and specifically Outer Cook Inlet (OC) increased their contributions as nursery areas with a transport proportion of 0.07. Nursery areas in the Bering Sea such as *BSSo*, *BSCo* and *BSCm* had transport probabilities of 0.09, 0.05 and 0.04 (Fig. 3.5c).

Patterns of retention and connectivity between spawning and nursery areas resembled those observed for March released eggs, with retention and transport probabilities ranging between 45 and 50% overall. Contributing spawning areas began as far north as *OC*, but the connectivity between *OC* and *SIin* was weaker than earlier in the year (Fig. 3.8). The same two routes to the *SIin* nursery area observed for February and March released eggs were present during April, with a primary route associated with the inner edge of the GOA shelf and a secondary route along the outer edge of the GOA shelf. Retention of juveniles also occurred in all of these areas (Fig.3.8). Two prominent nursery areas occurred in the Bering Sea : (1) *BSSb* the primary nursery area, and *BSSo*, which showed the same pattern of connectivity between spawning and nursery areas as previously observed, but with additional spawning areas further to the southwest than in March, and primarily along the outer edge of the continental shelf (from *KIN* to *UPo*). A secondary transport route existed along the inner edge of the continental shelf of the GOA extending from *SSE* to *UP*. For both routes, transport values increased over those observed during March. (2) Areas *BSCm* and *BSCo* also had two connectivity routes that were more contracted to the southwest than in March. As in previous months, the routes were along the inner edge of the GOA continental shelf, with increasing transport probabilities from *SIin* (5%) to *UP* (25%), and along the outer edge of the GOA continental shelf originating in *Sut* (5%) and ending in *UPo* (25%) (Fig. 3.8). The *BSNo* nursery area was connected to the *UP* (15-20%) spawning area.

A group of nursery areas including *OC* (15-30%), *Sin* (5-20%), *SSN* (5-15%), *Sin* (5%), and *KIN* (5%) all increased transport levels, with the same connectivity routes between spawning and nursery areas as observed in March. The *SSE* nursery area was connected with *OC* (5%) and *SemI* with *OC* (5%), *Sin* (5%) and *SSE* (5%).

### 3.3.6. Spawning in May

May released eggs followed the same patterns of retention and connectivity as observed in April, but the connectivity decreased with values ranging between 40 to 45%. Spawning areas were located further southwest than those contributing during April (e.g., connectivity from *Sin* to *SIn*, Fig. 3.9). Individuals arriving at *SIn* followed the inner and outer GOA shelf transport routes that were observed for individuals released in February, March and April. Fish continued to be retained in these areas (Fig. 3.9). In the *BS* the two main nursery areas were present, with intensified connectivity and contributing spawning areas further southwest than observed for fish spawned in April. Nursery areas *BSSb* and *BSSo* maintained transport routes between spawning and nursery areas, although spawning areas were located further southwest, along the outer edge of the continental shelf (from *KIS* to *UPo*) than in April, and secondarily along the inner edge of the continental shelf (from *Seml* to *UP*). In both cases, transport values or connectivity increased relative to those observed during April. Nursery areas *BSCm* and *BSCo* maintained the inner and outer edges of the GOA continental shelf primary spawning routes, with increasing transport from spawning area *SIn* to *UP* (5-30%) and *Sio* to *UPo* (5-30%) (Fig. 3.9). The *BSNo* nursery area maintained its connection to the *UP* (5%) spawning area, but with reduced connectivity relative to that observed in April.

Complex interactions in the connectivity of areas inside of the GOA exist in May. *OC*, *PWSin* and *InC* show significant retention levels. Areas *InC* and *PWSin* retained 20% and 30% of individuals spawned during May. The *SSN*, *KIN*, *SSE* and *Seml* nursery areas show complex connectivity with spawning areas during this month (see Figure 3.9). The *OC* nursery area was connected to *PWSin* (35%) and *OC* (35%). The *Sin* nursery area was connected to *PWSin* (15%) and *Sin* (5%). The *SSN* nursery area was connected with *OC* (20%) and *KIN* was connected with *PWSin*, *OC*, and *Sin* with a connectivity value of 5%. The *SSE* nursery area was connected with spawning area *InC* (5%), *OC* (10%), *Sin* (5%), *SSN*, and *KIN* at 5%. The nursery area *Seml* had two routes of connection, one along the inner edge of the continental shelf through the *SSN* (25%) and *SSE* (15%) spawning areas, and the other along the outer edge of the continental shelf via *KIN* (10%) and *KIS* (5%).

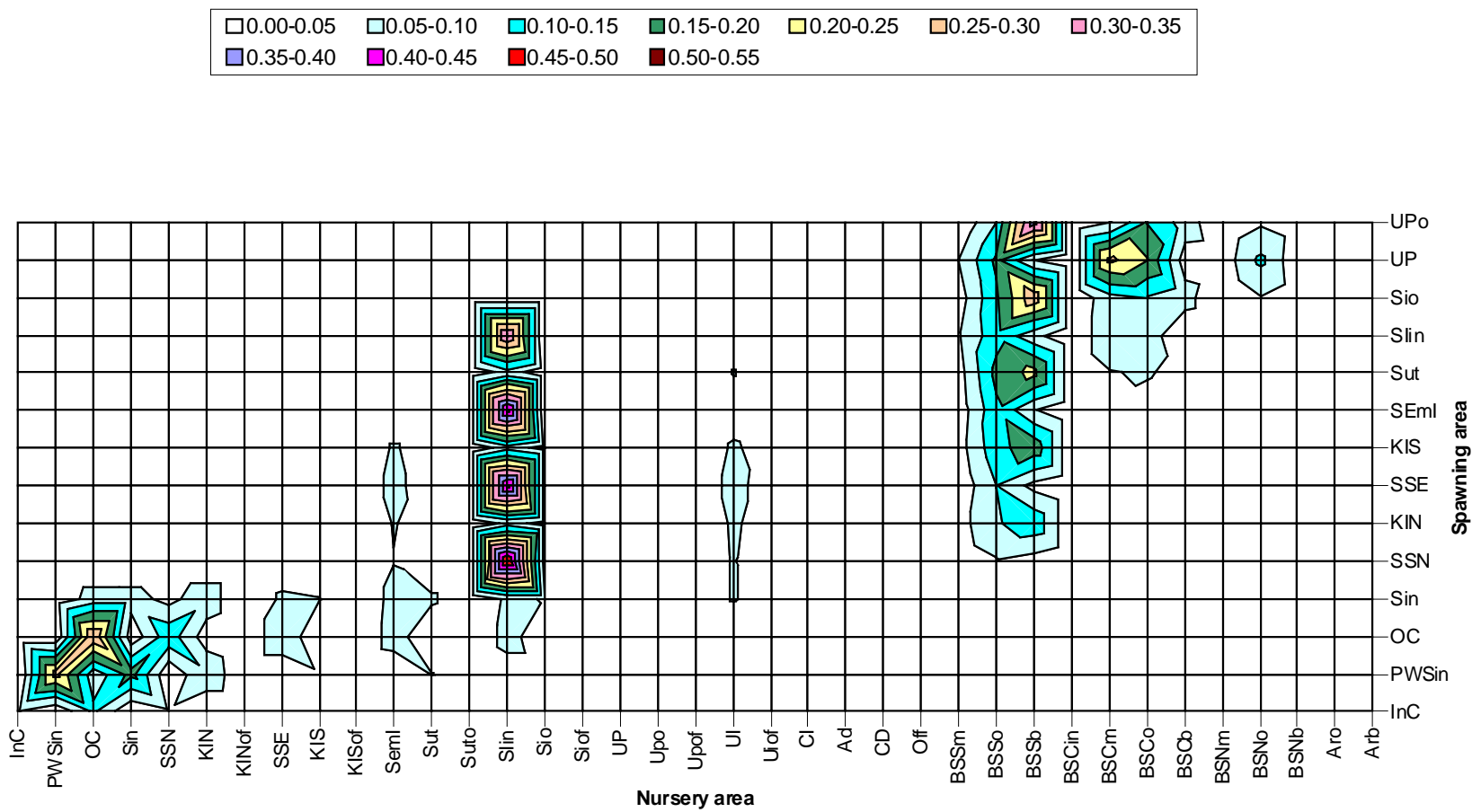


Figure 3.8. Connectivity matrix between spawning and nursery areas for the simulation where eggs were released in April.

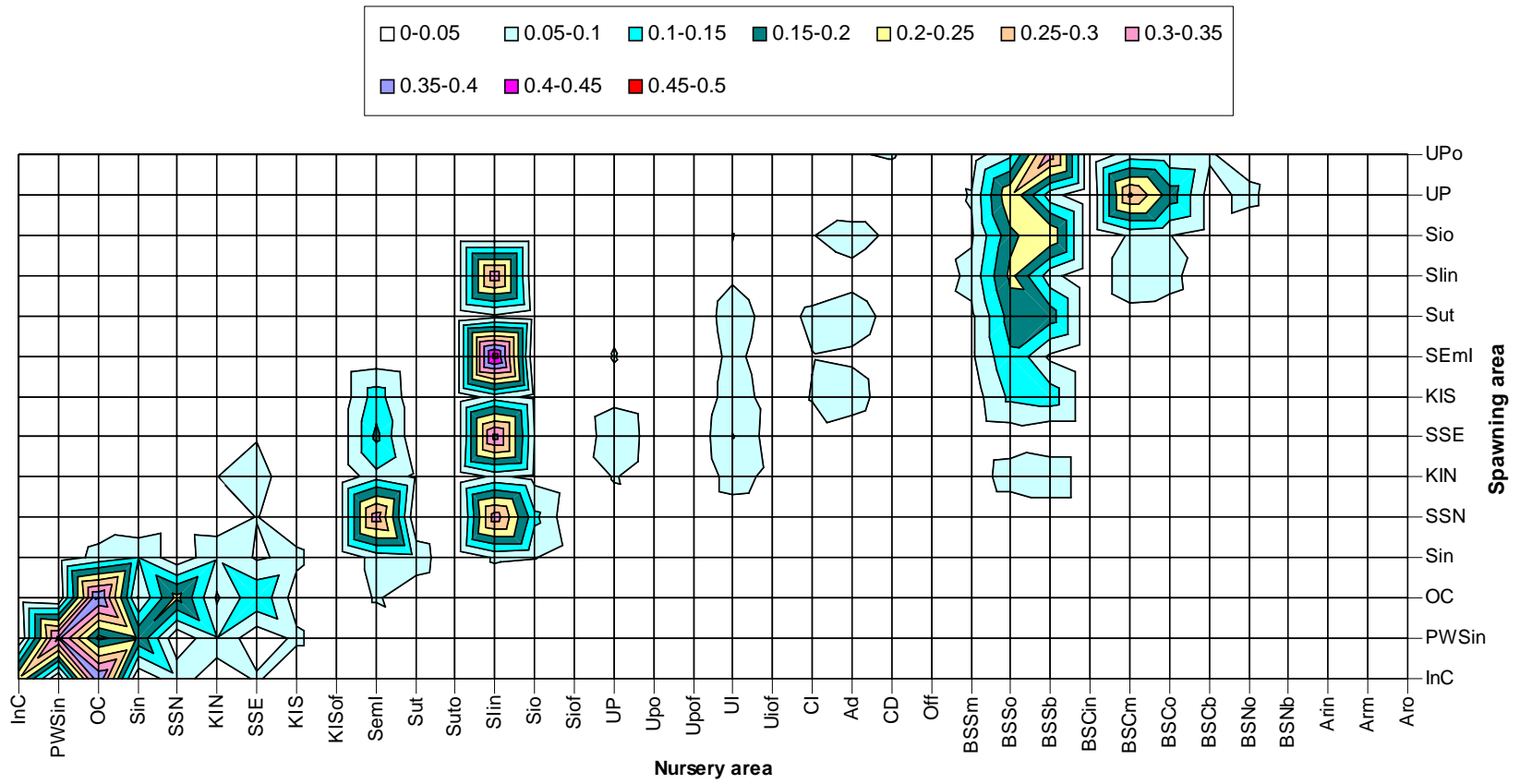


Figure 3.9 Connectivity matrix between spawning and nursery areas for the simulation where eggs were released in May.

### 3.4. Summary of Results

Common retention and transport routes from spawning to nursery areas were observed across all release months. Walleye pollock spawned in the GOA were transported to nursery areas in the GOA, to the Bering Sea, and to the Aleutians Islands. A constant feature was that the *Shumagin Islands Inner (Slin)* area functioned as a retention area (less so in February) and a nursery destination in the GOA for almost all months. Two primary connectivity routes were maintained during these simulated months: (1) along the inner edge of the GOA continental shelf, and (2) a secondary route along the outer edge of the shelf (see Figures 3.10 to 3.13). Nursery areas in the Bering Sea, *BSSb* and *BSSo*, also served as endpoints of routes connecting spawning areas in the outer and the inner edge of the continental shelf of the GOA to the BS. The dominance of the outer continental shelf route over the inner route in taking individuals to the Bering Sea contrasts to the routes taken by individuals to *Slin*, which was more often along the inner shelf. Another interesting feature is that the routes of connectivity and the spawning areas were similar during different spawning months with some variability and with very marked patterns. Figure 3.10 to 3.13 present summaries of the connectivity and retention in the GOA/AL and BS.

Transport routes between spawning and nursery areas are summarized by months in Figures 3.10 to 3.13. General patterns observed in the Gulf of Alaska include:

1. The Shumagin Islands inner nursery area, *Slin*, was connected to spawning areas via a primary route along the inner edge of the GOA shelf (*OC* to *Slin*, ie. through Shelikof Strait), and a secondary route along the outer edge of the shelf (*Sin* to *Slin*). These routes occurred in all simulated release months (i.e. February to May, Figs. 3.10 to 3.13). The highest connectivity to the *Slin* nursery area occurred from spawning occurring in March and April (Figs. 3.7 and 3.8).
2. In all months the *Slin* nursery area included retention of eggs that survived to age-0 juveniles. The highest retention values were observed for individuals spawned in April and May (30-35%, Figs. 3.8 and 3.9). However, retention was less from the February spawning, the month when spawning has been observed in this region.
3. As the spawning year progressed, the overall number of retention areas and the retention rates increased (Figs. 3.10 to 3.13). Prince William Sound and the surrounding areas provided age-0 walleye pollock retention areas later in the year. Retention in *PWS* and *OC* nursery areas was weak during February (Fig.3.10) and March (Fig.3.11), and increased during April (Fig. 3.12) and May (Fig. 3.13). Weak retention in *Sin* occurred in March and was

maintained until May. *SSE* and *SemI* were secondary nursery areas in terms of the connectivity between nursery and spawning areas. Other nursery areas appeared in March through May, such as *SSN* and *KIN*.

Two consistent patterns were observed in the retention and transport of walleye pollock early life stages to Bering Sea nursery areas:

1. The primary nursery area in the Bering Sea, *BSSb*, and *BSSo*, shared transport routes between spawning and nursery areas, where the routes were primarily along the outer edge of the GOA continental shelf and secondarily along the inner edge of the continental shelf.
2. Transport routes to secondary nursery areas *BSCm* and *BSCo* in the Bering Sea were primarily along the inner edge of the continental shelf (with increasing contributions to the nursery areas as distance from the spawning area decreased), and secondarily along the outer edge of the shelf, also with contributions increasing as proximity to spawning areas decreased. The exception, *Upo* had a decrease in transport and connectivity with distance from the spawning area. As the spawning months progressed, the origins of the inner and outer edge routes moved more to the southwest, with spawning areas closer to the nursery areas in the BS.
3. Other nursery areas important in the BS included *BSCb*, *BSCo*, and *BSCm*, which were equally connected to spawning areas along the inner and outer GOA shelf. The northernmost extent of these spawning areas tended to be restricted to the southwestern areas in the GOA.
4. In May, nursery areas along the southern Aleutian Islands showed increasing proportions of surviving juvenile walleye pollock.

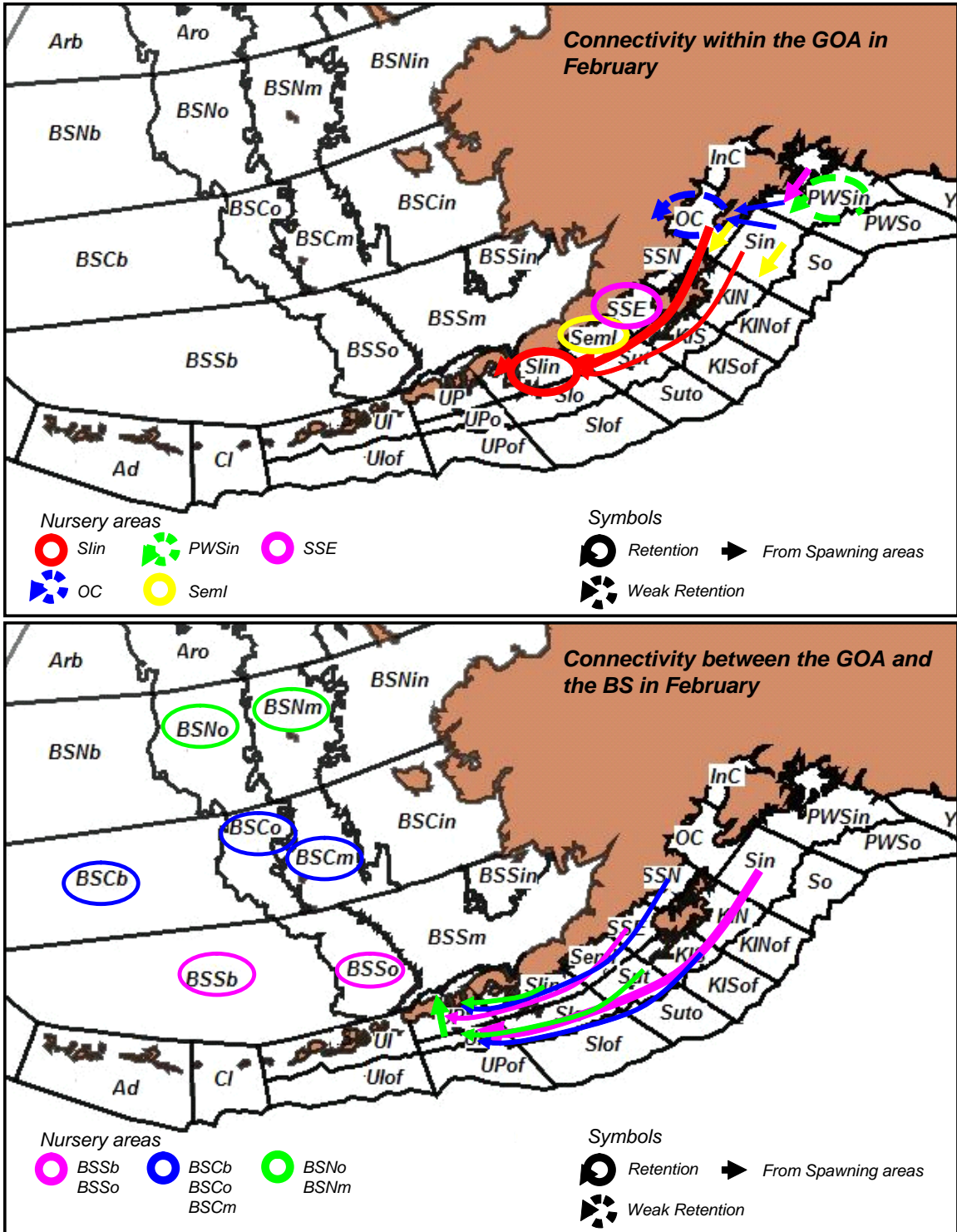


Figure 3.10. Diagram of connectivity between spawning and nursery areas for individuals spawned in February. The rings in the figure indicate the main nursery areas, rings with arrows represent retention areas. The trajectory arrows represent the routes of connection between spawning and nursery areas, with the width of the arrow proportional to the intensity of connectivity (for values, see Figure 3.6). The names of spawning and nursery areas are indicated

in Table 3.1, Table 3.2 and Figure 3.1. The color of the arrow indicates the route taken by individuals transport to the nursery area indicated by a circle of the same color.

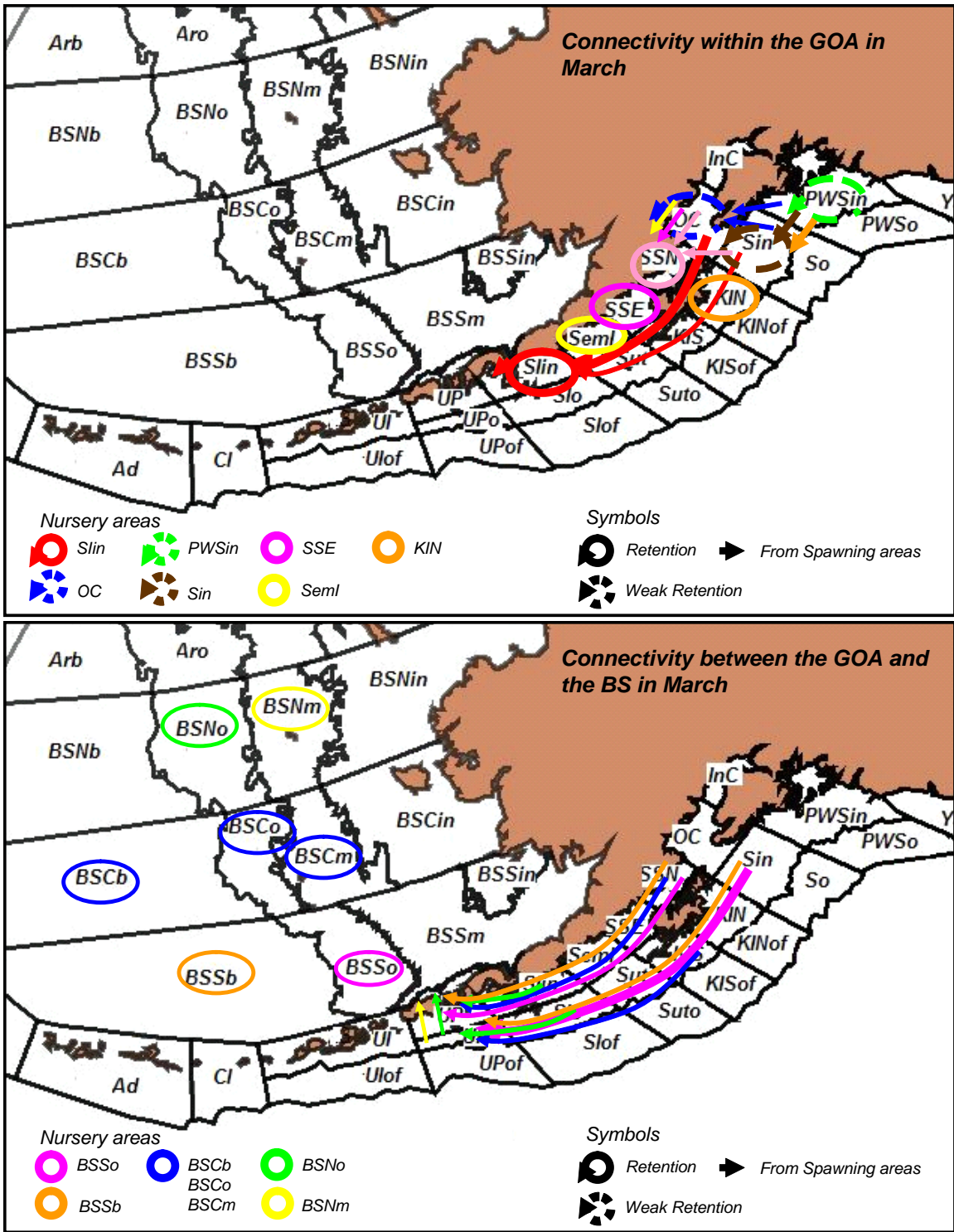


Figure 3.11. Diagram of connectivity between spawning and nursery areas for individuals spawned in March. The rings in the figure indicate the main nursery areas, rings with an arrow represent retention areas. The transport arrows represent the routes of connection between spawning and nursery areas, with the width of the arrow proportional to the intensity of connectivity (for values see Figure 3.7). The names of spawning and nursery areas are indicated

in Table 3.1, Table 3.2 and Figure 3.1. . The color of the arrow indicates the route taken by individuals transport to the nursery area indicated by a circle of the same color.

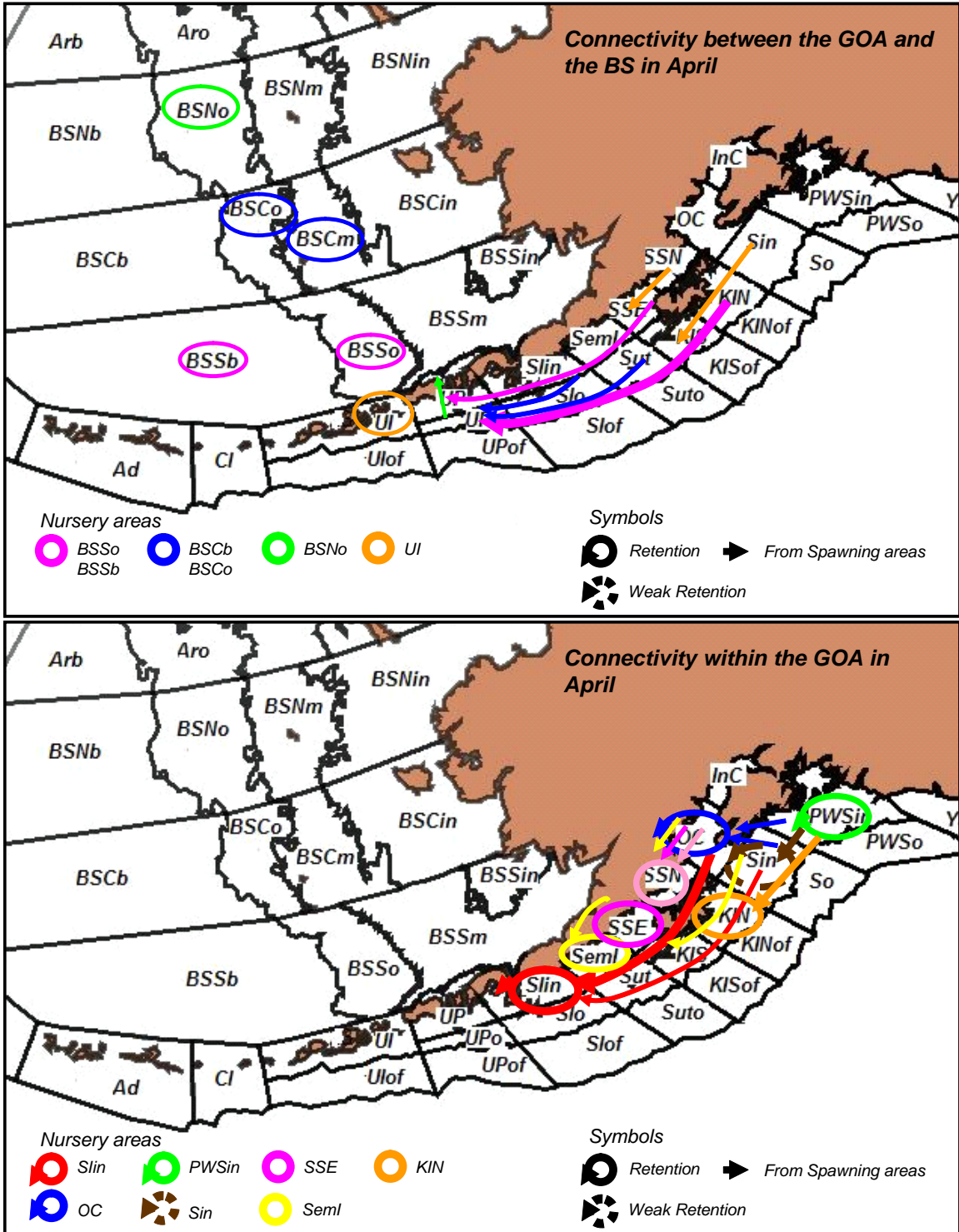


Figure 3.12. Diagram of connectivity between spawning and nursery areas for individuals spawned in April. The rings in the figure indicate the main nursery areas, rings with an arrow represent retention areas. The transport arrows represent the routes of connection between spawning and nursery areas, with the width of the arrow proportional to the intensity of

connectivity (for values see Figure 3.8). The names of spawning and nursery areas are indicated in Table 3.1, Table 3.2 and Figure 3.1. The color of the arrow indicates the route taken by individuals transport to the nursery area indicated by a circle of the same color.

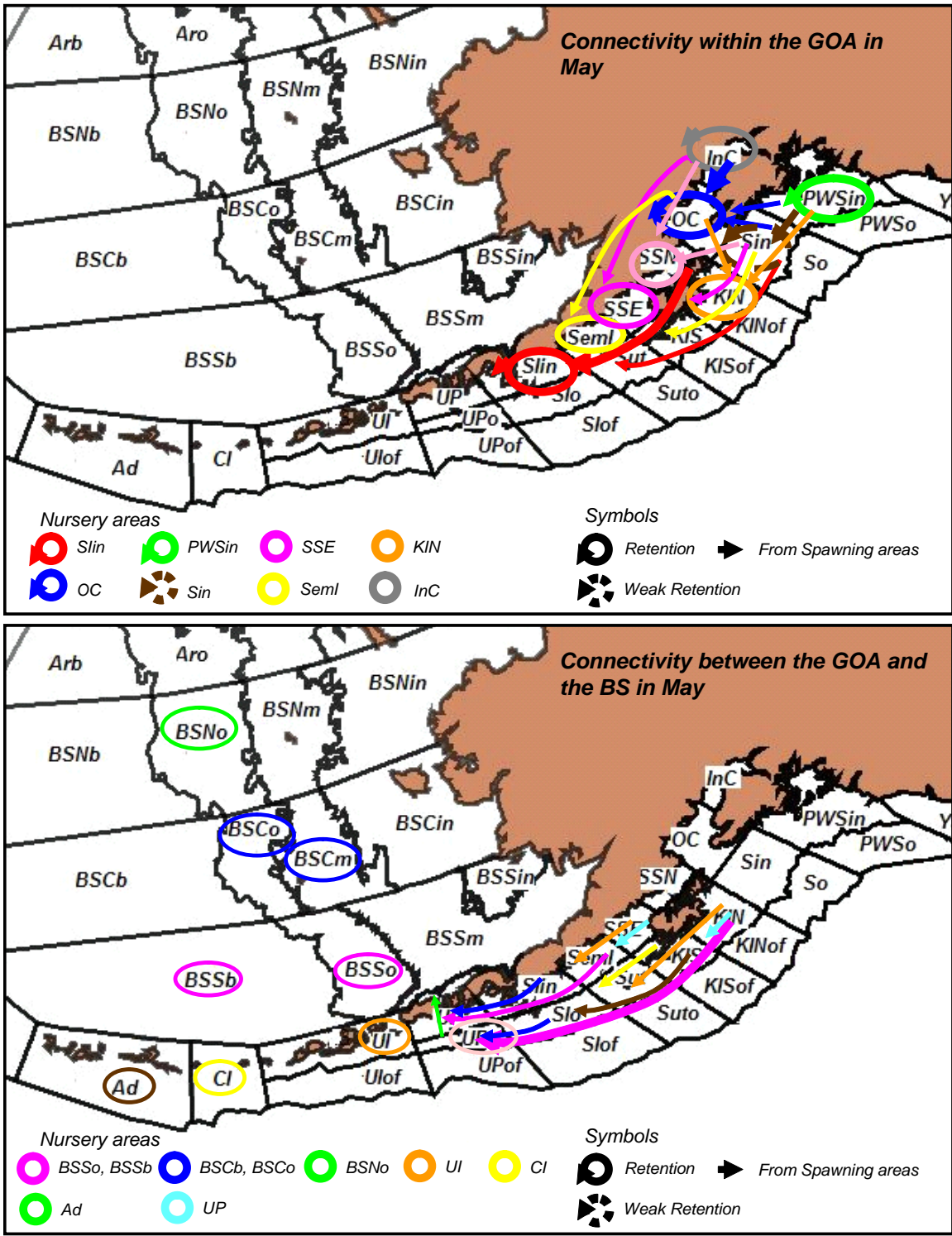


Figure 3.13. Diagram of connectivity between spawning and nursery areas for individuals spawned in May. The rings in the figure indicate the main nursery areas, rings with an arrow represent retention areas. The transport arrows represent the routes of connection between spawning and nursery areas, with the width of the arrow proportional to the intensity of

connectivity (for values see Figure 3.9). The names of spawning and nursery areas are indicated in Table 3.1, Table 3.2 and Figure 3.1. The color of the arrow indicates the route taken by individuals transport to the nursery area indicated by a circle of the same color.

### 3.5. Discussion

The coupled bio-physical IBM was used to examine connections between potential spawning and nursery areas, and how these patterns changed with changes in the time of spawning. An unknown portion of the observed variability in spawning area contributions resulted from not including cumulative mortality when tabulating age-0 juvenile survival, but a monotonic increase in connectivity with later spawning dates was not observed. Connectivity between spawning and nursery areas actually declined with later spawning dates in some nursery areas. But to ensure an equal comparison among spawning dates, cumulative mortality needs to be included when quantifying connectivity as a function of spawning date. This will be done for the paper on these results.

Model simulations demonstrated that destination areas for surviving age-0 walleye pollock juveniles were comparable to observed or suspected nursery areas (Table 3.4). The modelled nursery areas found in the Semidi Islands (*SemI*), Sutwik (*Sut*), and the inner Shumagin Islands (*Slin*) corresponded to the observed Shumagin Islands nursery area which extends from the Semidi Islands to Unimak Pass. The known nursery area north of Kodiak Island corresponded to modelled nursery areas Outer Cook Inlet (*OC*) and the inner continental shelf near Seward (*Sin*). The modelled nursery area Kodiak Island North (*KIN*) matched the area northeast of Kodiak Island where juvenile pollock are found, and the observed nursery area southwest of Unimak Pass corresponded to the model regions Unimak Pass (*UP*) and the outer Unimak Pass (*UPo*). In contrast to conventional thought, the model region Shumagin Islands Outer (*Slo*) was not found to be a regular destination for surviving age-0 walleye pollock in model simulations.

Walleye pollock spawning locations have shifted in recent years, and other spawning areas have been recently described. In past years, the majority of pollock spawning in the GOA was found between mid-March and early May in Shelikof Strait (Fig. 1.1, Kendall et al., 1987; Schumacher & Kendall 1991). Peak spawning occurred at the beginning of April in the deepest part of Shelikof Strait. After spawning, eggs and larvae were advected southwest by the Alaska Coastal Current (ACC) along the Alaska Peninsula and arrived in the Shumagin Islands 8 to 10 weeks later. Another portion of eggs and larvae may have been advected into the Alaskan Stream, where they could have been lost from the population (Bailey et al. 1999). Walleye pollock begin to recruit to the harvested population at age-2 and are fully recruited by age 4 or 5 (Bailey et al. 2005). The Shumagin Islands region has traditionally been considered the nursery

area that ensures the success of the population in the GOA (Hinckley et al. 1991, Wilson et al.1996).

In recent years, however, acoustic surveys have observed concentrations of spawning fish in the Shumagin Islands (Dorn et al., 2005). Little is known about the fate of walleye pollock spawned in this region, but in stock assessment models, this spawning biomass is assumed to contribute recruits to the GOA (Dorn et al., 2005). It should be noted that this work indicates that walleye pollock spawning in February in the Shumagin region mostly were transported to the Bering Sea; few were retained in this area.

Using model simulation results, destination nursery areas can be predicted for known or suspected spawning areas. Model results confirmed the connectivity between Shelikof Strait spawning and the Shumagin nursery region with 40-45% connectivity in March and 45-50% in April. Connections were also found between *SSN* and *SSE* spawning areas and Bering Sea destination areas such as *BSSo* (5-10%) and *BSSb* (5%). These results are relevant as they confirm that there is a strong connection between the Shelikof and Shumagin areas, and indicate potential spawning contributions from Shelikof Strait to southern parts of the Bering Sea.

The model also predicted that, of eggs spawned by walleye pollock in the inner parts of the Shumagin Islands (*SIin*) during February and March (the observed spawning time in this region), only 5% were retained in this area, with the rest transported to various nursery areas in the southern and central Bering Sea (*BSSo*, 10%; *BSSb*, 20%; and *BSCm*, *BSCo*, *BSCb* each at 5%). As noted above, this may mean that the Shumagin Islands do not contribute significant recruits to the GOA, which is what present management assumes.

Prince William Sound (*PWSin*), areas north of Kodiak Island (*KIN* and *SIN*), the Sutwik region (*Sut*), and the Unimak Pass region (*UP* and *UPo*) have also been observed to be spawning areas. During March and April spawning, *PWSin* showed a retention rate of 15-25%, with connectivity to Outer Cook Inlet (*OC* 10%), the inner shelf at Seward (*Sin* 5-15%), and Kodiak Island north (*KIN* 5%) nursery areas. Spawning-nursery area connectivity from Prince William Sound spawned walleye pollock may be restricted to the GOA.

Where do juveniles found to the northeast and east of Kodiak Island originate? Our model indicates that walleye pollock spawned off Seward (*Sin*), not far from the northern end of

Kodiak were only retained at a rate of about 5%. Fish spawned in the North Kodiak area itself are mostly transported out of the region to the southwest parts of the GOA, to the BS and to the AL areas in this simulation. A potential caveat to this result is that juvenile fish found in the bays around northern and eastern Kodiak (Wilson et al., 1996) may have been spawned on the shelf near Kodiak Island, and they may exhibit behavior and directed swimming not suitable modeled or simulated by the IBM. The ROMS model, which uses a 10 km grid, does not accurately resolve flow into and out of coastal bays, and we cannot examine the use of these bays by juvenile pollock as nursery areas at this time.

Other potential spawning and nursery areas in the GOA could contribute age-0 walleye pollock juveniles to GOA and BS populations. The Sutwik Island region (*Sut*) mimicked retention and transport pattern observed in the Shumagin area (*Slin*). Individuals from this region, as well as being retained, were transported to *Slin* and to the central and southern Bering Sea. Supporting evidence for contributions from this area is derived from a spatial bioenergetics model for the western GOA, which indicated that habitat conducive to juvenile walleye pollock growth was located along the eastern edge of Semidi Bank, in the vicinity of Castle Cape, Kupreanof Point, and south-west of Sutwik Island (Mazur et al., 2007).

Another important question that may be addressed by this study is whether young pollock from the GOA are transported to the Bering Sea. Model simulations indicated that the Bering Sea may be an important nursery area for several spawning grounds in the GOA. This result raises the possibility of GOA spawning success and transport rates influencing walleye pollock recruitment in the BS. It is also not known if variability in GOA recruitment can be attributed to the number of walleye pollock transported to the BS. If surviving GOA juveniles in the BS develop, grow, and recruit to the BS fishery, then transport of individuals to the BS potentially influences walleye pollock cohort strength in both the GOA and the BS. The BS pollock stock, however, is ten times larger than the GOA stock. Also, as juvenile fish in the Bering Sea (age-1's and 2's) tend to be found in the northern half, i.e., west of 170°, any of the juveniles transported to the BS from the GOA would have to run the gantlet of cannibalistic adult pollock and increasing numbers of arrowtooth flounder that are found in the southern half of the Bering. Another possibility, of course, might be that GOA juveniles that settle in the BS may eventually find their way back to the GOA. Some of the GOA fishery data are suggestive of an influx of pollock from the Bering Sea (M. Dorn, Alaska Fisheries Science Center, Seattle, WA; pers. comm.).

The bio-physical coupled IBM can potentially contribute to the annual walleye pollock stock assessments for the BS and GOA. At this time, the model only simulates egg through age-0 juvenile life history stages. There are at least two additional years before individuals are recruited to the commercial fishery. If GOA spawned walleye pollock are transported to the BS and stay in the BS, then there are important implications for the assessment and management of Bering Sea and Gulf of Alaska walleye pollock. If there is an occasional large year class in the Bering Sea due to an influx of recruits from the GOA, it could distort the stock-recruit relationship, and make the BS stock seem more productive than it actually is. Additional information on the stock structure and dynamics of walleye pollock in the northeast Pacific, including potential transport of walleye pollock early life stages from the GOA to the BS, may decrease error in recruitment estimates for both regions and help interpret odd patterns in the catch and survey data. Annual surveys of GOA spawning locations, perhaps from acoustic surveys, would be needed to predict potential transport to the BS. Ideally, tagging or marking age-0 juveniles would provide additional information on actual recruit destination and site fidelity of spawning adults. Validation of model-predicted transport rates would enable the addition of IBM-predicted survivorship and transport components to the annual stock assessment of BS and GOA walleye pollock populations.

### 3.6. Literature Cited

Bailey, K.M., Bond, N.A., Stabeno, P.J., 1999. Anomalous transport of walleye pollock larvae linked to ocean and atmospheric patterns in May 1996. *Fisheries Oceanography* 8: 264-273.

Bailey, K.M. 2000. Shifting control of recruitment of walleye pollock *Theragra chalcogramma* after a major climatic and ecosystem change. *Mar Ecol Prog Ser* 198:215-224.

Bailey, K. M., L. Ciannelli, N.A. Bond, A. Belgrano, and N. C. Stenseth. 2005. Recruitment of walleye pollock in a physically and biologically complex ecosystem: A new perspective. *Prog. Oceanogr.* 76:24-42.

Beck, M.W., Heck, K.L., Able, K.W. Jr., Childers, D.L., Eggleston, D.B., Gillanders, B.M., Halpern, B., Hays, C.G., Hoshino, H., Minello, T.J., Orth, R.J., Sheridan, P.F., and Weinstein, M.P. 2001. The identification, conservation, and management of estuarine and marine nurseries for fish and invertebrates. *BioScience* 51: 633-641.

- Botsford L.W., Hastings A, Gaines S.D. 2001. dependence of sustainability on the configuration of marine reserves and larval dispersal distance. *Ecology letters* 4:144-150.
- Cowen R.K., Lwiza K.M.M., Sponaugle S., Paris C.B., Olson D.B. 2000. Connectivity of marine populations: Open or closed? *Science* 287:857-859.
- Cowen R.K., Gawarkiewicz G., Pineda J., Thorrold S.R., Werner F. 2007. Population connectivity in marine systems An overview. *Oceanography* 20(3):14-21.
- Curchitser, E.N, D.B. Haidvogel, A.J. Hermann, E.L. Dobbins, T. Powell and A. Kaplan, 2005. Multi-scale modeling of the North Pacific Ocean: Assessment of simulated basin-scale variability (1996-2003). *J. Geophys. Res.*, 110, C11021, doi:10.1029/2005JC002902.
- da Silva, A.M., Young, C.C., and S. Levitus. 1994. Atlas of Surface Marine Data 1994. Vol 1. Algorithms and Procedures, NOAA Atlas NESDIS, vol 6, 83 pp., NOAA, Silver Spring, MD.
- Dorn M, Aydin K, Barbeaux S, Guttormsen M, Megrey B, Spalinger K, Wilkins M. 2005. Assessment of walleye pollock in the Gulf of Alaska In: Appendix B. Stock assessment and fishery evaluation report for the Groundfish Resources of the Gulf of Alaska, North Pacific Fishery Management Council, P.O. Box 103136, Anchorage, AK 99510
- Gaines S.D., Caylord B., Gerber L.R., Hastings A., Kinlan B.P. 2007. Connecting places. The ecological consequences of dispersal in the sea. *Oceanography* 20 (3): 90-99.
- Grant, W.S. and F.M. Utter. 1980 Biochemical genetic variation in walleye pollock, *Theragra chalcogramma*: population structure in the southeastern Bering Sea and the Gulf of Alaska. *Can J Fish Aquat Sci* 37:1093–1100.
- Haidvogel, D.B., H.G. Arango, K. Hedstrom, A. Beckmann, P. Malanotte-Rizzoli, P. and A.F. Shchepetkin. 2000. Model evaluation experiments in the North Atlantic Basin: Simulations in nonlinear terrain-following coordinates, *Dynamics Atmosphere Oceans* 32: 239-281.
- Hastings, A. and S. Harrison, 1994. Metapopulation dynamics and genetics. *Annual Review of Ecology and Systematics*, 25: 167-188.
- Hermann, A. J., S. Hinckley, B. A. Megrey and P. J. Stabeno. 1996. Interannual variability of the early life history of walleye pollock near Shelikof Strait, as inferred from a spatially explicit, individual-based model. *Fish. Oceanogr.* 5 (Suppl. 1): 39-57.
- Hinckley, S., Bailey, K.H., Picquelle, S.J., Shumacher, J.D., Stabeno, P.J., 1991. Transport, distribution, and abundance of larval and juvenile walleye pollock (*Theragra chalcogramma*) in the western Gulf of Alaska. *Can. J. Fish. Aquat. Sci.* 48, 91-98.
- Hinckley S., Hermann A.J., Megrey B.A. 1996. Development of a spatially explicit, individual-based model of marine fish early life history. *Marine Ecology progress series* 139: 47-68.
- Kendall AW Jr, Clarke ME, Yoklavich MM, Boehlert GW (1987) Distribution, feeding, and growth of larval walleye pollock, *Theragra chalcogramma*, from Shelikof Strait, Gulf of Alaska. *Fish Bull*, US 85: 499-521.

- Kim, S-S, Moon, D-Y and W-S, Yang. 2000. Mitochondrial DNA analysis for stock identification of walleye pollock, *Theragra chalcogramma*, from the North Pacific Ocean. *Bull Nat Fish Res Dev Inst Korea* 58:22–27.
- Levins R. 1969. Some demographic and genetic consequences of environmental heterogeneity for biological control. *Bulletin of the Entomological Society of America* 15:237-240.
- Marchesiello, P., McWilliams, J.C., and A. Shchepetkin, 2001: Open boundary conditions for long-term integration of regional ocean models. *Ocean Modelling*, 3, 1-20.
- Marchesiello, P., McWilliams, J.C., and A. Shchepetkin, 2003. Equilibrium Structure and Dynamics of the California Current System, *J. Phys. Oceanogr.*, 33, 753-783.
- Mazur MM, Wilson MT, Dougherty AB, Buchheister A, Beauchamp DA (in press) Temperature and prey quality effects on growth of juvenile walleye pollock *Theragra chalcogramma*: a spatially explicit bioenergetics approach. *J Fish Biol*
- Moore, J. K., D.M. Doney, C. Scott, and K. Lindsay, 2004. Upper ocean ecosystem dynamics and iron cycling in a global three-dimensional model. *Global Biogeochemical Cycles* 18, [np].
- Mulligan, T.J., Chapman, R.W. and B.L., Brown. 1992. Mitochondrial DNA analysis of walleye pollock, *Theragra chalcogramma*, from the eastern Bering Sea and Shelikof Strait, Gulf of Alaska. *Can J Fish Aquat Sci* 49:319–326.
- North et al. in press
- [Anon2]Olsen, J.B., Merkouris, S.E., Seeb, J.E. 2002. An examination of spatial and temporal genetic variation in walleye pollock (*Theragra chalcogramma*) using allozyme, mitochondrial DNA, and microsatellite data. *Fish Bull* 100:752–764.
- O'Reilly, P.T., Canino, M.F., Bailey, K.M. And P., Bentzen. 2004. Inverse relationship between FST and microsatellite polymorphism in the marine fish, walleye pollock (*Theragra chalcogramma*): implications for resolving weak population structure. *Mol Ecol* 13:1799–1814
- Pineda J., Hare J., Sponaugle S.U. 2007. Larval transport and dispersal in the coastal ocean and consequences for population connectivity. *Oceanography*, 20(3): 22-39.
- Sale P.F., Cowen R.K., Danilowicz B.S., Jones G.P., Kritzer J.P., Lindeman K.C., Planes S., Polunin N.V.C., Russ G.R., Sadovy Y.I., Steneck R.S. 2005. Critical science gaps impede use of no-take fisheries reserves. *Trends in Ecology and Evolution* 20(2):74-80.
- Schumacher JD, Kendall AW Jr (1991) Some interactions between young pollock and their environment in the western Gulf of Alaska. *Calif Coop Oceanic Fish Invest Rep* 32:22-929
- Shchepetkin, A.F. and J.C. McWilliams. 2005. The Regional Ocean Modeling System: A split-explicit, free-surface, topography-following coordinate ocean model, *Ocean Modeling*, 9: 347-404.
- Shields, G.F. and J.R., Gust. 1995. Lack of geographic structure in mitochondrial DNA sequences of Bering Sea walleye pollock, *Theragra chalcogramma*. *Mol Mar Biol Biotechnol* 4:69–82.

Werner, F.E., Mackenzie, B.R., Perry, R.I., Lough, R.G., Naimie, C.E., Blanton, B.O., and J.A. Quinlan, Larval trophodynamics, turbulence, and drift on Georges Bank: A sensitivity analysis of cod and haddock. *Sci. Mar.*, 63 (Suppl. 1): 99-115, 2001.

Willis T.J., Millar R.B., Babcock R.C., Tolimieri N. 2003. Burdens of evidence and the benefits of marine reserves: Putting Descartes before des horse? *Environmental Conservation* 30:97-103.

Wilson, M.T., Brodeur, R.D., Hinckley, S., 1996. Distribution and abundance of age-0 walleye pollock, *Theragra chalcogramma*, in the western Gulf of Alaska during September 1990. In: Brodeur RD, Livingston PA, Loughlin TR, Hollowed AB (eds) *Ecology of Juvenile Walleye pollock , Theragra chalcogramma*, U.S. Dep. Commer., NOAA Tech. Rep. NMFS 126 p 11-24.

Wilson, M.T., 2000. Effects of year and region on the abundance and size of age-0 walleye pollock, *Theragra chalcogramma*, in the western Gulf of Alaska, 1985-1988. *Fish. Bull.*, U.S. 98, 823-834.

## CONCLUSIONS

Cutting edge methodology has been used to advance our scientific knowledge of walleye pollock in the North Pacific in this project. Methodological advances include the coupling of a state-of-the-art hydrodynamic model to our individual-based model of walleye pollock early life history using a fast and flexible Java interface, and the addition of new features to the IBM to reflect recent thinking about important recruitment processes for this species. Simulations were done to test algorithms and parameters, and these resulted in reasonable estimates of growth and other characteristics of young pollock and their variability, and allowed us to show that we could replicate known phenomena such as a year of anomalous transport. We now have an application which was to test the main hypotheses of this project, and indeed which has been used for recruitment studies of other species in Alaskan waters, such as snow crab (NPRB project 624).

We performed a simulation intended to test whether the coupled models could replicate the temporal and spatial distribution of several life stages of young pollock for the year 1987, in which there were multiple surveys of sequential life stages, from early larvae to autumn 0-age juveniles to compare with model output. The model replicated these patterns of distribution well, demonstrating the ability of this biophysical model suite to predict the location and timing of early life stages of walleye pollock in the GOA. The modeled juveniles in this test were found near the Shumagin Islands, a known nursery area for GOA pollock. This test corroborated the connection which has been observed between Shelikof Strait spawning and the Shumagin nursery area (Hinckley et al., 1991). The horizontal movement submodel used for juvenile pollock, based on a correlated random walk, produced a distribution of early juveniles that agreed with the survey data, indicating that horizontal movements of 0-age juveniles are important in predicting their distribution. The model also correctly identified most of the known or hypothesized juvenile nursery areas in the GOA, such as the Shumagins (as mentioned), the area to the north and east of Kodiak Island, and around the Semidi Islands. The model corroborated the finding from parasite studies which found that juvenile walleye pollock found in bays east of Kodiak Island (Fig. 2.1) did not originate in Shelikof Strait, unless there were anomalous currents (Bailey et al., 1999). Also, the Bering Sea was predicted to be an important potential nursery area for GOA spawned pollock, a result that has been hypothesized but had not been tested until this study. This result has implications for management of walleye pollock in the GOA and the BS, as the two are currently managed as separate stocks.

The results of the connectivity analysis are relevant and important to the ecology of pollock in the North Pacific. There were some important findings from this analysis. As well as confirming that the coupled bio-physical model could correctly identify most of the known or suspected juvenile walleye pollock nursery areas in the GOA, the analysis allowed us to examine possible destinations of young pollock derived from different spawning locations in the GOA, and to examine the sources of juvenile pollock found in different nursery areas. Model results, as mentioned above, confirmed the connectivity between Shelikof Strait spawning and the Shumagin nursery area, but also indicated that some young pollock spawned in Shelikof Strait may transit to the Bering Sea. The model experiment also indicated that fish spawning in February in the Shumagin Islands, as has been observed, may not be retained in the GOA. This spawning aggregation has been suspected of replacing the former large aggregation in Shelikof Strait in recent years as the most important GOA pollock spawning site in the GOA. The model results indicate, however, that this area may not represent a significant source of recruits to the Gulf (recently, the spawning biomass in the Shumagin Islands has only been a small fraction of that in Shelikof).

Perhaps the most interesting finding from this study is the high percentage of GOA spawned pollock that may be transported to the Bering Sea from spawning areas widely dispersed over large portions of the Gulf. Transport of young pollock through Unimak Pass has been suspected, but for the most part not to the degree indicated by this work. If these juveniles eventually recruit to the Bering Sea populations, the management of pollock in these two areas as two separate stocks may be called into question, and recruitment estimates for the two areas may be confounded. Studies are needed that shed light on this question, and the question of natal homing of walleye pollock to answer the question of whether juvenile pollock transported from the GOA to the BS could return to the Gulf to recruit and spawn.

Even if this connection between the GOA and the BS proves to be of lesser magnitude than indicated by this study, the patterns it has shown may be useful in explaining unusual patterns in recruitment that are sometimes seen in the data, such as unusually large year classes in the Bering Sea perhaps due to an influx from the GOA, and perhaps in decreasing the error in recruitment estimates used in stock assessment models. If the results of this model study could be validated, IBM-predicted survivorship and transport could be added to the annual stock assessments of walleye pollock.

The immense model-generated “dataset” generated for this work can also be analyzed to examine qualities that differentiate “survivors” from “nonsurvivors”, ie. young fish that do or do not make it to nursery areas, and what differentiates them. In recruitment studies it is often said that, due to the high mortality rates in early life stages and the fact that only about 1% or less of the initial number of eggs released ever makes it to the age of recruitment, it is the unusual individual that survives. A unique aspect of individual-based models is that the entire history for each individual is retained and can be analyzed for patterns of encounter with different environmental characteristics such as temperature, prey, or currents, or other factors which may make some individuals more or less likely to be the unusual individual that survives. We hope to follow this work with a longitudinal analysis of this dataset to discover some of the important features that allow for survival, and perhaps are key to recruitment success. This type of analysis, along with this analysis of connectivity between spawning and nursery areas, should allow us to design model-based indices derived from this coupled model set which could be useful in forecasting recruitment of walleye pollock.

## **PUBLICATIONS**

Parada, C., Hinckley, S., Horne, J., Dorn, M., Hermann, A., Megrey, B. Comparing simulated walleye pollock recruitment indices to data and stock assessment models from the Gulf of Alaska. Accepted. Marine Ecology Progress Series

Parada, C., Hinckley, S., Horne, J. and Mazur, M. Empirical corroboration of IBM-predicted walleye pollock (*Theragra chalcogramma*) spawning-nursery area transport and survival in the Gulf of Alaska. In preparation. Planned submission date: December, 2008. **JOURNAL???**

Parada, C., Hinckley, S., and Horne, J. Connectivity of Walleye Pollock (*Theragra chalcogramma*) Spawning and Nursery Areas in the Gulf of Alaska. In preparation. Planned submission date: December, 2008. **JOURNAL???**

## **OUTREACH**

### **Web Pages**

Ecosystems and Fisheries Oceanography (EcoFOCI) Physical and Biophysical Modeling. Gulf of Alaska and Bering Sea numerical simulation models exploring physical and biological dynamics. [http://www.ecofoci.noaa.gov/efoci\\_models.shtml](http://www.ecofoci.noaa.gov/efoci_models.shtml)

(In prep) Recruitment Processes Program, Alaska Fisheries Science Center subpage on Ecosystems and ecological modeling subprogram. Will be linked to:  
[http://www.afsc.noaa.gov/RACE/recruitment/default\\_rp.php](http://www.afsc.noaa.gov/RACE/recruitment/default_rp.php)

### **Conference Presentations**

Parada, C., S. Hinckley, A.J. Hermann and M. Dorn. “A biophysical model of walleye pollock in the Gulf of Alaska: model to model and model to data comparisons” Advances in Marine Ecosystem Modelling Research Symposium. Plymouth, UK, June 2005.

Hermann, A. J., S. Hinckley, C. Parada, E. Dobbins, C. W. Moore and D. B. Haidvogel, “Immersive visualization: a modern approach for the rapid exploration of coastal ecosystem model dynamics”, Advances in Marine Ecosystem Modelling Research symposium, Jun. 27-29, 2005, Plymouth Marine Laboratory, Plymouth, UK

Hermann, A., M. Dorn and S. Hinckley, “Multi-decadal simulations of circulation and walleye pollock in the Northern Gulf of Alaska”, Fisheries and the Environment (FATE) Science Meeting, Jun. 8-9, 2005, Seattle, WA.

Hinckley, S. and C. Parada. “NPZ & IBM modeling: current Gulf of Alaska biological models, their applications, and future plans”. Presentation to North Pacific Fisheries Management Council. Seattle, WA. February, 2006

Megrey, B., S. Hinckley and C. Parada. “Using IBM’s to compare two hypotheses for the effect of turbulence on feeding rates in larval fishes”. Workshop on advancements in modelling

physical-biological interactions in fish early-life history: recommended practices and future directions. Nantes, France. April, 2006.

S. Hinckley. "Future Directions: Integration with observing systems, operational models, monitoring programs, and management recommendations". Workshop on advancements in modelling physical-biological interactions in fish early-life history: recommended practices and future directions. IFREMER, Nantes, France. April, 2006.

Hermann, A. J., S. Hinckley, C. Parada, E. Dobbins, C. W. Moore and D. B. Haidvogel, "Immersive visualization: a modern approach for the rapid exploration of Eulerian and Individual-Based models", Workshop on advancements in modelling physical-biological interactions in fish early-life history: recommended practices and future directions (WKAMF), 3-5 April 2006, IFREMER, Nantes, France.

Parada, C., S. Hinckley, J. Horne, A.J. Hermann, B. Megrey and M. Dorn. "Hindcasting walleye pollock recruitment and examining pollock stock structure in the Gulf of Alaska using a biophysical model". Marine Science Symposium, Anchorage, Alaska. January, 2007.

Hermann, A. J., S. Hinckley, C. Parada, E. Dobbins, C. W. Moore and D. B. Haidvogel, "Immersive visualization: a modern approach for the rapid exploration of Eulerian and Individual-Based models", Gordon Conference on Coastal Ocean Modeling, 17-22 June 2007, Colby-Sawyer College, New London NH.

### **Workshop Participation**

Hermann, A.J., S. Hinckley. "A brief history of IBM/NPZ/Hydrodynamic modeling in FOCI". Joint Centre de Recherche Halieutique (CRH) seminar, June, 2005, Sete, France.

Hermann, A. J. "Immersive visualization techniques for the exploration of hydrodynamic and biological model output", Fisheries Oceanographic Modeling Workshop, Centre de Recherche Halieutique (CRH), , June 24, 2005, Sete, France.

Hinckley, S. "NPZ and individual-based models in the Bering Sea/Aleutian Islands". Workshop on evaluation of ocean circulation models for the Bering Sea and Aleutian Islands Region". NPRB Project 402. February, 2005.

Workshop on advancements in modelling physical-biological interactions in fish early-life history: recommended practices and future directions (WKAMF). Nantes, France. April, 2006.

### **Presentations in Schools**

Hermann, A. J., E. N. Curchitser, D. B. Haidvogel, E. L. Dobbins, S. Hinckley and C. W. Moore, "Immersive visualization of the circulation and biology of the Northeast Pacific using spatially nested models", Physical Oceanography Seminar, College of Oceanic and Atmospheric Sciences, Oregon State University, Feb 16, 2005, Corvallis, OR USA

Parada, C. Introduction to coupled biophysical models with IBMs. University of Concepcion summer school, December, 2005.

Hermann, A. J., "Immersive 3D visualization of Lagrangian and Eulerian phenomena in oceanography", University of Washington Physical Oceanography seminar, May 31, 2006, University of Washington, Seattle, WA USA.

Hermann, A. J. "3D Astronomy and Oceanography", Whittier Elementary Science Fair, March 28, 2006, Seattle, WA USA.

Parada, C. Individual-based models in fisheries oceanography. University of Concepcion. December, 2007.

Hinckley, S. "Applied individual-based models in fisheries oceanography". Ecological modeling class, University of Washington, Seattle. May, 2007 and May, 2008

## **ACKNOWLEDGEMENTS**

Be brief and include other funding agencies if appropriate.

## **LITERATURE CITED**

List only those references not listed in the chapters, i.e., those used in the *Introduction* or *Conclusions*.

## PROJECT SYNOPSIS

**Introduction:** Walleye pollock – backbone of an ecosystem a fishery, and many people’s livelihood

Walleye pollock (*Theragra chalcogramma*) in Alaska supports one of the largest fisheries in the world, as well as being a pivotal species in the ecosystems in the Gulf of Alaska. Walleye pollock spawn in many different locations in the Gulf of Alaska (GOA), and the nursery areas for juvenile fish (less than 1 year old) are found in many other locations. At the present time, little is known about where the young fish from each spawning area end up, or to put it another way, where the juveniles found in a particular location were spawned. In other words the connectivity or pathways between spawning and nursery grounds is not well understood.

Female walleye pollock spawn millions of eggs, but 99% of these die before the end of their first year, due to some combination of three factors: lack of food, high levels of predation, and transport by ocean currents out of their preferred habitat. The number of fish left to support both the ecosystem and the fisheries (“recruits”) varies widely among years. This variability can put stress on species in the ecosystem that depend on juvenile or adult pollock for food such as Steller sea lions, fur seals, many groundfish and bird species, among others, and also on the pollock fishery itself.

**Why we did it:** Managers of Alaskan ecosystems and fisheries need to understand how the number of recruits varies with the number of spawners and with variability in the physical and biological environment. They must have an understanding of whether spawning and juvenile nursery areas for walleye pollock represent separate populations or a single Gulf of Alaska or Bering Sea stock, to correctly parameterize the stock assessment models, set the management regime and ultimately, correctly establish catch quotas. Only when spawning-nursery area connections are understood, can the reasons for variations in “recruitment” both for near-term (1-3 years) and long-term (decades) be clarified. This is important to manage removals by the fishery in a responsible way, leaving enough pollock for other “mouths” in the ecosystem. Projections of how walleye pollock recruitment may be affected as climate changes will also help in long-term management of this species.

**How we did it:** We developed a set of coupled physical and biological simulation models to track the trajectories through the ocean, the feeding and growth, predation and survival of young pollock in the first year of their life. The physical model gives us a 3D “movie” of the currents, and temperature and salinity patterns as they change over time. In the biological model, young fish are moved around by the currents, and physical factors at different locations affect processes such as encounter with food, metabolic and development rates, growth and mortality. With these models, we can do “experiments” designed to tell us what combination of factors affect survival in any year, and how this may change as the environment changes. In the main experiment done for this project, we released virtual walleye pollock eggs over the whole spawning range of the species in the GOA, and followed them until the fall of their first year when they were juveniles. This way we could track the links between spawning time and location, and nursery areas, and the conditions along the way.

**What we discovered:** We verified with the model that in the GOA many young pollock use the Shumagin Island region as a nursery area. The model tells us that these fish could be spawned along the inner part of the continental shelf of the GOA, in areas such as Outer Cook Inlet, Shelikof Strait and the Semidi Islands, as well as in the Shumagin region itself. An interesting

result is that many young pollock may be born in the GOA, but end up in the Bering Sea, especially if they were spawned on the outer edges of the continental shelf or slope; or in the Shumagin region. This is important, as it raises two questions: (1) are the GOA and Bering Sea walleye pollock populations really separate, or is recruitment in the Bering Sea affected by spawning in the Gulf?, and (2) the Shumagin Island region has recently found to contain many spawning pollock – but is this a self-sustaining population, or are all the young fish produced in this region “lost” to the Gulf? What percentage of those spawned here remain? These are critical factors for managers to understand.

**What’s next:** Our coupled model set may be a useful tool to forecast recruitment in such a way that includes **mechanisms**, i.e. the physical and biological factors that are most important in controlling recruitment variability. To do this, we need to understand what differentiates “survivors” (those that eventually will recruit) and “non survivors”. The output of the model experiment done for this project should be the foundation to a subsequent effort to telling us this. We can track each individual to understand why it survived or didn’t – too little food? Too much cold water? Was it carried out to sea? Once these factors are better understood, we can design model-derived indices that may allow us to forecast future recruitment.

**Outreach:**

- Nine presentations at scientific conferences, including the Advances in Marine Ecosystem Modelling Research Symposium, the Fisheries and the Environment Science Meeting, the Advancements in Modelling Physical-Biological Interactions in Fish Early-Life History Conference, the Alaska Marine Science Symposium, and the Gordon Conference on Coastal Ocean Modeling.
- One presentation to the North Pacific Fisheries Management Council.
- Participation in three workshops: (1) the Fisheries oceanographic modeling workshop, Centre de Recherche Halieutique (CRH), (2) the Workshop on evaluation of ocean circulation models for the Bering Sea and Aleutian Islands Region (NPRB Project 402), and (3) the Workshop on advancements in modelling physical-biological interactions in fish early-life history: recommended practices and future directions.
- Several school presentations, including Whittier Elementary School, the University of Washington Physical Oceanography Department, the UW School of Fisheries and Aquatic Sciences and the UW Quantitative Ecology and Resource Management program, at Oregon State University Physical Oceanography Department, and at the University of Concepcion (Chile).
- The EcoFOCI website ([www.ecofoci.noaa.gov](http://www.ecofoci.noaa.gov)) posted some of the presentations of the walleye pollock project results and work on a specific website for this work is in progress.
- Two courses on individual-based modeling for graduate students were organized and conducted, for training and dissemination of the biophysical coupling techniques with emphasis on the Gulf of Alaska walleye pollock case study.

**The Big Picture:** Biophysical modeling is an important tool to help us understand how to better manage fish stocks for both the fisheries that depend on them and other creatures in the environment that also depend on them. This is because we can perform “experiments” with models in ways that tell us about mechanisms – ie. how the systems actually work, and how climate change may affect these systems. In this study, we discovered important relationships between walleye pollock spawning in different places within the Gulf of Alaska, and between the

GOA and the Bering Sea juvenile nursery areas. This should help managers effectively manage this species.

***NPRB Research Interest:*** The overall mission of NPRB is to support research “*designed to address pressing fishery management or marine ecosystem information needs.*” This research will add to the ability of managers to protect the walleye pollock fishery, and the marine ecosystems in the GOA and the BS for which pollock is a pivotal species. It will add to the knowledge required to use this coupled biophysical model to forecast recruitment levels for pollock in both the short and the long term. We have developed a tool that can be used with other species in other areas as well.